Czech Technical University in Prague
Faculty of Electrical Engineering
Department of Power Engineering
&
Department of Electric Drives and Traction

MASTER THESIS

Simulation of a Brushless DC Motor in ANSYS – Maxwell 3D

Student: Prathamesh Mukund Dusane

Guide: Ing. Karel Buhr, PhD.

Czech Technical University in Prague
Faculty of Electrical Engineering

Department of Electrical Power Engineering

DIPLOMA THESIS ASSIGNMENT

Student: **Prathamesh Dusane**

Study programme: Electrical Engineering, Power Engineering and Management
Specialisation: Electrical Power Engineering

Title of Diploma Thesis: **Simulation of brushless direct current machine in ANSOFT Maxwell 3D software environment**

Guidelines:

1. BLDC hub configuration machines literary research
2. ANSOFT Maxwell 3D software interface familisation
3. 1500 W BLDC machine electromagnetic design
4. Machine 3D model design in RMxprt module
5. BLDC machine as drive parts simulationResult analysis

Bibliography/Sources:

[1] Pyrhonen J., Jokinen T., Hrabovcova V., Design of Rotating Electrical Machines, Wiley 2014
[2] Krishnan R., Permanent Magnet Synchronnous and Brushless DC Motor Drives, CRC Press, 2010
[3] Maxwell_v16_3D, ANSYS Academic Teaching EM, pdf manuals 2013

Diploma Thesis Supervisor: Ing. Karel Buhr, CSc.

Valid until the end of the winter semester of academic year 2017/2018

L.S.

doc. Ing. Zdeněk Müller, Ph.D.
Head of Department

prof. Ing. Pavel Ripka, CSc.
Dean

Prague, April 18, 2016

Declaration

I hereby declare that the work 'Simulation of a BLDC Motor in ANSYS – Maxwell 3D' is my own work. This thesis is a presentation of my original research work. Wherever contributions of others are involved, every effort is made to indicate this clearly, with due reference to the literature, and acknowledgement of collaborative research and discussions.

Written and Submitted in partial fulfillment of the requirements for the degree of Master of Power Engineering and Management

The work was done under the esteemed guidance of Professor Ing. Karel Buhr, PhD and Ing. Radek Fajtl of the Czech Technical University in Prague.

Prathamesh Mukund Dusane

For the Czech Technical University, Prague

Date: 2nd June 2016

Abstract:

This thesis is about the simulation of a Brush-Less Direct Current Machine in the ANSYS – Maxwell Environment. The machine is selected for a high-performance electric-bike as a motor over the UNEP (United Nations Environment Program) metropolitan drive cycle. Analytical study of the forces influencing the machine along with industry references and literature review led to estimation of rated operating parameters. Four models of a 1,500Watt, 380Rpm, 40Nm & 48Volt BLDC Motor are designed and simulated in the RMxprt module of Maxwell [24 Slot, 36 Slot, 48 Slot, 72 Slot] The software enabled solving and simulation of magneto-static and transient fields based on Maxwell's equations in 2D & 3D. The solution set of each machine is described and tabulated in the appendix of this thesis. 2D and 3D analysis reveals inconsistencies in the waveform of winding currents, induced voltages and losses of 24 Slot and 36 Slot Machines due to an error in the internal software conversion from 2D to 3D in RMxprt, also the field plots show abnormally low magnetic field density in stator teeth and high current magnitude in the winding of these two machines. The 48 Slot and 72 Slot machines had consistent 2D and 3D waveform characteristics although field overlays show localized hot spots of magnetic field density in the stator sections. Overall the 72 Slot machine suits best for the given application.

Aim & Objective:

In the 1890s, electric bicycles were described and documented within numerous patents. For example, in 1895, Ogden Bolton Jr. was granted a patent for a battery-powered bicycle with "6-pole brush-and-commutator direct current (DC) hub motor mounted in the rear wheel." There were no gears and the motor could draw up to 100 amperes (A) from a 10-volt battery. [1]

Still today for much of our world, especially in countries of Asia like China, India, South-Korea, Japan etc. and European countries like Netherlands, Denmark, Hungary, Germany, France, Spain, Sweden etc. bicycles have been a major form transportation for the masses because the working and housing areas in most of these densely populated cities are within walking or cycling distance.

An E-Bike is a bicycle that has an integrated motor for the purpose of propulsion. Brushless DC Motors are commonly used for propulsion of these bikes nowadays. The Brushless DC Motor design has tremendous advantages. It combines the long life of the induction motor and linearity of the permanent magnet motor, plus adds higher speed range capability (productivity), size weight reduction (compact design), and improved torque capability (precision). [2]

The aim of this thesis is to design and simulate a direct drive outer rotor BLDC Machine as a motor for a high-power and performance electric bike. ANSYS – Maxwell is used for designing and simulating the machine.

Contents

1. Background of the BLDC Machine

Brushless DC motors are rapidly evolving, thanks to the advancements in solid state semiconductor technology and further improvements in magnetic materials. A BLDC (Brush-less direct current) motor, also known as an *electronically commutated motor* is a type of synchronous motor powered by a DC source integrated with an inverter or switching power supply, which converts DC to AC signal to power the motor. Here, AC does not refer to the sinusoidal shape of the wave, but rather a bi-directional current with no restriction on its waveform. [3]

Just like all other motors a BLDC motor consists of a Stator and a Rotor, permanent magnets are mounted on the rotor while the stator is usually made by stacking slotted steel laminations wound with a specific number of poles. The stator can also be slotless, a slotless core has lower inductance, and thus it can run at very high speeds. [4]

The power convertor is responsible for commutation, which is the act of changing the motor phase currents at the appropriate times to create a Rotating Magnetic Field (RMF) thereby producing rotational torque. The RMF is maintained by using the appropriate phase sequence to supply the stator phases. One pole of energized stator phase attracts one of the rotor poles, while the second pole of the energized stator phase repels the corresponding pole of the rotor. This action of the rotor chasing the electromagnet poles on the stator is the fundamental working principle of BLDC motors.

Based on relative position of the Stator & Rotor, the BLDC motor can be classified as,

1. Inner Rotor/Inrunner – The rotor along with its embedded permanent magnets are in the center of the machines whereas the windings of the stator surround the rotor.
2. Outer Rotor/Ourunner – The stator coils form the center (core) of the motor while the permanent magnets spin within a rotor that surrounds the stator. [5]

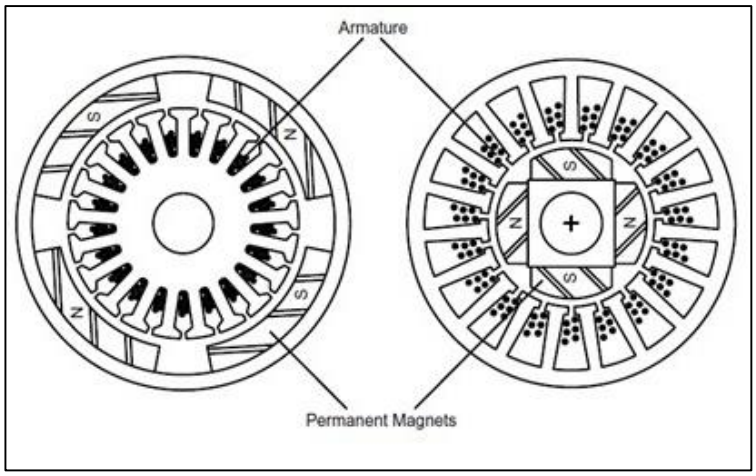

Figure 1: Outer Rotor Motor (Left), Inner Rotor Motor (Right) [6]

The BLDC motor's control is based on the information about position of its rotor. The estimation of rotor position in brushless DC motors can be either sensored or sensorless.

In the case of sensor based control a Hall-effect position sensor I.C. (Integrated Circuit) detects the position of the rotating magnet in the rotor and excites the corresponding windings through logic and driver circuitry. The rotating permanent magnet moving across the front of the sensor causes it to change state. The sensor operates when each South Pole approaches. [7]

In sensorless control the principle used for rotor position estimation and control is to analysis of the Back-Electromotive Force (BEMF) from the motor. Back-EMF is the voltage induced in the stator winding of the motor by a rotating magnetized rotor. The magnitude of back-EMF is proportional to the speed of the motor. [8] A BLDC motor has trapezoidal waveform of back-EMF, as opposed to the sinusoidal waveform back-EMF found in permanent magnet synchronous motor. [9]

There are two types of electrical wiring configurations for the winding,

1. Delta (Δ) Configuration – The 3 phase winding of the stator are connected to each other in a series combination resembling a triangle like circuit. Here, 3 terminals are available for control.
2. Star (Y) Configuration – The 3 phase winding of the stator are connected to each other in a parallel combination to a central point (star point/neutral point). Here, 4 terminals are available for control.

Based on the form factor of the permanent magnet synchronous machine, the BLDC motor is classified below in *Figure 2*, also present are Circumferential and Transverse flux machines.

1. Axial Flux – The axial flux motors have a flux that runs parallel to the output shaft, that is, along the axis of the shaft, thus, '*axial*'. These type of machines can be stacked in parallel making them multi-staged.
2. Radial Flux – A radial flux motor has its flux running in and out from the center of the shaft, on the radius, hence '*radial*'.

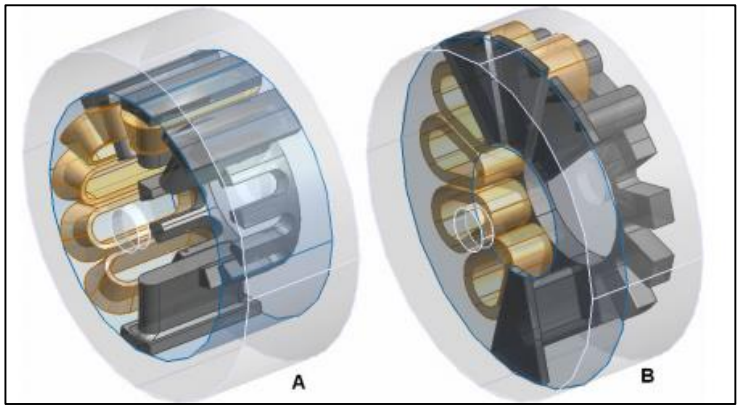

Figure 2: A) Radial Flux Motor, B) Axial Flux Motor [10]

2. BLDC Machine literature review

The paper [11] describes design scope and analysis issues about the BLDC machine like selection of pole number, winding layout, rotor topology, drive strategy, field weakening and cooling. The scope of the paper is limited to radial flux motors, the paper discussed some ratings to dimension the motor, it also differentiated between AC & DC control. The following section sheds light on the factors determining the pole number of the machine and its importance and characteristics in the operation of the motor, in this section the authors have also mentioned strategies in slot design to reduce cogging torque. The authors placed importance on the number of slots & poles along with the number of coil sides in a slot for choosing the AC winding design, whereas the authors resolved that a fully pitched concentrated winding is necessary for DC winding design. Then next section mentions about the selection magnets and their dimensioning for designing the rotor, the authors pointed out the importance of not operating magnets in their non-linearity zone, they also laid constraints on the thermal loading of the magnets. The authors also warned about having impractically high stator slot fill percentages and advised caution. In the next section of the paper the author has discussed thermal considerations for selecting current density in the winding along with some popular cooling methods. The last section of the paper shows I-Psi & Efficiency plots of a PMDC machine to judge it torque and performance, the authors also mentioned effect of phase angle advance setting of the converter on the efficiency of the machine. Overall, the authors have presented a comprehensive design analysis of the brushless permanent magnet machine with many notable references.

In [12], Srivastava and Brahmin describe the design and simulation of a 3-phase double layer coil BLDC motor (Hub Drive Machine) for Electric Vehicles (EV) using ANSYS software. Two 15 kW brushless BLDC motors are designed, simulated and compared, one has 36 Slots/24 Poles while the other has 36 Slots/16 Poles. FEM is used by the authors to resolve the electromagnetic field using Variational Calculus of Poisson's type from the basic Magneto-Static Maxwell's equations. The authors have graphically depicted their observations of Torque v/s Rotation Angle for all three phases. 2D mesh analysis in ANSYS - Maxwell revealed that the rated torque requirement is achieved from configuration - II (36S/16P). They concluded that with reduced number of poles high speed of rotation could be achieved easily.

In [5], the authors have aimed to design an optimal outer rotor BLDC motor parameterized for low cogging torque. They have used ANFOT – Maxwell to model the rotor & stator of the motor and also verify its Pole/Slot combinations. The authors concluded that cogging torque was lowest in 26 Slot motors and was heavily influenced by slot aperture, wider slot openings leading to higher cogging torque, the authors also suggest that, the number of poles have a significant influence of the cogging torque of the machine, lower number of poles produced lower cogging torque.

The paper published by IEEE Transactions in Magnetics [13], the authors have presented an efficiency study of a 1.5kW 2 & 6 Pole Induction Motor converted to 1.5kW 2 & 6 Pole BLDC Motor, they have modified the rotor of an induction motor to a PM rotor (NdFeB) and reported a higher average efficiency of 14% and consequent increase in speed and torque range. Afterwards, the authors have replaced the stator steel of the IM with M253-35A steel type in the BLDC motor with the same geometric design and reported a further 2% increase in efficiency.

The journal paper by [14], the author examines the effect of stator slot structure and switching angle on a cylindrical single-phase brushless direct current motor (BLDC). Three types of default slot designs are compared in RMxprt of Ansys – Maxwell, then the motor is analyzed in Maxwell 3D electromagnetically using FEM, and at the end with the use of MATLAB the author the examined influence of switching angle on motor performance. The author indicates that with correct choosing of stator slots & its structure along with switching angle, maximum efficiency can be attained. His results are, that motors operate better when the windings are switched ON earlier with respect to the emfs induced in them, which means that if voltage inverters are applied to the inverters they should operate at an advanced switching angle for maximum efficiency (β = - 45deg), the default slot structure number 3 of RMxprt was found to have largest flux density and the smallest inductance leakage.

A paper by James R. Hendershot of the Magna Physics Corporation [15] analyzes the phase , rotor poles and stator slots such that the best selection can be made before the actual motor design is attempted, the author has analyzes and compared various phase, pole and slot configurations. It is shown by the author that with increase in number of phases, the ripple content in the machine's torque decreases although the number of switches & sensors needed for commutation increases along with the system cost. The author has summarized the effect of number of poles as, higher the number of poles lower is the motor speed and vice a versa. Considering the number of slots the author has advised that if a low cost, sinusoidal motor is desired then 3.75 Slots/Pole configuration is best. The author has then listed numerous Slot/Pole configurations along with the number of slots & poles respectively. In the final section the author has analyzed the back EMF of the slot/pole groups using Fourier series on an IBM PCAT computer for star and delta connections.

3. ANSYS – Maxwell familiarization

ANSYS, Inc. is an American Computer-aided engineering software developer headquartered south of Pittsburgh in Pennsylvania, United States. Ansys publishes engineering analysis software across a range of disciplines like finite element analysis, structural analysis, computational fluid dynamics, explicit/implicit methods, and heat transfer.

ANSYS Maxwell is a high-performance, low frequency electromagnetic field simulation interactive software package that uses finite element analysis (FEA) to solve electromagnetic problems by solving *Maxwell's equations* in a finite region of space with appropriate boundary and user-specified initial conditions for 2D/3D electromagnetic and electromechanical devices, including motors, actuators, transformers, sensors and coils. Maxwell uses the accurate finite element method to solve static, frequency-domain, and time-varying electromagnetic and electric fields. The software can only use a triangular/tetrahedral elements to mesh the domain and linear interpolation functions to approximate the solution. [16]

The physical equations that describe the electromagnetic field given by James Clerk Maxwell are [17],

Gauss' Law for Electricity $\nabla . \boldsymbol{D} = \boldsymbol{p}$

Gauss' Law for Magnetism $\nabla . \boldsymbol{B} = \boldsymbol{0}$

Faraday's Law of Induction $\nabla \times \boldsymbol{E} = -\frac{\partial \boldsymbol{B}}{\partial \boldsymbol{t}}$

Amperes' Law $\nabla \times \boldsymbol{H} = \boldsymbol{J} + \frac{\partial \boldsymbol{D}}{\partial \boldsymbol{t}}$

E = Electric field
ρ = Charge density
B = Magnetic field
ε_0 = Permittivity
J = current density
D = Electric displacement
μ_0 = Permeability
H = Magnetic field strength
M = Magnetization
P = Polarization

$D = \varepsilon_0 E + P$ *General case*	$D = \varepsilon_0 E$	*Free space*
	$D = \varepsilon E$	*Isotropic linear dielectric*
$B = \mu_0 (H + M)$ *General case*	$B = \mu_0 H$	*Free space*
	$B = \mu H$	*Isotropic linear magnetic medium*

Numerical techniques are necessary to solve equations above, which is the cause of software simulation.

3.1. ANSYS RMxprt:

(RMxprt) Rotating Machine Expert is a template-based design tool of the ANSYS – Maxwell suite used to create a customized machine design flow to meet demand for higher efficiency. Using classical analytical motor theory and equivalent magnetic circuit methods, RMxprt can calculate machine performance, make initial sizing decisions and perform numerous "what if" analyses. RMxprt is able to automatically set up a complete Maxwell project (2-D/3-D) including geometry, materials and boundary conditions. The set up includes the appropriate symmetries and excitations with coupling circuit topology for electromagnetic transient analysis. [18] [19]

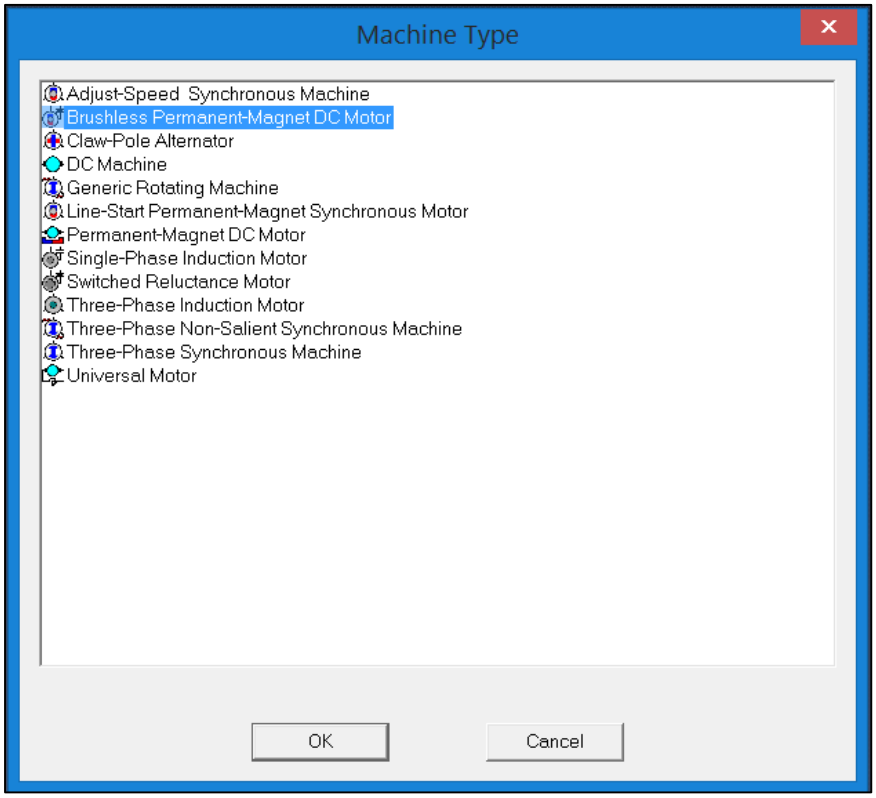

Figure 3: Machine selection interface in RMxprt

3.1.1. The Machine Selection Window in *Figure 3* includes all possible AC & DC rotating machines within the Maxwell RMxprt mainframe, with each machine having its own predefined dimensions & mechanical properties.

On selection of any machine a graphical user interface opens on the screen which includes five windows and four toolbars each having various functions, out of them the most important is the Project Window.

3.1.2. The Project Window in *Figure 4* includes a dropdown tool list whose main components are,

1. Machine
    - Circuit
    - Stator
    - Rotor
    - Shaft
2. Analysis
3. Optimetrics
4. Results

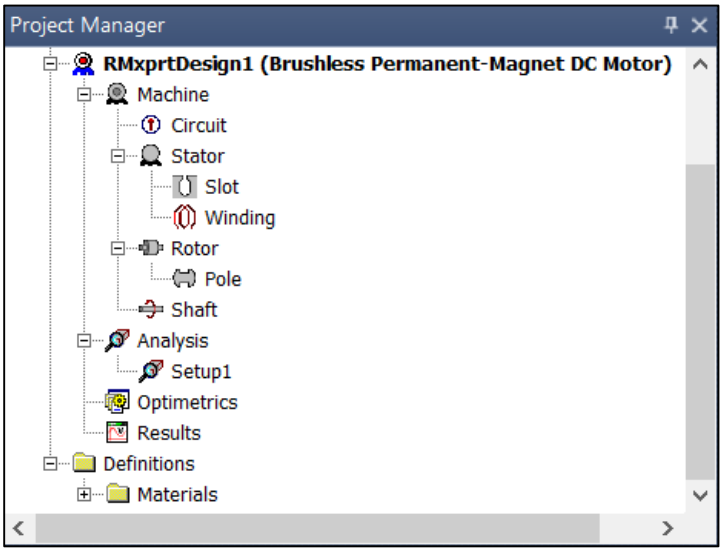

Figure 4: Project Manager Window

3.1.3. The Machine Properties Window includes general information depicted in *Figure 5*, the number of poles has to be an even number integer, the position of the rotor can be either inner or outer rotor, the frictional & winding (air-resistance) loss along with reference speed are user defined quantities. The control type can be DC or CCC (Current Chopped Control).

The circuit type can be,

1. Y3 – Y Type, 3Φ
2. L3 – Loop Type, 3Φ
3. S3 – Star type, 3Φ
4. C2 – Cross Type, 2Φ
5. L4 – Loop Type, 4Φ
6. S4 – Star Type, 4Φ

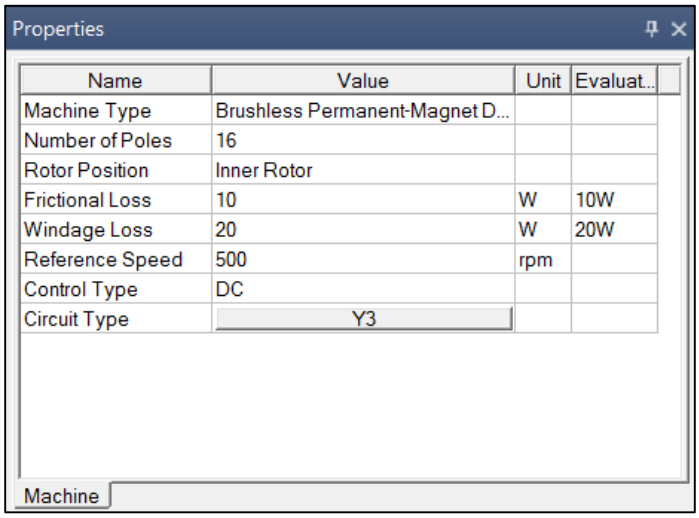

Figure 5: Machine Properties Window

Name	Value	Unit	Evaluated Value
Lead Angle of Trigger	0	deg	0deg
Trigger Pulse Width	120	deg	120deg
Transistor Drop	2	V	
Diode Drop	2	V	

Figure 6: Circuit Properties Window

3.1.5. The Circuit Data Properties Window depicted in *Figure 6* defines excitation circuit data for a BLDC machine, the Lead Angle of Trigger is illustrated in *Figure 7*, and the graph shows open circuit induced voltage v/s rotor position in electrical degrees. An angle of zero means that induced voltage in the triggered phase is maximum. A positive value denoted a lead angle while a negative value is a lag angle. The Trigger Pulse Width is the 'on-time' of a transistor in electrical degrees. The Transistor drop defines the voltage drop across one transistor in the ON state. The Diode Drop is to quantify the voltage drop across a diode in the discharge loop.

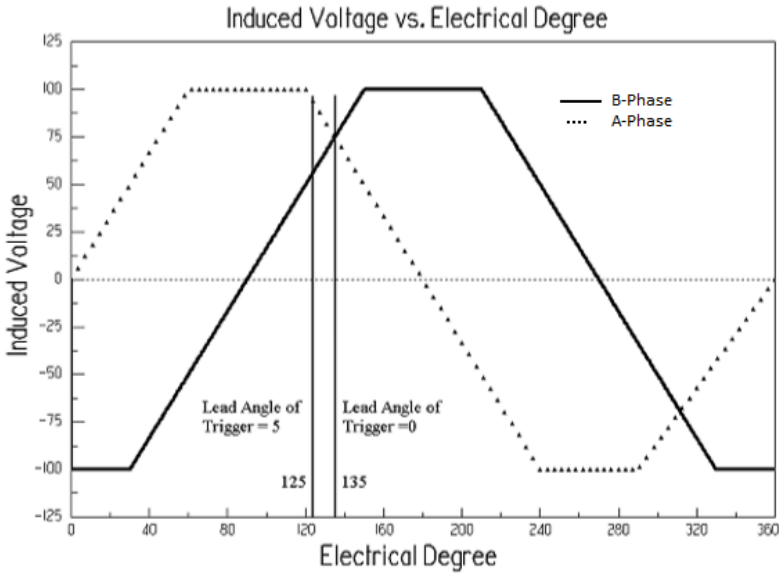

Figure 7: Lead Angle of Trigger [19]

3.1.6 The Stator is a slotted lamination stack where poly-phase windings reside, the Stator Entry option is shown in *Figure 8*. The Outer & Inner Diameters along with Length and Slot Number are user defined inputs and change with the type of motor modelled. Stacking factor is to quantify the total stator steel area to the area covered by lamination varnish. Various types of steel can be described by the software, also steel types can be added and modelled if their parameters are known is known along with coefficients of core loss Ke, Kc, Kh. There are six types of slots provided in RMxprt for rotating machines. Skew Width quantifies the skew angle of a slot defined as in slot width unit.

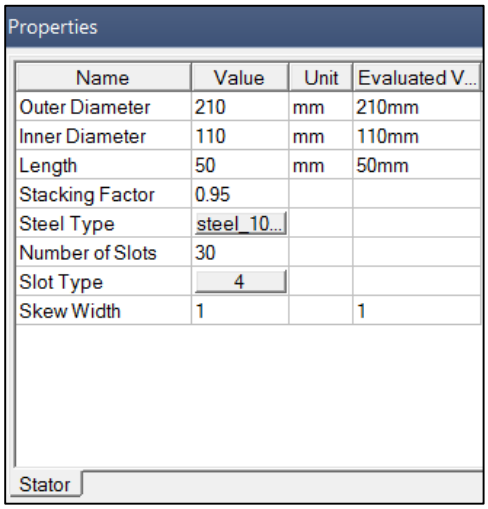

Figure 8: Stator Properties Window

3.1.7. Slot Dimensions: the Stator option in RMxprt for BLDC motors includes slot properties and Winding Properties, the possible slot dimensions are depicted in *Figure 9*, while a slot model is depicted in *Figure 10.*

Properties

Name	Value	Unit
Auto Design	☐	
Parallel Tooth	☐	
Hs0	2	mm
Hs1	1	mm
Hs2	30	mm
Bs0	2	mm
Bs1	6	mm
Bs2	12	mm
Rs	0.6	mm

Slot

Figure 9: Slot Dimensions Window

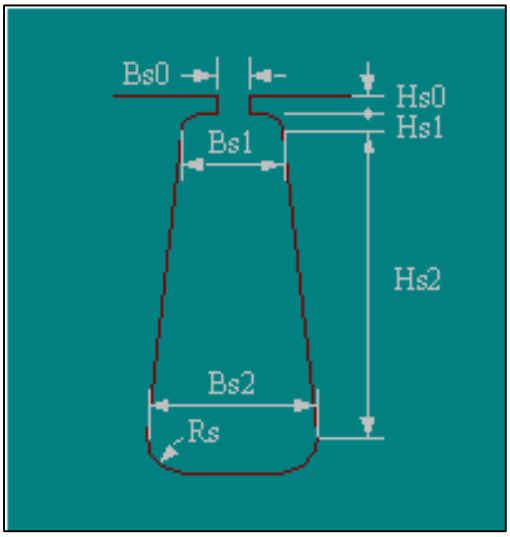

Figure 10: Slot Model

3.1.8. The Stator Winding Properties Window is shown in *Figure 11* lists the inputs relating to the winding of the machine, the number maximum winding layers can be two, the type of winding can user defined in an editor along with Whole-Coiled or Half-Coiled winding shown in *Figure 12*. Six windings are possible three for single layer and three for double layer.

Properties

Name	Value
Winding Layers	2
Winding Type	Whole-Coiled
Parallel Branches	1
Conductors per Slot	15
Coil Pitch	1
Number of Strands	5
Wire Wrap	0.2
Wire Size	Diameter: 1.369mm

Winding | End/Insulation

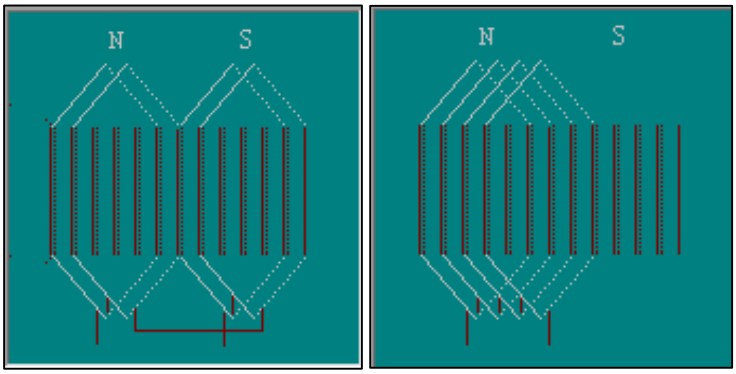

Figure 12: Whole Coiled (Left) & Half Coiled (Right)

Figure 11: Winding Properties Window

The number of Parallel Branches in one phase of the winding is specified in the Parallel Branches field of the Winding Properties Window. The number of Conductors per Slot is the value of number of turns per coil multiplied by number of layers.

The Coil Pitch is number of slots separating one winding, for example, if a coil starts in slot 1 and ends in slot 6, its coil pitch is 5. Number of Strands defines the number of wires per conductor. Wire Wrap is the double sided thickness (2Y) of insulation on a conductor illustrated in *Figure 13*. The Wire Size includes the wire diameter in a pull down list along with an appropriate wire gauge.

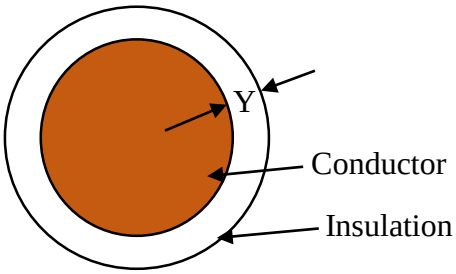

Figure 13: Wire Wrap of a Conductor

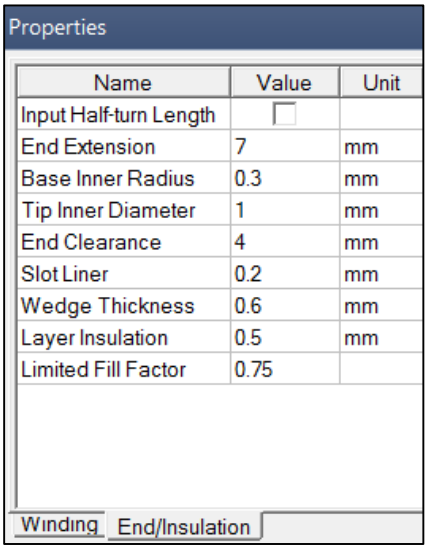

Figure 14: End/Insulation Tab

3.1.9. The End/Insulation Tab shown in *Figure 14* is for the dimensioning of Coil Ends and Slot Insulation, illustrated in *Figure 15* & *Figure 16* respectively. The End Extension is the distance between the end of stator and one end of a conductor. The Base Inner Radius is the radius of the base inner corner, while the Tip Inner Diameter is the inner diameter of the coil tip. End Clearance is the distance between two stator coils. Slot Liner is the measure of thickness of the slot liner insulation, while Wedge Thickness is the measure of thickness of the wedge insulation in the stator slot. Layer Insulation is the thickness of the insulation layer. Limited Fill Factor is the ratio between cross-sectional areas of all conductors in one slot to the whole area of the slot.

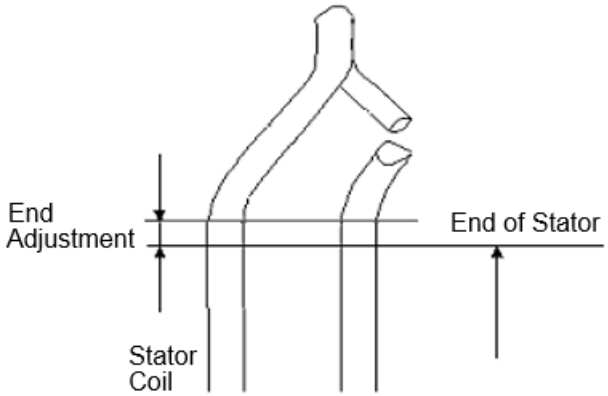

Figure 15: Coil End of the Winding [19]

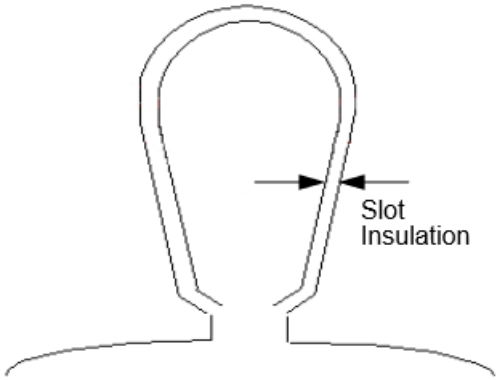

Figure 16: Slot Insulation of the Stator [19]

3.1.10. The Rotor of a BLDC machine is a stack of laminated steel stampings with permanent magnets on the periphery or embedded inside. The magnetic field of the stator coils react to the field of the rotor thereby resulting in a force causing rotary motion. The Rotor Data Properties Window is depicted in *Figure 17*. The general properties like Outer & Inner Diameter along with Length are user defined fields. The software describes various Steel Types and also has the option for user defined additions. The Stacking Factor is the measure of ratio of cross sectional area of all laminations to the area of steel which is varnish insulated. RMxprt supports five types of Pole Models, some of the Rotor Data Fields change or get inactive depending on the type of pole selected.

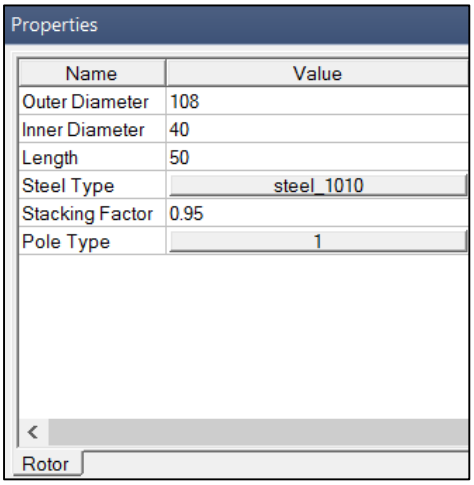

Figure 17: Rotor Data Properties Window

3.1.11. The Pole Properties Window is depicted in *Figure 18.* Embrace is defined as the ratio of actual pole arc distance to the maximum possible arc distance, the value is between 0 & 1 and is illustrated in *Figure 19*. Offset is the pole arc center offset from the rotor center (0 for uniform air gap). RMxprt describes many types of magnetic materials and has the option of adding new materials. Magnet Thickness field describes the maximum thickness of the magnet for all pole types.

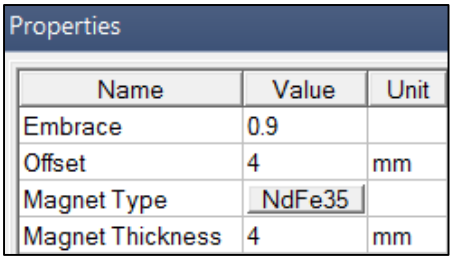

Figure 18: Pole Properties Window

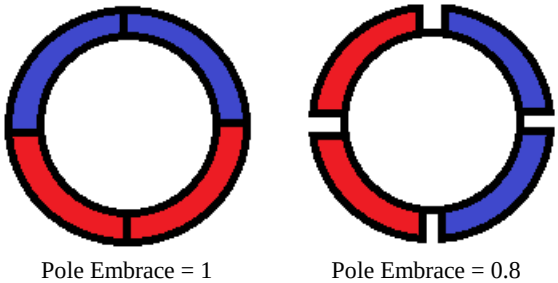

Figure 19: Pole Embrace

3.1.12. The Shaft Data Properties Window of the BLDC machine is depicted in *Figure 20.* The only input filed here is the Magnetic Shaft Checkbox which enable the shaft of the machine to be made of magnetic material.

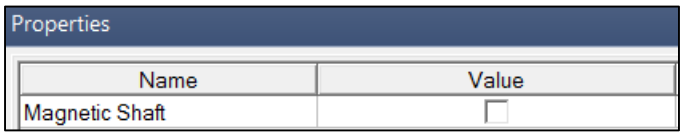

Figure 20: Shaft Properties Window

3.1.13. The Analysis Setup Window shown in *Figure 21* of the BLDC Motor in RMxprt is used to define the rated input/output parameters of the motor. The Operation Type is Motor in this case.

The Load Type can be,

1. Constant Speed – Speed of the motor is constant
2. Constant Power – Output power of motor is constant
3. Constant Torque – Torque remains constant regardless of speed ($T_{LOAD} = T_{RATED} = P_{OUT}/N_{RPM}$).
4. Linear Torque – Torque increases linearly with speed ($T_{LOAD} = T_{RATED} * N_{RPM}/N_{RATED}$)
5. Fan Load – The load varies non-linearly with speed ($T_{LOAD} = T_{RATED} * (N_{RPM}/N_{RATED})^2$)

The Rated Output Power field describes the power developed at the shaft of the motor. The Rated Voltage field represents the RMS line-to-line voltage. Rated Speed defines the output speed of the motor at which measurements are recorded. Operating Temperature, as the name suggests is for quantifying the functional temperature of the motor.

	Name	Value	Unit	Evaluated Value	Description
	Name	Setup1			
	Enabled	☑			
	Operation Type	Motor			Motor or generator
	Load Type	Const Power			Mechanical load type
	Rated Output Power	1500	W	1500W	Rated mechanical or electrical output power
	Rated Voltage	48	V	48V	Applied rated AC (RMS) or DC voltage (see circuit type)
	Rated Speed	500	rpm	500rpm	Given rated speed
	Operating Temperature	75	cel	75cel	Operating temperature

Figure 21: Analysis Setup Window

3.1.14. Solution Data: RMxprt is now ready & eligible to analyze the machine, the Solution Data is divided into three tabs Performance, Design Sheet and Curves, which are expanded in the following section

3.1.14.1. Performance - This contains a Data field with a drop-down menu (*Figure 22*) that allows you to view many different data tables, which vary with the machine type.

• Aux Winding • Full Load Operation • Material Consumption • No Load Operation • Permanent Magnet • Rotor Data • Rated Parameters • Stator Slot • Stator Winding • Steady State Parameters

3.1.14.2. Design Sheet - The file contains tables with information of the performance (*Figure 23*) depending on the machine type.

• General Data • Stator Data • Rotor Data • Permanent Magnet Data • Material Consumption • Rated Operation • No-Load Operation • Steady State Parameters • No Load Magnetic Data • Full Load Data • Winding Arrangement • Transient FEA Input Data

3.1.14.3. Curves - This displays the plots that were automatically generated by the solver (*Figure 24*).

• Input DC Current vs Speed • Efficiency vs Speed • Output Power vs Speed • Output Torque vs Speed • Cogging Torque in Two Teeth • Induced Coil Voltage at Rated Speed • Air Gap Flux Density • Induced Winding Phase Voltage at Rated Speed • Winding Currents under Load • Phase Voltage under Load

Figure 22: Efficiency v/s Speed

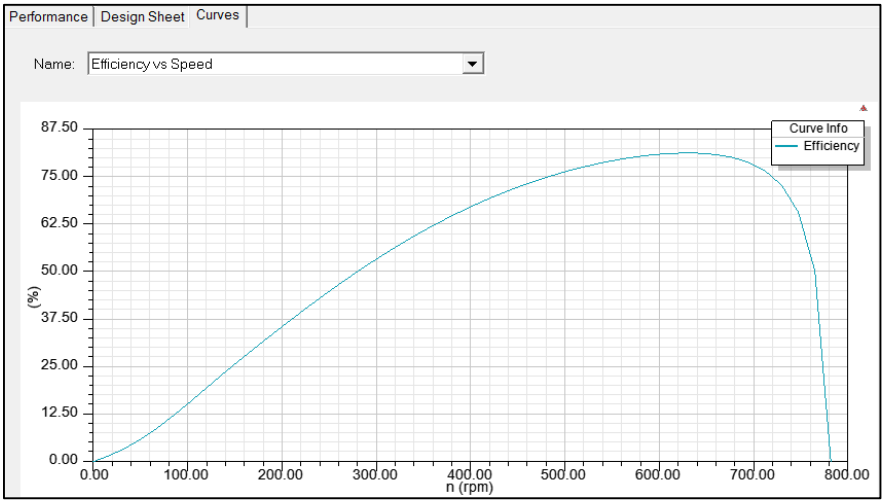

Figure 22: Stator Winding Performance

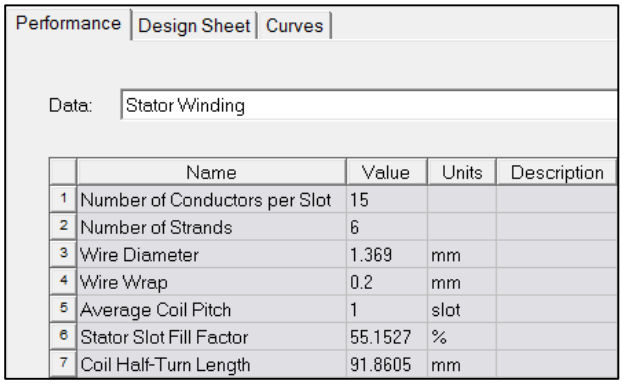

	Name	Value	Units	Description
1	Number of Conductors per Slot	15		
2	Number of Strands	6		
3	Wire Diameter	1.369	mm	
4	Wire Wrap	0.2	mm	
5	Average Coil Pitch	1	slot	
6	Stator Slot Fill Factor	55.1527	%	
7	Coil Half-Turn Length	91.8605	mm	

Figure 23: Full-Load data Design Sheet

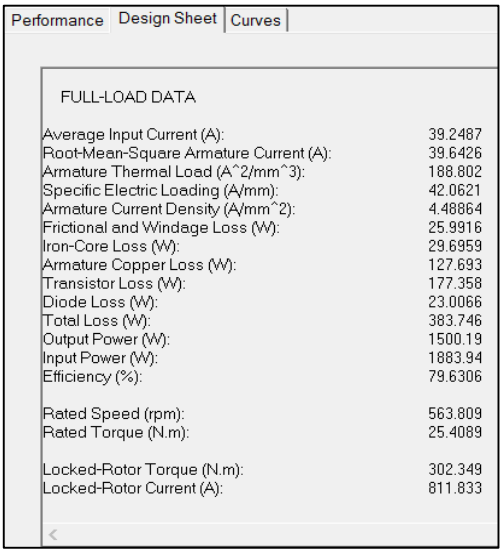

4. 1500 W, BLDC Machine Analytical Model

The machine is selected for the application of a high - power electric - bike. The first step in order to design the machine is to establish the objectives of the work according to the energy consumption and the performance of the vehicle for individual use.

The amount of power a vehicle needs in order to travel at a given speed can be approximately calculated by adding the resistances (Forces) it has to overcome. Three types of road resistances have to be taken into account. [20] [21]

1. Passive vehicle resistances

2. Resistances for overcoming the inertial forces of moving masses

3. Resistances given by the profile of the track

For dimensioning of the system, the inputs are as follows, the e-bike is assumed to travel at **40Km/Hr. (11.11m/s) at 0˚ slope**. Tabulated below (*Table 1)* are the approximate weights of the system.

Component	Weight (Kg)
Bicycle	20
Motor & Transmission	12
Control & Electronics	3
Battery	12
Cyclist	80
Total (m)	127 to 130

Table 1: System component weights

The resistances which must be considered for the dimensioning of the system are,

1. F_A - Air resistance/Aerodynamic drag
2. F_R - Rolling resistance
3. F_G - Climbing resistance/Gravity Force Component
4. F_M - Acceleration force

1. Air Resistance/Aerodynamic Drag $$F_A = C \times S \times \frac{\rho}{2} \times \left[\frac{{V_R}^2}{3.6^2}\right] \quad (1)$$

2. Rolling Resistance $$F_R = f m g \cos\alpha \quad (2)$$

3. Climbing Resistance $$F_G = m g \sin\alpha \quad (3)$$

4. Acceleration Force $$F_M = m\frac{dV}{dt} \quad (4)$$

Where,

- F – Force (N)
- C – Coefficient of air-resistance/Nose form factor
- S – Cross-Sectional Windward Area (m^2)
- ρ – Air Density (Kg/m^2)
- V_R – Velocity of the bike relative to the wind velocity (Km/Hr.)
- *f* – Coefficient of rolling-resistance
- *m* – Mass of the whole bike (Kg)
- *g* – Gravitational Constant (m/s^2)
- α – Slope angle/Climbing Angle (˚)
- V – Velocity of the bike (m/s)

4.1. Air Resistance/Aerodynamic Drag:

The motor must provide power to overcome the resistance provided by air. This power is influenced by the nose form factor (C) of the vehicle and its cross-sectional area (S).

Air density depends on the temperature and on atmospheric pressure. In European conditions, where the ambient temperature & pressure conditions vary from -25˚C to +40˚C and the pressure varies from 98.5 – 103.5 kPa, **air density ρ** can be taken as **1.326** Kg/m^2. Typical values of the nose form factor/coefficient of aerodynamic drag are tabulated below [20].

Vehicle Type	Nose form factor
One-track (bicycle/motor-cycle)	0.6 - 1.2
Passenger vehicle	0.25 - 0.4
Open passenger vehicle	0.5 - 0.65
Van	0.4 - 0.5
Motor-truck	0.8 - 1.0

Table 2: Nose Form Factor of Vehicle

The force to overcome aerodynamic drag can be calculated from equation (1) as:

$$\boldsymbol{F_A = \frac{(0.6 \times 0.5 \times 1.326)}{2}\left(\frac{40 \times 40}{3.6 \times 3.6}\right) = 24.55N}$$

1W is the power required by an object of 1Kg to accelerate at $1m/s^2$ through a distance of 1m in 1 second. W = Nm/s, therefore, the total watts needed are $\boldsymbol{P_A = 24.55 \times 11.11 = 272.75W.}$

4.2. Rolling Resistance:

The force required to overcome the resistance provided by grading of the track, is a function of the slope α & the normal component of the gravity force. For an e-bike traveling on a standard asphalt road on radial tyre the coefficient of **rolling resistance** is selected as $\boldsymbol{f = 0.0112}$. Some values for the coefficient of rolling resistance for different vehicles and road type are tabulated below. [20]

Wheel Type	**Road Type**	**Rolling-Resistance Coefficcient** $[N \cdot kN^{-1}][10^{-2}]$
Passenger vehicle Diagonal tyre Radial tyre	Asphalt track	 15 - 22 12 - 18
Motor-truck Diagonal tyre Radial tyre	Asphalt track	 10 - 15 8 - 12
Motor-truck	Terrain	150 - 200
Motor-truck / tractor	Ploughed Terrain	250 - 500
Rail vehicle	Rail	0.3 - 1

Table 3: Coefficients of Rolling Resistance

The force to overcome the rolling resistance can be calculated from equation (2) as,
$\boldsymbol{F_R = 0.0112 \times 130 \times 9.81 \times \cos 0 = 14.28N}$,
which in Watts is $\boldsymbol{P_R = 14.28 \times 11.11 = 158.68W.}$

4.3. Acceleration Force:

The reference acceleration of the vehicle can be calculated from the European drive cycle (Extra-Urban) shown below in the *(Figure 24).*

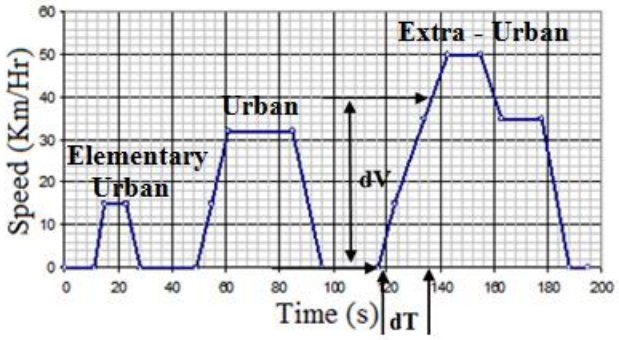

Figure 24: ECE+EUDC test cycle - also known as the MVEG-A cycle [22]

Hence, the acceleration can be calculated as $\boldsymbol{a = \frac{dV}{dt} = \frac{40000(m)}{3600(s) \times 16(s)} = 0.694\ m/s^2}$

The acceleration force is then calculated from equation (4) as
$\boldsymbol{F_M = m \times a = 0.694 \times 130 = 90.22N}$, which when multiplied by the e-bike speed in m/s gives us the total acceleration power $\boldsymbol{P_M = 11.11 \times 90.22 = 1002.34W.}$

4.4. Total Power:

The total power to keep the e-bike at 40Km/Hr. is given as the summation of resistances (W) which the motor has to overcome & is to be taken as the nominal power of the machine.

$$\boldsymbol{P_{Total} = P_A + P_R + P_M = 273 + 160 + 1003 = 1436W}$$

Hence, the total rated output power of the motor is selected as **1500W.**

4.5. Angular Velocity:

The angular velocity of the e-bike with a **700c/29er** wheel at **40Km/Hr.**, is the analytical rated Rpm of the motor & can be calculated as,

$$\boldsymbol{V_{rpm} = 9.549 \frac{V(m/s)}{r(m)} = 9.549 \times \frac{11.11}{0.311} = 341.12\ Rpm}$$

4.5. Torque:

The torque produced by the machine is a function of the angular velocity of the wheel and the output power of the motor which is expressed as follows,

$$\boldsymbol{T(Nm) = \frac{P(W)}{\omega\left(\frac{rad}{s}\right)} = \frac{1436}{\frac{2\pi \times 341.12(Rpm)}{60}} = 40.20Nm}$$

5. 1500W BLDC Outer Rotor Machine Electro-Magnetic Design

The above analytical (4) model will now be designed in accordance with the calculated rated input/output parameters the RMxprt module of ANSYS – Maxwell. For this purpose four variants of the 1500W, BLDC motor are designed and simulated in the software interface.

1. 24 Slots, 16 Pole BLDC machine
2. 36 Slots, 16 Pole BLDC machine
3. 48 Slots, 22 Pole BLDC machine
4. 72 Slots, 32 Pole BLDC machine

5.1. 24 Slot, 16 Pole BLDC Machine in ANSYS – Maxwell - RMxprt:

A 24 Slot, 16 Pole machine configuration is selected based on the optimum phase/pole/slot configurations mentioned in [15]. Its dimensioning will be discussed in the following sections.

5.1.1. Machine & Circuit:

The general machine and circuit parameters are as follows,

Parameter	Value	Unit
Number of Poles	16	
Frictional Loss	10	W
Windage Loss	20	W
Reference Speed	380	Rpm
Lead angle of trigger	0	°
Trigger Pulse Width	120	°
Transistor/Diode Drop	2	V

Table 4: General Machine & Circuit data

The friction and windage losses account to approximately 2% of the total out power capacity. The transistor and diode drop are usually neglected for power converter dimensioning but here their value impacts the efficiency significantly.

It is calculated as, $V_{DROP} = 0.6V + [\, I_{AVG} \times (R_{armature} + R_{diode})]$

5.1.2. Stator Dimensions:

Parameter	Value	Unit
Outer Diameter	180	mm
Inner Diameter	90	mm
Stacking Factor	0.95	
Length	50	mm
Steel Type	M100-23P	
Number of Slots	24	
Slot Type	4	
Skew Width	1	Slots

Table 5: Stator Data

5.1.2.1. Slot Design:

The selected slot type 4 in RMxprt is based on the research done by [14]. Its design are dimensions are depicted and tabulated below.

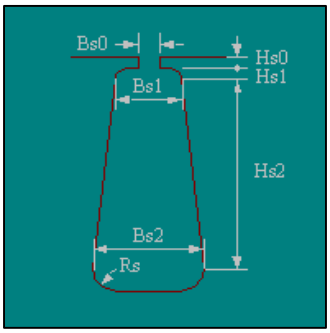

Figure 25: Slot Design (Type 4)

Parameter	Value	Unit
Hs0	3	mm
Hs1	3	mm
Hs2	30	mm
Bs0	3	mm
Bs1	16	mm
Bs2	8	mm
Rs	0.6	mm

Table 6: Slot Dimensions

Parameter	Value	Unit
End Extension	4	mm
Base Inner Radius	0.5	mm
Tip Inner Diameter	1	mm
End Clearance	1	mm
Slot Liner	0.5	mm
Wedge Thickness	0.3	mm
Layer Insulation	0.1	mm
Limited Fill Factor	0.75	

Table 7: End/Insulation Data

5.1.2.2. Winding Design:

The stator winding data & geometry is depicted and tabulated below, while the end/insulation data is depicted above the aim of the design is to minimize the armature copper losses while keeping the stator slot fill factor in practical limits.

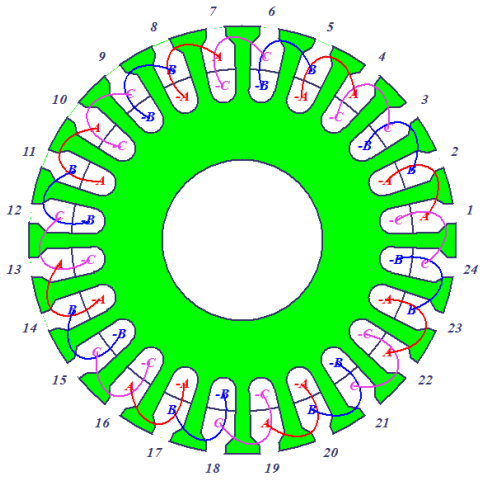

Figure 26: Stator Winding

Parameter	Value	Unit
Winding Layers	2	
Winding Type	Whole Coiled	
Parallel Branches	1	
Conductors per slots	18	
Coil Pitch	1	
Number of Strands	5	
Wire Wrap	0.2	mm
Wire Size (Diameter)	1.369	mm

Table 8: Winding Data

5.1.3. Rotor Dimensions:

The general data for the machine rotor is tabulated below,

Parameter	Value	Unit
Outer Diameter	200	mm
Inner Diameter	182	mm
Stacking Factor	0.95	
Length	50	mm
Steel Type	M100-23P	
Pole Type	1	

Table 9: General Rotor Data

Due to the outer rotor geometry of the BLDC machine only pole type 1 is allowed for analysis depicted below in *Figure 27.*

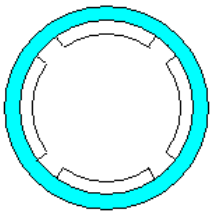

Pole Type 1

Figure 27: Pole Shape 1 in ANSYS – Maxwell RMxprt.

5.1.3.1. Pole Data:

The pole data is tabulated below,

Parameter	Value	Unit
Embrace	0.9	
Offset	4	mm
Magnet Type	NdFeB	
Magnet Thickness	4	mm

Table 10: Pole Data

5.1.4. Analysis Setup:

The machine's rated operating state input/output parameters are tabulated below,

Parameter	Value	Unit
Load Type	Constant Power	
Rated Output Power	1500	W
Rated Voltage	48	V
Rated Speed	380	Rpm
Operating Temperature	75	˚C

Table 11: Analysis Setup

5.1.5. Solution Data:

RMxprt provides an entire range of data types and variables, some important output parameters and plots are described below.

Parameter	Value	Unit
Armature Current (RMS)	36.23	A
Total Loss	324.78	W
Output Power	1500.2	W
Input Power	1825	W
Efficiency	82.20	%
Rated Speed	359	Rpm
Rated Torque	39.92	Nm
Total Net Weight	7.30	Kg
Total Steel Consumption	15.3	Kg
No-Load Speed	465.25	Rpm
Residual Flux Density(Rotor)	1.23	T
Minimum Air-Gap	1	mm
Stator Slot Fill Factor	60.32	%
Stator Winding Factor	0.86	
Single Phase Resistance	0.030	Ω
Time Constant	0.005	s
Back EMF Constant (K_E)	0.908	V/rad
Rated Torque Constant	1.06	Nm/A
Armature Current Density	4.92	A/mm^2
Locked Rotor Torque	665	Nm
Locked Rotor Current	732	A
Stator Teeth Flux Density	3.95	T

Table 12: Solution Data of 24 Slot, 16 Pole, 1500W Motor

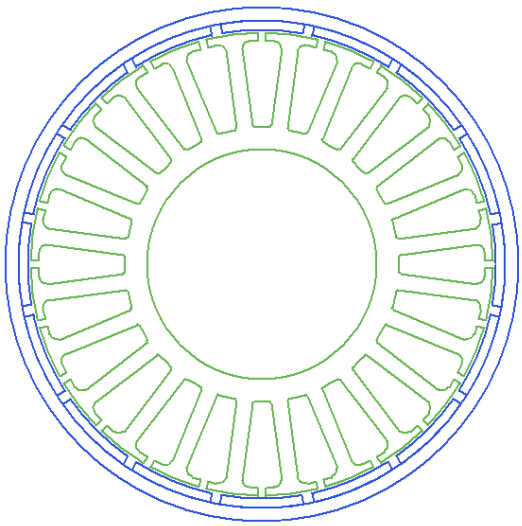

Figure 28: 24 Slot, 16 Pole BLDC Motor Cross - Section

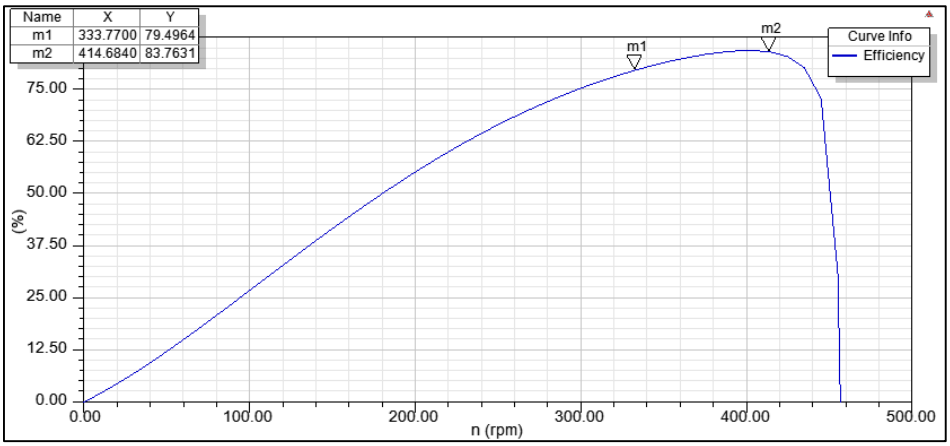

Figure 29: Efficiency (%) V/s Speed (Rpm)

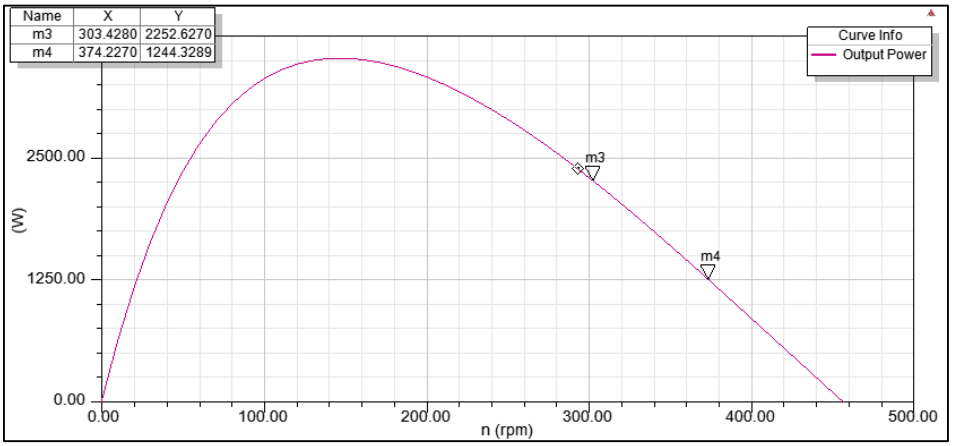

Figure 30: Output Power (W) V/s Speed (Rpm)

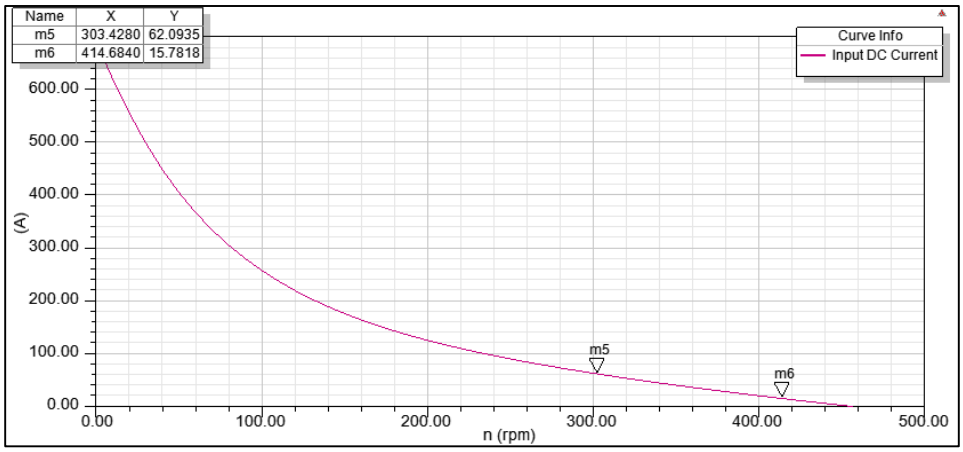

Figure 31: Input DC Current (A) V/s Speed (Rpm)

5.2. 36 Slot, 18 Pole BLDC Machine in ANSYS – Maxwell - RMxprt:

The text below describes the RMxprt design of a 36 Slot, 18 Pole based on configuration described in [15].

5.2.1. Machine & Circuit:

The general machine and circuit parameters are as follows,

Parameter	Value	Unit
Number of Poles	16	
Frictional Loss	10	W
Windage Loss	20	W
Reference Speed	380	Rpm
Lead angle of trigger	0	°
Trigger Pulse Width	120	°
Transistor/Diode Drop	2	V
Circuit Type	Y3	

Table 13: General Machine & Circuit data

Delta connection is not recommended in a brushless PM machine. If there is any third time harmonic in the phase back EMF, then this will induce a circulating zero- order current. This will cause excessive current and copper losses and potential burnout of the winding. [9]

5.2.2. Stator Dimensions:

The general data for the stator is tabulated below.

Parameter	Value	Unit
Outer Diameter	220	mm
Inner Diameter	130	mm
Stacking Factor	0.95	
Length	50	mm
Steel Type	M100-23P	
Number of Slots	36	
Slot Type	4	
Skew Width	1	Slots

Table 14: General Stator Data

5.2.2.1. Slot Design:

The selected slot type 4 in RMxprt is based on the research done by [14]. Its design are dimensions are depicted and tabulated below.

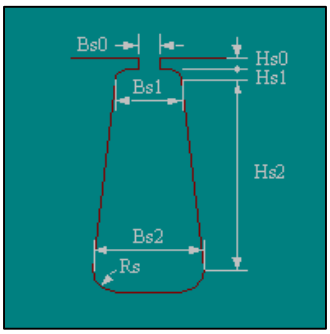

Figure 32: Slot Design (Type 4)

Parameter	Value	Unit
Hs0	3	mm
Hs1	3	mm
Hs2	30	mm
Bs0	3	mm
Bs1	13	mm
Bs2	8	mm
Rs	0.6	mm

Table 15: Slot Dimensions

5.2.2.2. Winding Design:

The stator winding data and geometry along with its end terminations and insulations is depicted and tabulated below, the aim of the design is to minimize the armature copper losses while keeping the stator slot fill factor in practical limits.

Parameter	Value	Unit
Winding Layers	2	
Winding Type	Whole Coiled	
Parallel Branches	1	
Conductors per slots	12	
Coil Pitch	1	
Number of Strands	6	
Wire Wrap	0.2	mm
Wire Size (Diameter)	1.369	mm

Table 16: Winding Data

Parameter	Value	Unit
End Extension	4	mm
Base Inner Radius	0.5	mm
Tip Inner Diameter	1	mm
End Clearance	1	mm
Slot Liner	0.5	mm
Wedge Thickness	0.3	mm
Layer Insulation	0.1	mm
Limited Fill Factor	0.75	

Table 17: End/Insulation Data

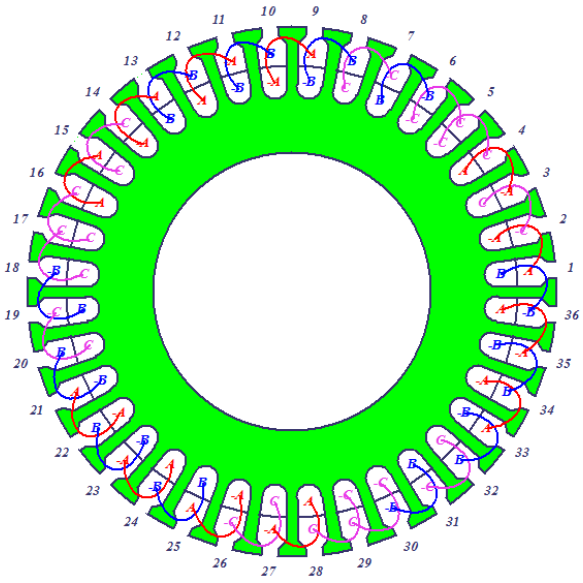

Figure 33: Stator Winding

5.2.3. Rotor Dimensions:

The general data for the machine rotor is tabulated below,

Parameter	Value	Unit
Outer Diameter	240	mm
Inner Diameter	222	mm
Stacking Factor	0.95	
Length	50	mm
Steel Type	M100-23P	
Pole Type	1	

Table 18: General Rotor Data

Due to the outer rotor geometry of the BLDC machine only pole type 1 is allowed for analysis.

5.2.3.1. Pole Data:

The pole data is tabulated below,

Parameter	Value	Unit
Embrace	0.9	
Offset	4	mm
Magnet Type	NdFeB	
Magnet Thickness	4	mm

Table 19: Pole Data

5.2.4. Analysis Setup:

The machine's rated operating state input/output parameters are tabulated below,

Parameter	Value	Unit
Load Type	Constant Power	
Rated Output Power	1500	W
Rated Voltage	48	V
Rated Speed	380	Rpm
Operating Temperature	75	˚C

Table 20: Analysis Setup

5.2.5. Solution Data:

The important output parameters and plots are described below.

Parameter	Value	Unit
Armature Current (RMS)	32.67	A
Total Loss	274.93	W
Output Power	1500.22	W
Input Power	1775.21	W
Efficiency	84.50	%
Rated Speed	408.38	Rpm
Rated Torque	35.07	Nm
Total Net Weight	9.23	Kg
Total Steel Consumption	22.1	Kg
No-Load Speed	473.53	Rpm
Residual Flux Density(Rotor)	1.23	T
Minimum Air-Gap	1	mm
Stator Slot Fill Factor	61	%
Stator Winding Factor	0.61	
Single Phase Resistance	0.025	Ω
Time Constant	0.0038	s
Back EMF Constant (K_E)	0.892	V/rad
Rated Torque Constant	0.971	Nm/A
Armature Current Density	3.7	A/mm^2
Locked Rotor Torque	798	Nm
Locked Rotor Current	894	A
Stator Teeth Flux Density	3.80	T

Table 21: Solution Data of 36 Slot, 16 Pole, 1500W Motor

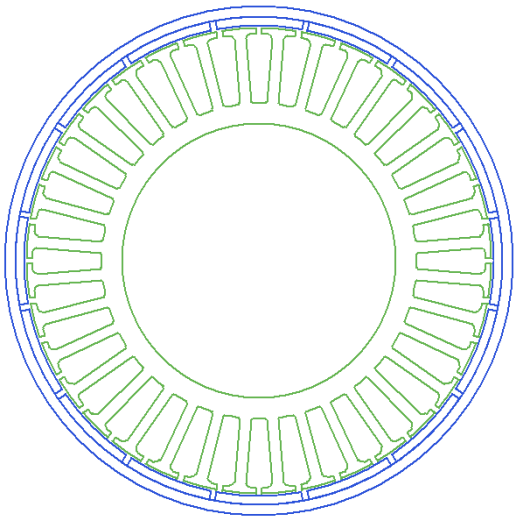

Figure 34: 36 Slot, 16 Pole, Motor Cross - Section

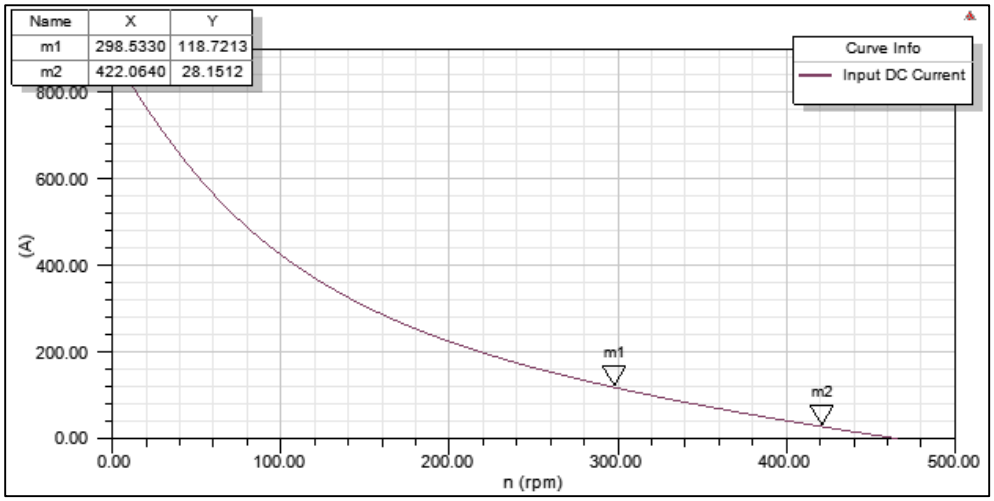

Figure 35: Input DC Current (A) V/s Speed (Rpm)

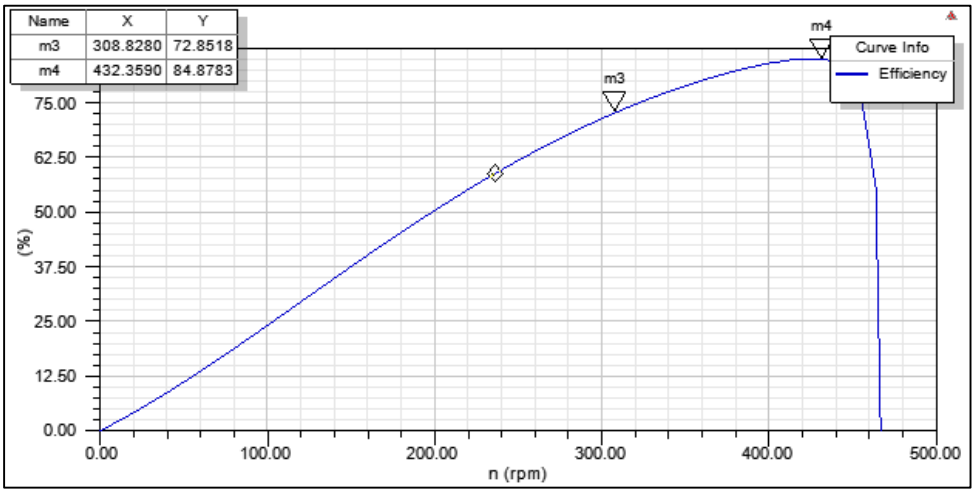

Figure 36: Efficiency (%) V/s Speed (Rpm)

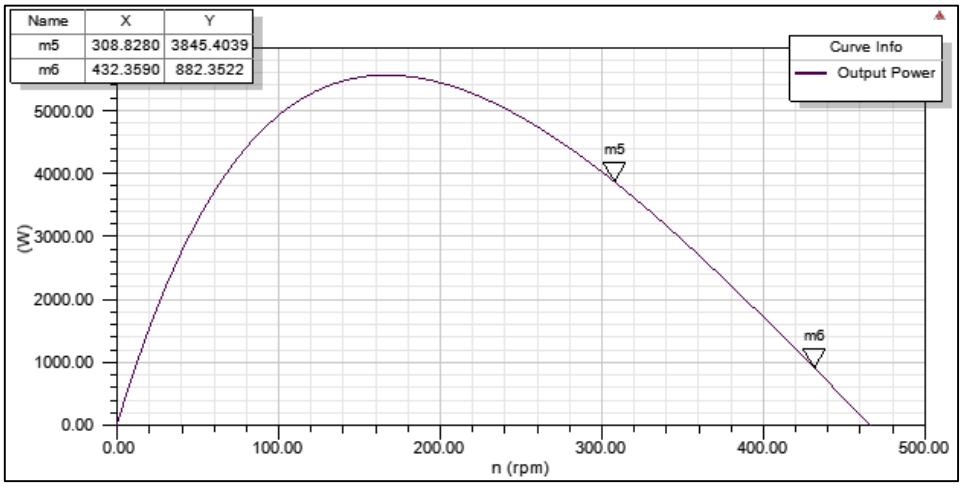

Figure 37: Output Power (W) V/s Speed (Rpm)

5.3. 48 Slot, 22 Pole BLDC Machine in ANSYS – Maxwell - RMxprt:

The text below describes the RMxprt design of a 48 Slot, 22 Pole with the aim to maximize performance at rated parameters. [15].

5.3.1. Machine & Circuit:

The general machine and circuit parameters are as follows,

Parameter	Value	Unit
Number of Poles	22	
Frictional Loss	10	W
Windage Loss	20	W
Reference Speed	380	Rpm
Lead angle of trigger	0	°
Trigger Pulse Width	120	°
Transistor/Diode Drop	2	V
Circuit Type	Y3	

Table 21: General Machine & Circuit data

5.3.2. Stator Dimensions:

The general data for the stator is tabulated below.

Parameter	Value	Unit
Outer Diameter	240	mm
Inner Diameter	140	mm
Stacking Factor	0.95	
Length	50	mm
Steel Type	M100-23P	
Number of Slots	48	
Slot Type	4	
Skew Width	1	Slots

Table 22: General Stator Data

5.3.2.1. Slot Design:

The selected slot type 4 in RMxprt is based on the research done by [14]. Its design are dimensions are depicted and tabulated below.

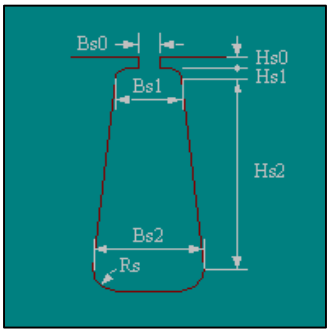

Figure 38: Slot Design (Type 4)

Parameter	Value	Unit
Hs0	2	mm
Hs1	2	mm
Hs2	30	mm
Bs0	3	mm
Bs1	10	mm
Bs2	6	mm
Rs	0.5	mm

Table 23: Slot Dimensions

5.3.2.2. Winding Design:

The stator winding data and geometry along with its end terminations and insulations is depicted and tabulated below, the coil pitch is kept minimum to reduce eddy current losses and end extensions.

Parameter	Value	Unit
Winding Layers	2	
Winding Type	Whole Coiled	
Parallel Branches	1	
Conductors per slots	9	
Coil Pitch	1	
Number of Strands	6	
Wire Wrap	0.2	mm
Wire Size (Diameter)	1.369	mm

Table 24: Winding Data

Parameter	Value	Unit
End Extension	5	mm
Base Inner Radius	1.2	mm
Tip Inner Diameter	2	mm
End Clearance	2	mm
Slot Liner	0.7	mm
Wedge Thickness	0.3	mm
Layer Insulation	0.1	mm
Limited Fill Factor	0.75	

Table 25: End/Insulation Data

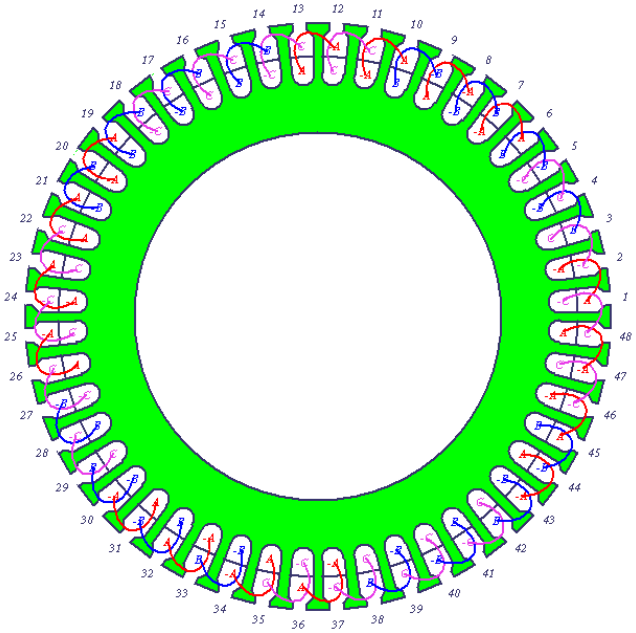

Figure 39: Stator Winding

5.3.3. Rotor Dimensions:

The general data for the machine rotor is tabulated below,

Parameter	Value	Unit
Outer Diameter	262	mm
Inner Diameter	242	mm
Stacking Factor	0.95	
Length	50	mm
Steel Type	M100-23P	
Pole Type	1	

Table 26: General Rotor Data

Due to the outer rotor geometry of the BLDC machine only pole type 1 is allowed for analysis.

5.3.3.1. Pole Data:

The pole data is tabulated below,

Parameter	Value	Unit
Embrace	0.9	
Offset	4	mm
Magnet Type	NdFeB	
Magnet Thickness	4	mm

Table 27: Pole Data

5.3.4. Analysis Setup:

The machine's rated operating state input/output parameters are tabulated below,

Parameter	Value	Unit
Load Type	Constant Power	
Rated Output Power	1500	W
Rated Voltage	48	V
Rated Speed	380	Rpm
Operating Temperature	75	˚C

Table 28: Analysis Setup

5.3.5. Solution Data:

The important output parameters and plots are described below.

Parameter	Value	Unit
Armature Current (RMS)	32.22	A
Total Loss	265	W
Output Power	1500	W
Input Power	1765	W
Efficiency	84.98	%
Rated Speed	378.86	Rpm
Rated Torque	37.81	Nm
Total Net Weight	11.57	Kg
Total Steel Consumption	25.2	Kg
No-Load Speed	434.64	Rpm
Residual Flux Density(Rotor)	1.23	T
Minimum Air-Gap	1	mm
Stator Slot Fill Factor	68.72	%
Stator Winding Factor	0.63	
Single Phase Resistance	0.025	Ω
Time Constant	0.0022	s
Back EMF Constant (K_E)	0.97	V/rad
Rated Torque Constant	1.04	Nm/A
Armature Current Density	3.64	A/mm^2
Locked Rotor Torque	864.32	Nm
Locked Rotor Current	888.61	A
Stator Teeth Flux Density	3.1	T

Table 29: Solution Data of 48 Slot, 22 Pole, 1500 W Motor

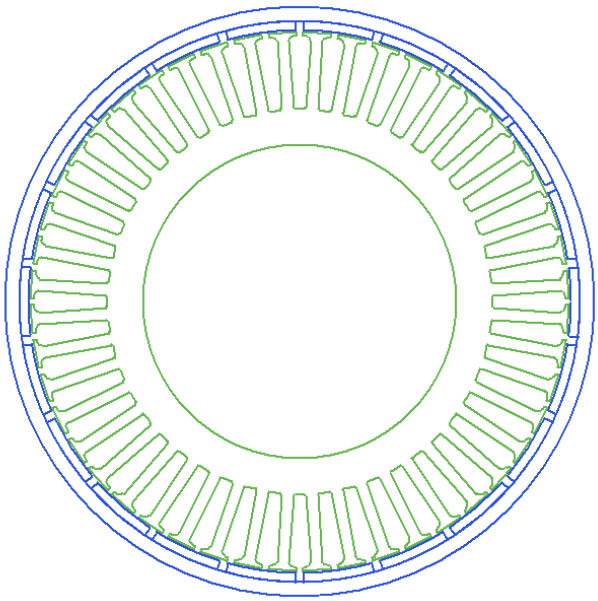

Figure 40: 48 Slot, 22 Pole Motor Cross - Section

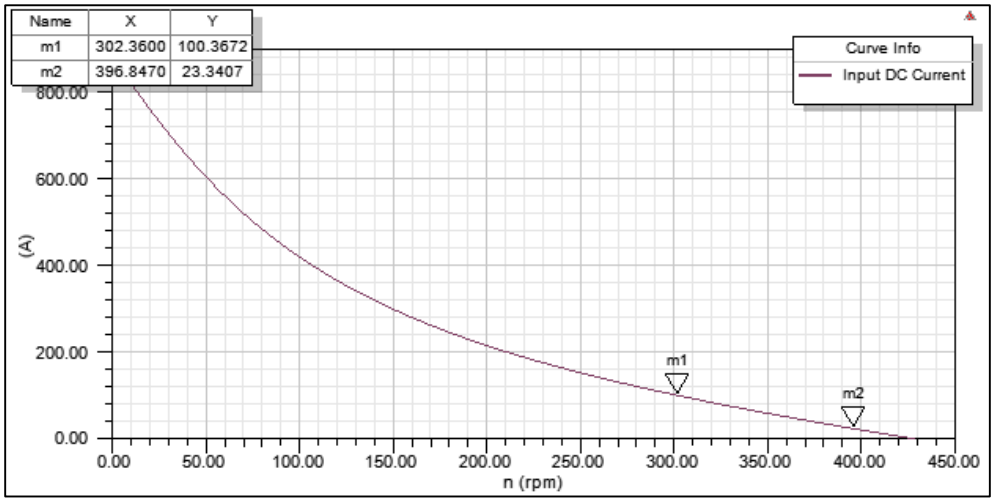

Figure 41: Input DC Current (A) V/s Speed (Rpm)

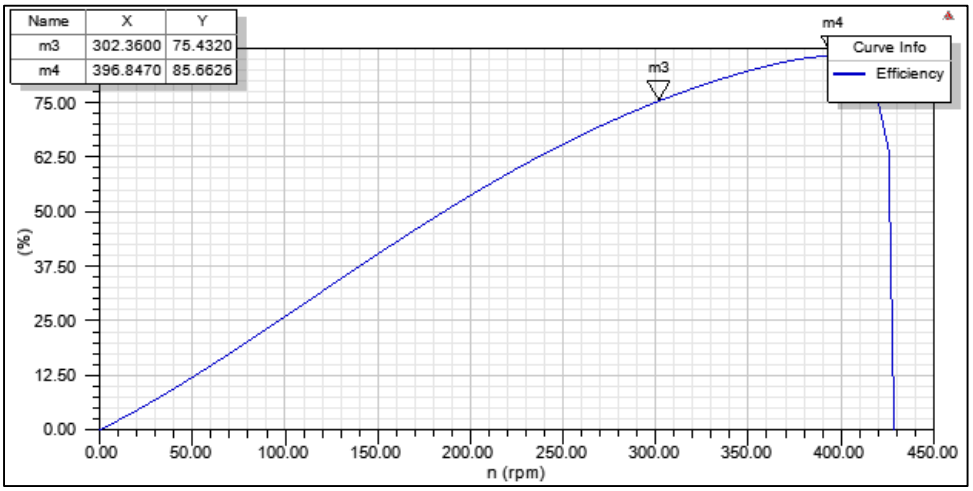

Figure 42: Efficiency (%) V/s Speed (Rpm)

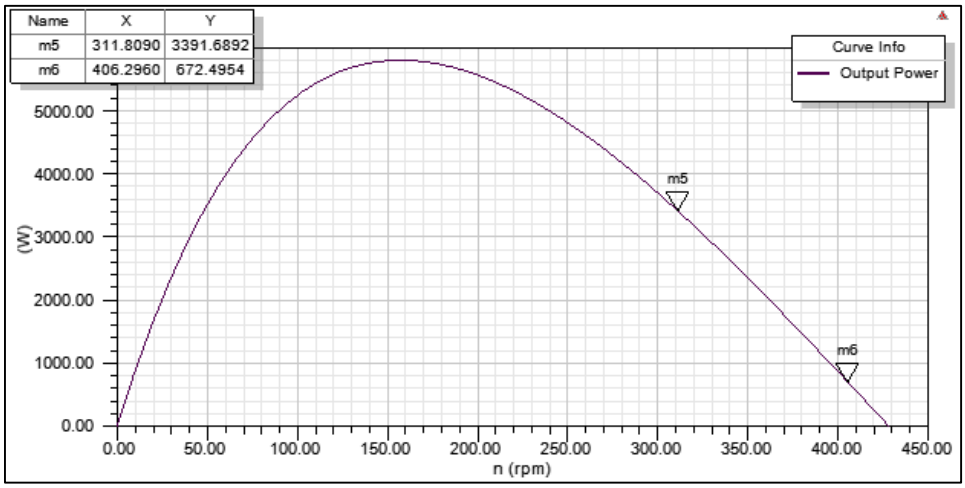

Figure 43: Output Power (W) V/s Speed (Rpm)

5.4. 72 Slot, 32 Pole BLDC Machine in ANSYS – Maxwell - RMxprt:

The text below describes the RMxprt dimensions of a 72 Slot, 32 Pole with the aim to maximize performance at rated parameters. [15].

5.4.1. Machine & Circuit:

The general machine and circuit parameters are as follows,

Parameter	Value	Unit
Number of Poles	32	
Frictional Loss	10	W
Windage Loss	20	W
Reference Speed	380	Rpm
Lead angle of trigger	0	°
Trigger Pulse Width	120	°
Transistor/Diode Drop	2	V
Circuit Type	Y3	

Table 30: General Machine & Circuit data

5.4.2. Stator Dimensions:

The general data for the stator is tabulated below.

Parameter	Value	Unit
Outer Diameter	270	mm
Inner Diameter	180	mm
Stacking Factor	0.95	
Length	47	mm
Steel Type	M100-23P	
Number of Slots	72	
Slot Type	4	
Skew Width	1	Slots

Table 31: General Stator Data

5.4.2.1. Slot Design:

The selected slot type 4 in RMxprt is based on the research done by [14]. The design is based on the commercial products out in the market during recent times which are depicted and tabulated below.

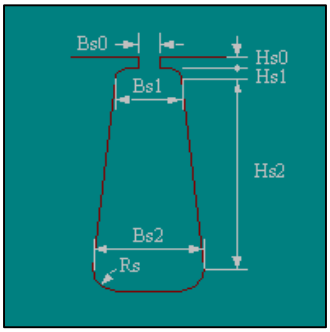

Figure 44: Slot Design (Type 4)

Parameter	Value	Unit
Hs0	2.5	mm
Hs1	1	mm
Hs2	30	mm
Bs0	3	mm
Bs1	8	mm
Bs2	5.3	mm
Rs	0.5	mm

Table 32: Slot Dimensions

5.4.2.2. Winding Design:

The stator winding data and geometry along with its end terminations and insulations is depicted and tabulated below, the coil pitch is kept minimum to reduce the eddy current losses & end extensions

Parameter	Value	Unit
Winding Layers	2	
Winding Type	Whole Coiled	
Parallel Branches	1	
Conductors per slots	6	
Coil Pitch	1	
Number of Strands	6	
Wire Wrap	0.2	mm
Wire Size (Diameter)	1.369	mm

Table 33: Winding Data

Parameter	Value	Unit
End Extension	3	mm
Base Inner Radius	0.5	mm
Tip Inner Diameter	1	mm
End Clearance	1.1	mm
Slot Liner	0.5	mm
Wedge Thickness	0.2	mm
Layer Insulation	0.1	mm
Limited Fill Factor	0.75	

Table 34: End/Insulation Data

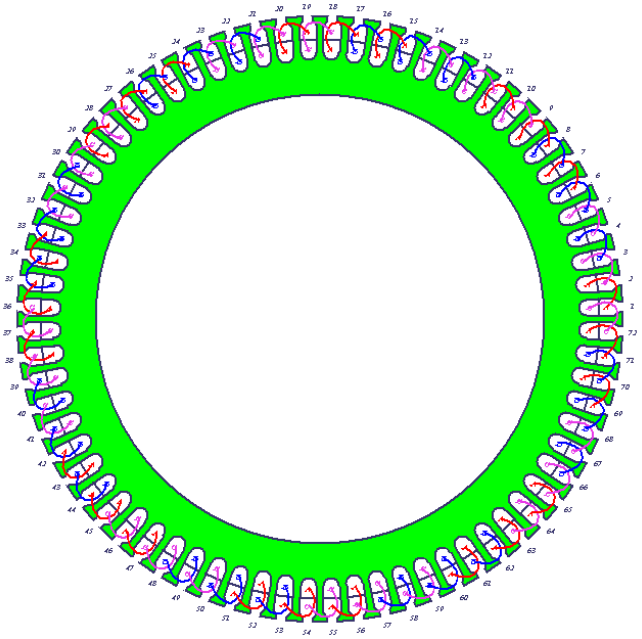

Figure 45: Stator Winding

5.4.3. Rotor Dimensions:

The general data for the machine rotor is tabulated below,

Parameter	Value	Unit
Outer Diameter	290	mm
Inner Diameter	272	mm
Stacking Factor	0.95	
Length	47	mm
Steel Type	M100-23P	
Pole Type	1	

Table 35: General Rotor Data

Due to the outer rotor geometry of the BLDC machine only pole type 1 is allowed for analysis.

5.4.3.1. Pole Data:

The pole data is tabulated below,

Parameter	Value	Unit
Embrace	0.9	
Offset	0	mm
Magnet Type	NdFeB	
Magnet Thickness	4	mm

Table 36: Pole Data

5.4.4. Analysis Setup:

The machine's rated operating state input/output parameters are tabulated below,

Parameter	Value	Unit
Load Type	Constant Power	
Rated Output Power	1500	W
Rated Voltage	48	V
Rated Speed	380	Rpm
Operating Temperature	75	˚C

Table 37: Analysis Setup

5.4.5. Solution Data:

The important output parameters and plots are described below.

Parameter	Value	Unit
Armature Current (RMS)	31.57	A
Total Loss	248.33	W
Output Power	1500	W
Input Power	1748	W
Efficiency	85.79	%
Rated Speed	376	Rpm
Rated Torque	38.10	Nm
Total Net Weight	10.40	Kg
Total Steel Consumption	31.1	Kg
No-Load Speed	422.83	Rpm
Residual Flux Density(Rotor)	1.23	T
Minimum Air-Gap	1	mm
Stator Slot Fill Factor	53.92	%
Stator Winding Factor	0.61	
Single Phase Resistance	0.021	Ω
Time Constant	0.0012	s
Back EMF Constant (K_E)	1	V/rad
Rated Torque Constant	1.06	Nm/A
Armature Current Density	3.57	A/mm^2
Locked Rotor Torque	1024	Nm
Locked Rotor Current	1024	A
Stator Teeth Flux Density	3.43	T

Table 38: Solution Data of 72 Slot, 32 Pole, 1500 W Motor

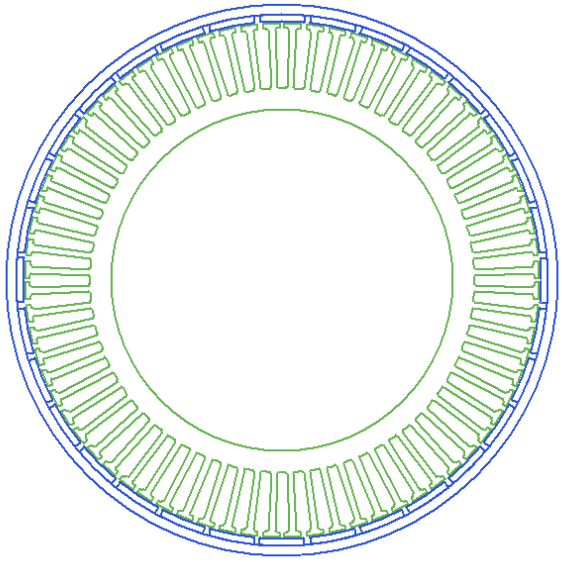

Figure 46: 72 Slot, 32 Pole Motor Cross – Section

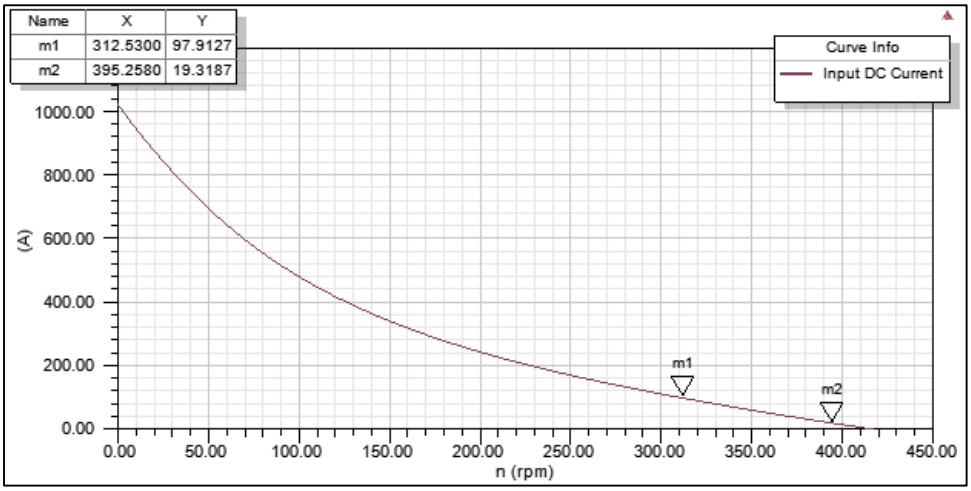

Figure 47: Input DC Current (A) V/s Speed (Rpm)

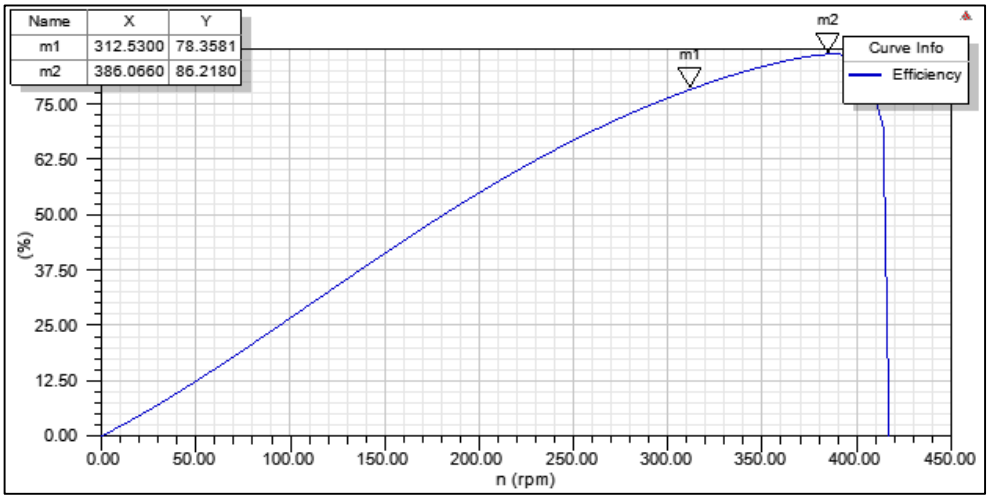

Figure 48: Efficiency (%) V/s Speed (Rpm)

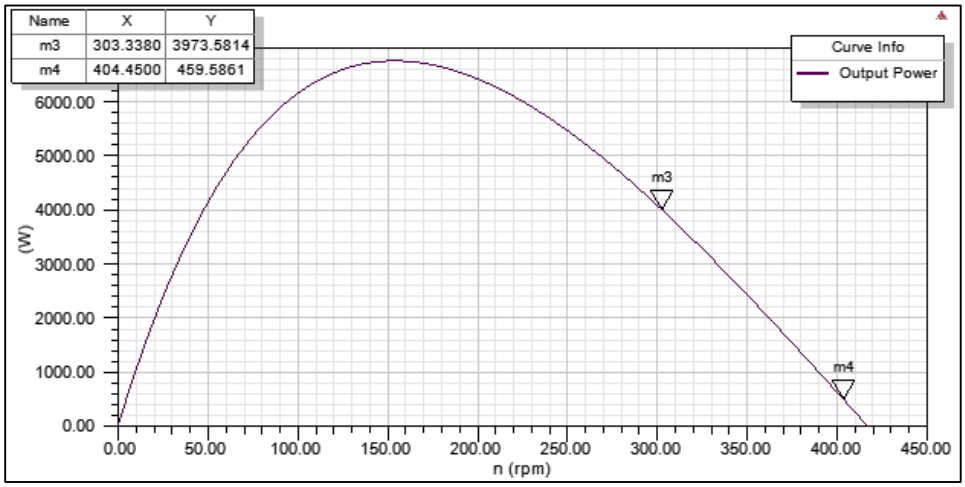

Figure 49: Output Power (W) V/s Speed (Rpm)

6. 1500 W, BLDC Machine 2D/3D design in Maxwell – RMxprt module:

The analyzed model of RMxprt can now be exported to create Maxwell 2D/3D models that include FE mesh modeling algorithms to solve the machine's Magneto Static and Transient equations along with an external electronic circuit editor called Simplorer, to integrate the machine & the power convertor, which decides its excitation and there by operating performance.

Shown below *(Figure 50)* is the external excitation circuit which is modelled automatically in the software and is used for magneto static and transient analysis. The solid state diodes and switches are considered by a modelling window where the user can input data like contact resistance, emission coefficient, barrier height, reverse breakdown voltage and current. The switch model includes variable inputs like on/off state resistance and control voltages.

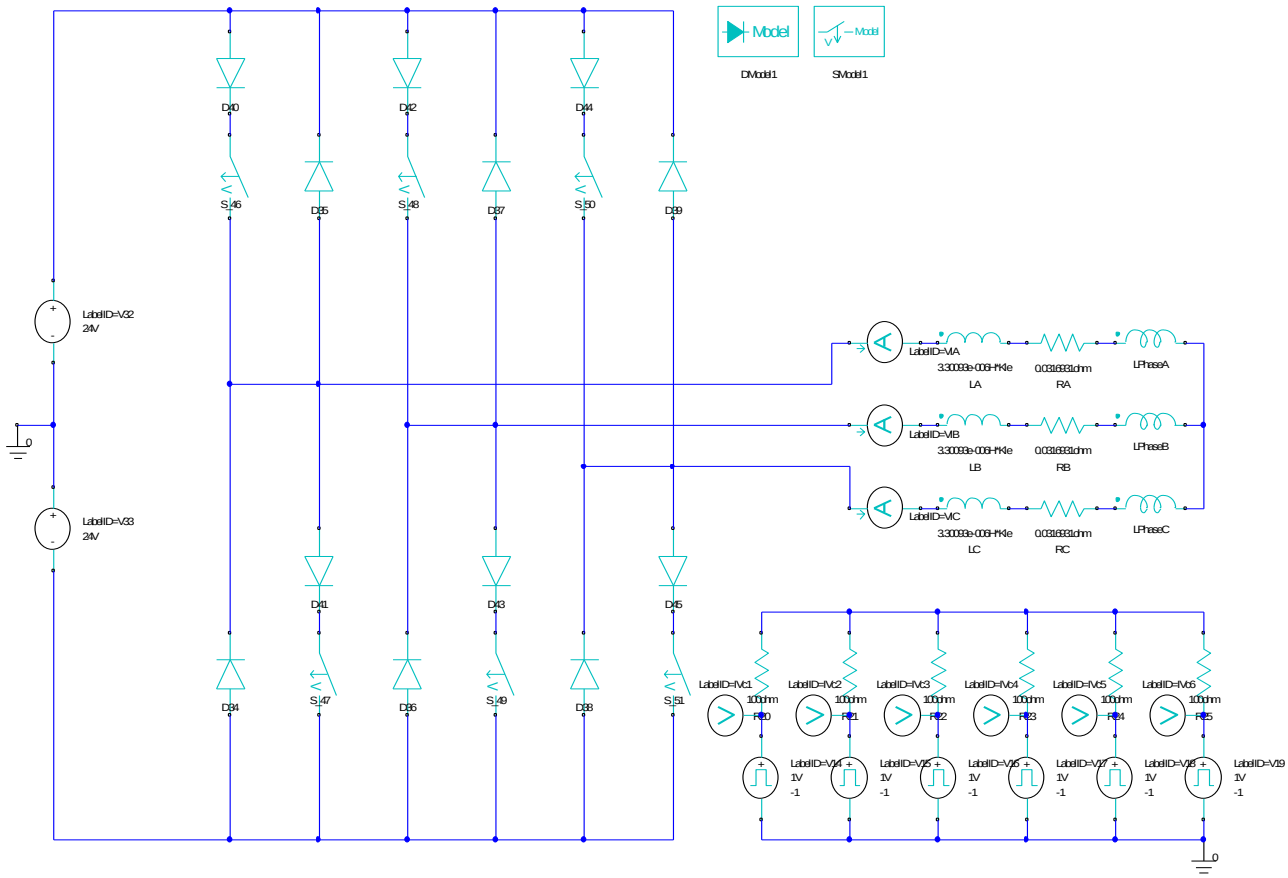

Figure 50: ANSYS – Simplorer Excitation Circuit

The eddy current effects were neglected in the above excitation scheme due to single coil pitch winding.

6.1. 24 Slot, 16 Pole Machine 2D Model in ANSYS – Maxwell - RMxprt:

Depicted below is the 2D model along with its FE mesh plot of the machine, the grey sections are Electric Steel, the green sections are Permanent Magnets, while the golden ones are copper conductors.

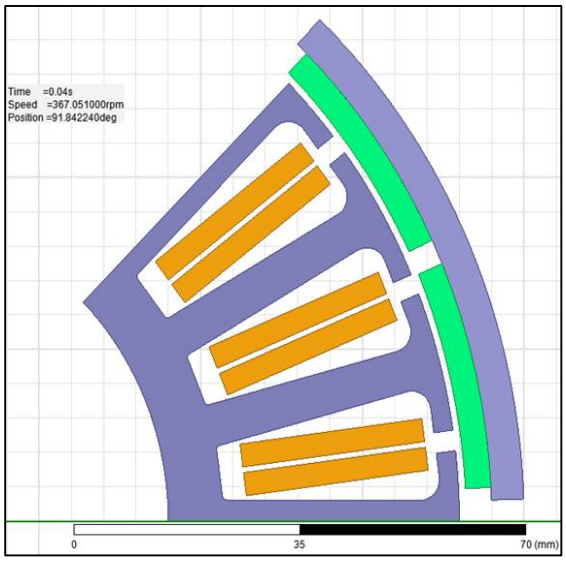

Figure 51: 2D Machine Cross - Section

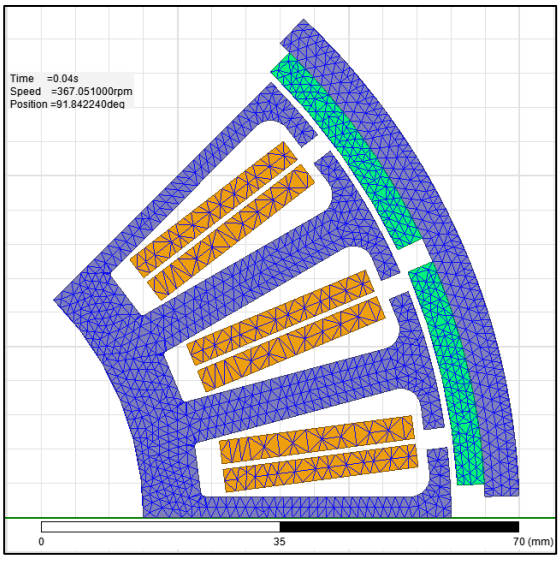

Figure 52: 2D Mesh Plot

6.1.1. Results and Field Overlays:

Before analyzing the 2D design it is important to apply and plot mesh operations along with integration of external excitation circuit. Shown below are the plots for Moving Torque and Winding Currents v/s time.

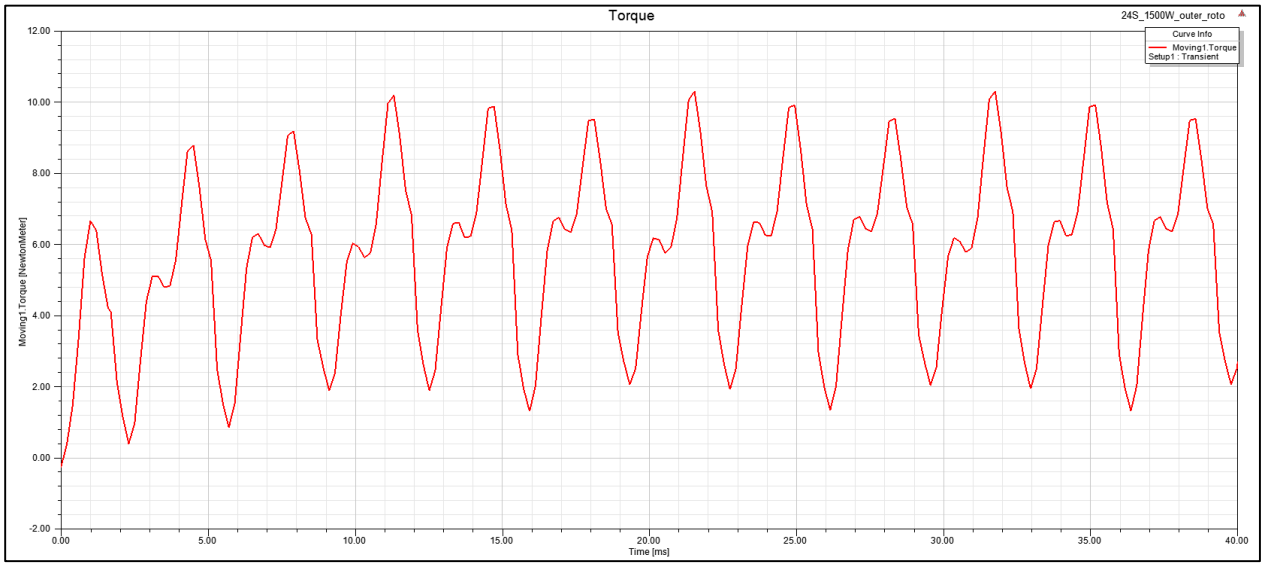

Figure 53: Moving Torque (Nm) V/s Time (ms)

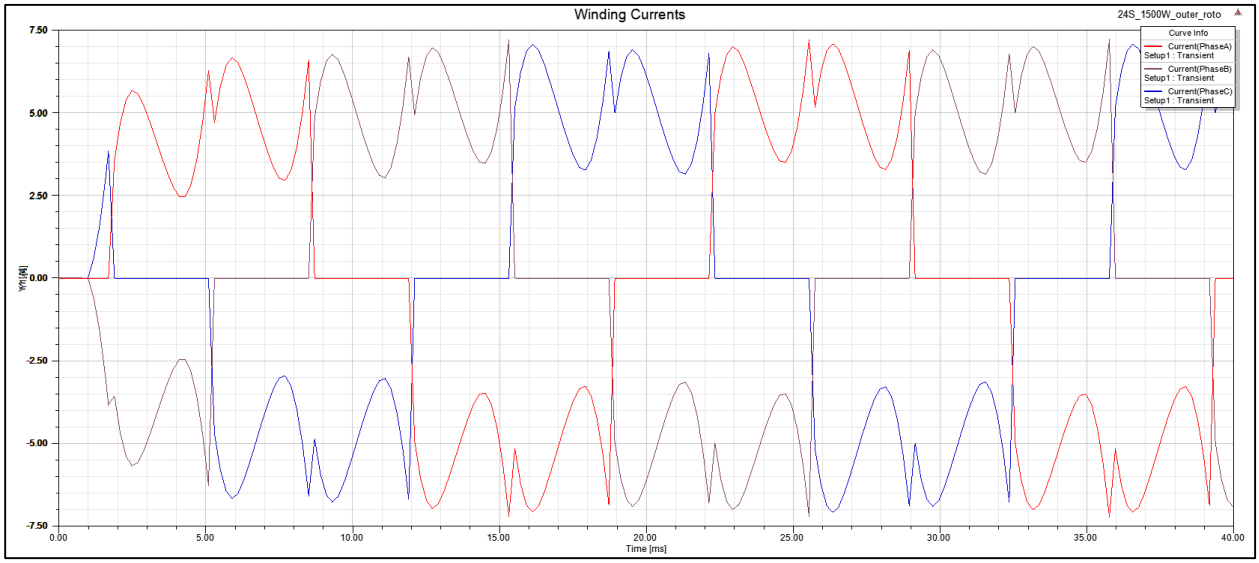

Figure 54: Winding Currents (A) V/s Time (ms).

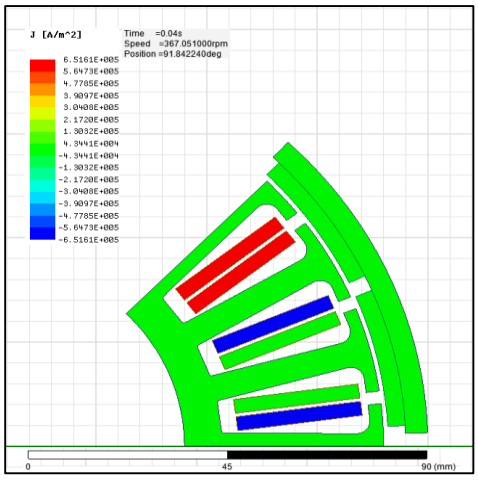

Figure 55: Electric Current Density (A/m^2)

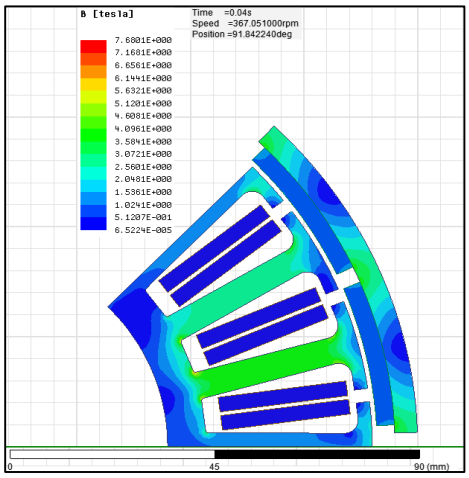

Figure 56: Magnetic Field Strength (T)

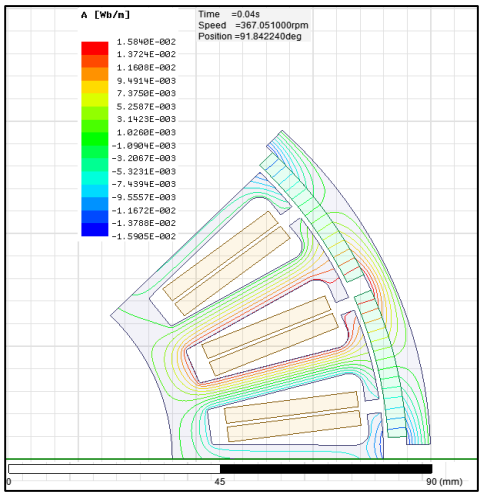

Figure 57: Flux Lines (Wb/m)

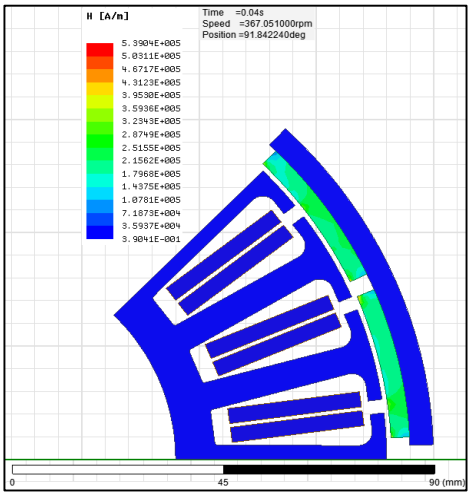

Figure 58: Magnetic Field Strength (A/m)

6.2. 36 Slot, 16 Pole Machine 2D Model in ANSYS – Maxwell – RMxprt:

Depicted below is the 2D model along with its FE mesh plot of the machine, the grey sections are Electric Steel, the green sections are Permanent Magnets, while the golden ones are copper conductors.

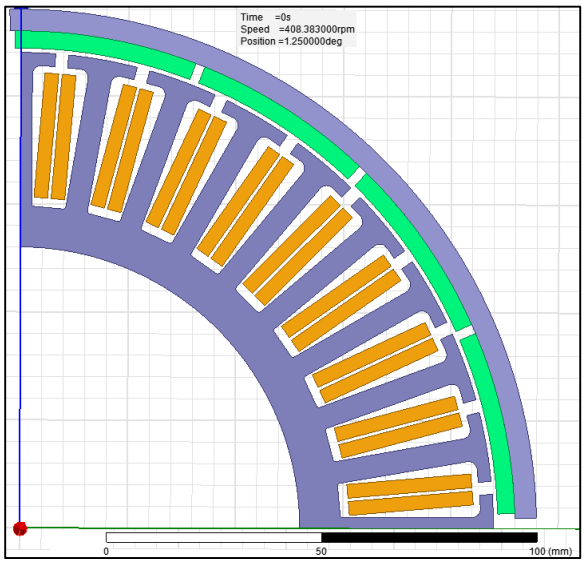

Figure 59: 2D Machine Cross - Section

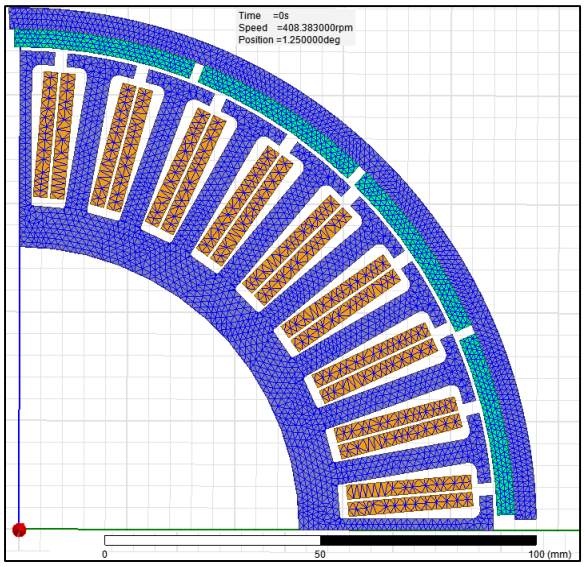

Figure 60: 2D Mesh Plot

6.2.1. Results and Field Overlays:

Shown below are the plots for Moving Torque and Winding Currents v/s time.

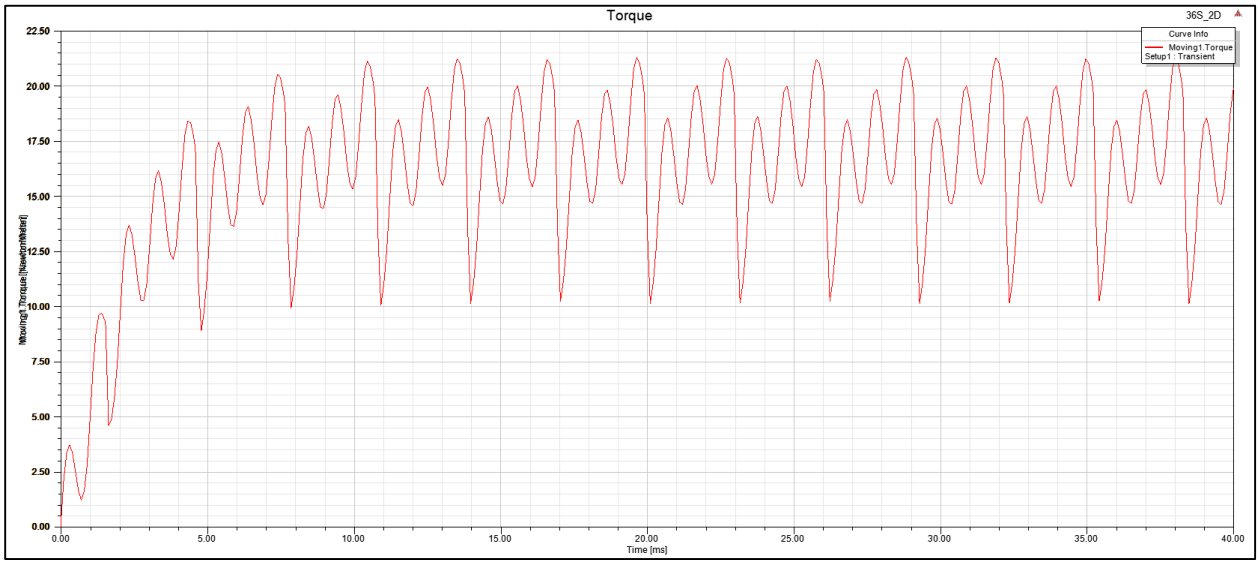

Figure 61: Moving Torque (Nm) V/s Time (ms)

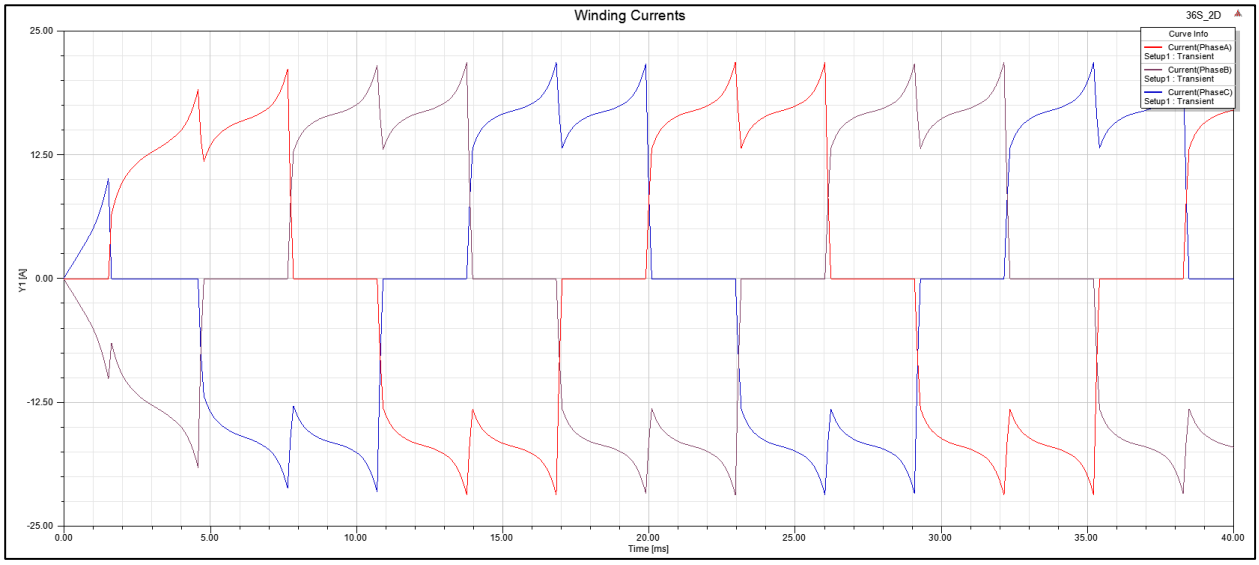

Figure 62: Winding Currents (A) V/s Time (ms)

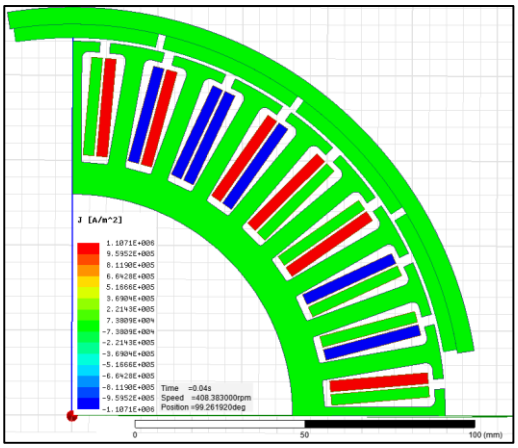

Figure 63: Electric Current Density (A/m^2)

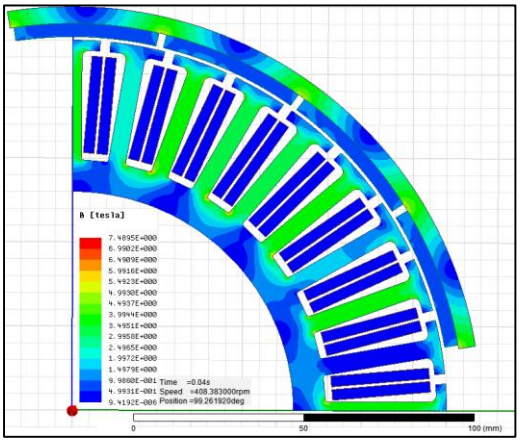

Figure 64: Magnetic Field Strength (T)

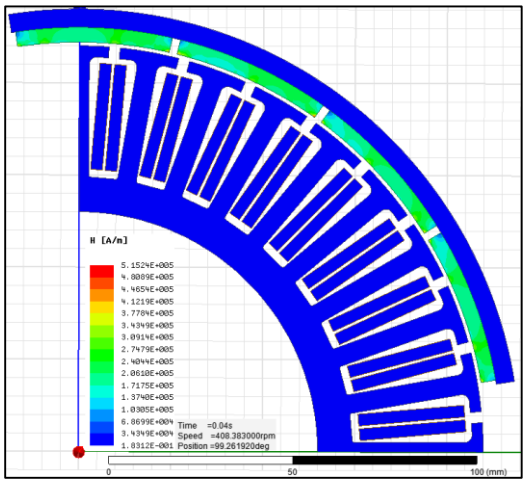

Figure 65: Magnetic Field Strength (A/m)

Figure 66: Flux Lines (Wb/m)

6.3. 48 Slot, 22 Pole Machine 2D Model in ANSYS – Maxwell – RMxprt:

Depicted below is the 2D model along with its FE mesh plot of the machine, the grey sections are Electrical Steel, the green sections are Permanent Magnets, while the golden ones are copper conductors.

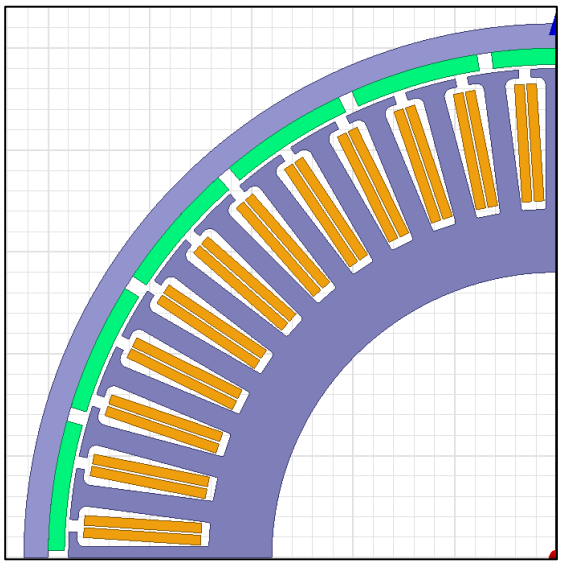

Figure 67: 2D Machine Cross – Section

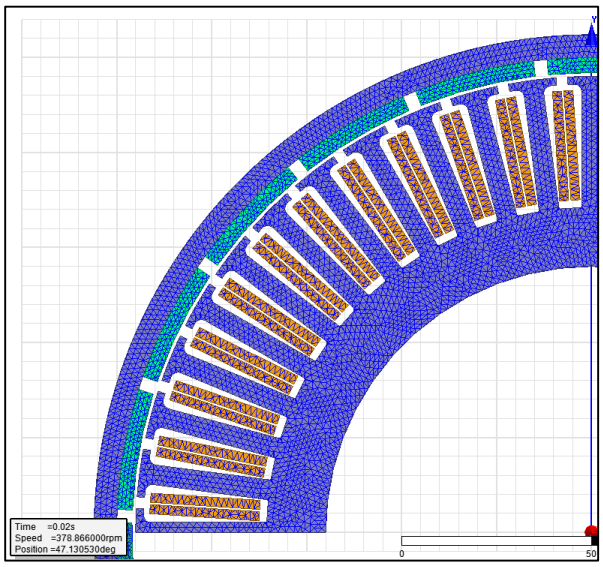

Figure 68: 2D Mesh Plot

6.3.1. Results and Field Overlays:

Shown below are the plots for Moving Torque and Winding Currents v/s time.

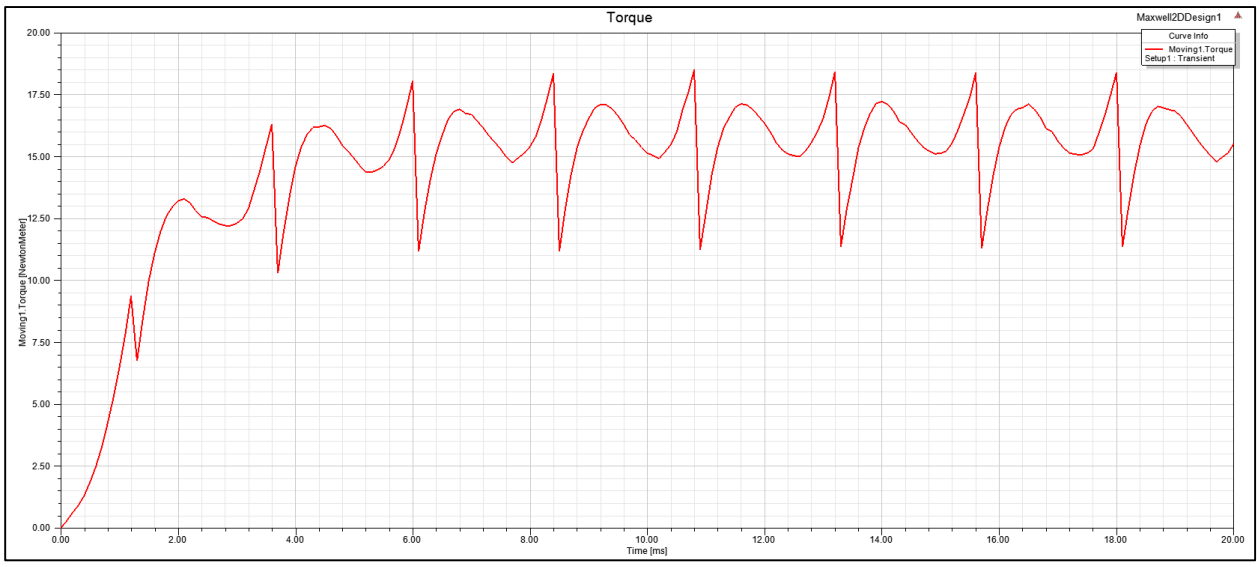

Figure 69: Moving Torque (Nm) V/s Time (ms)

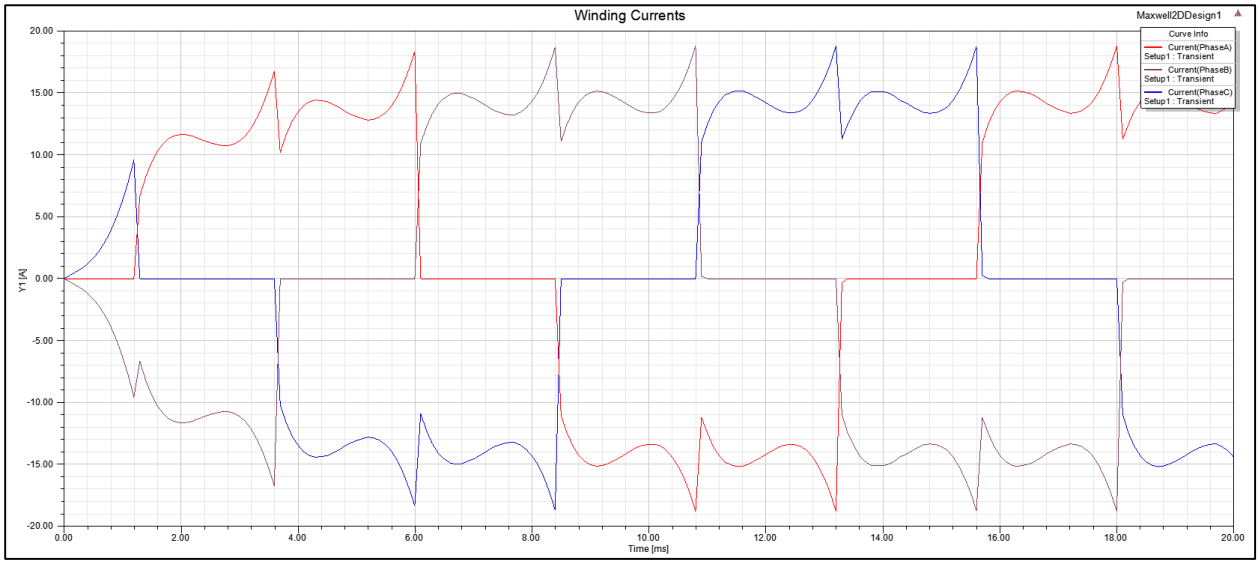

Figure 70: Winding Currents (A) V/s Time (ms)

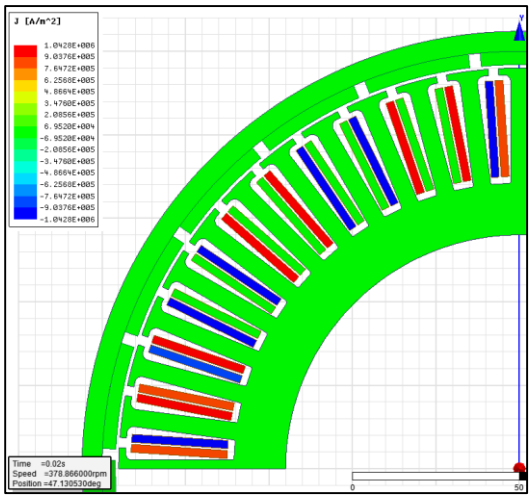

Figure 71: Electric Current Density (A/m^2)

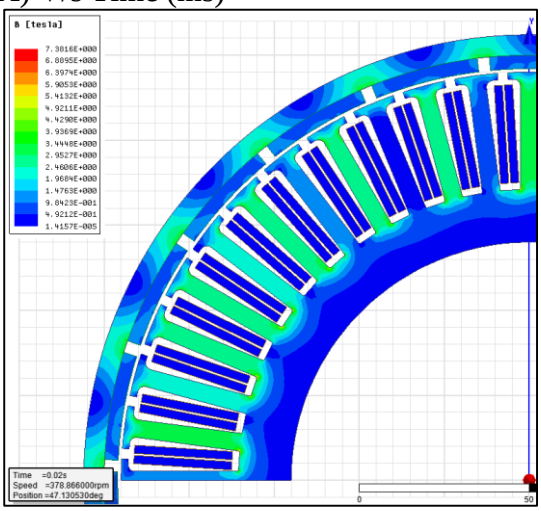

Figure 72: Magnetic Field Strength (T)

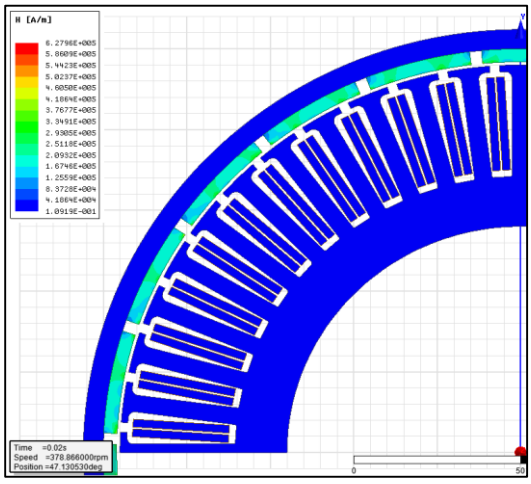

Figure 73: Magnetic Field Strength (A/m)

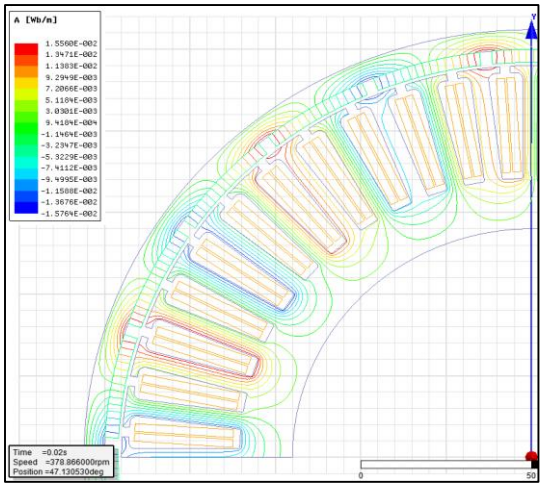

Figure 74: Flux Lines (Wb/m)

6.4. 72 Slot, 32 Pole Machine 2D Model in ANSYS – Maxwell – RMxprt:

Depicted below is the 2D model along with its FE mesh plot of the machine, the grey sections are Electrical Steel, the green sections are Permanent Magnets, while the golden ones are copper conductors.

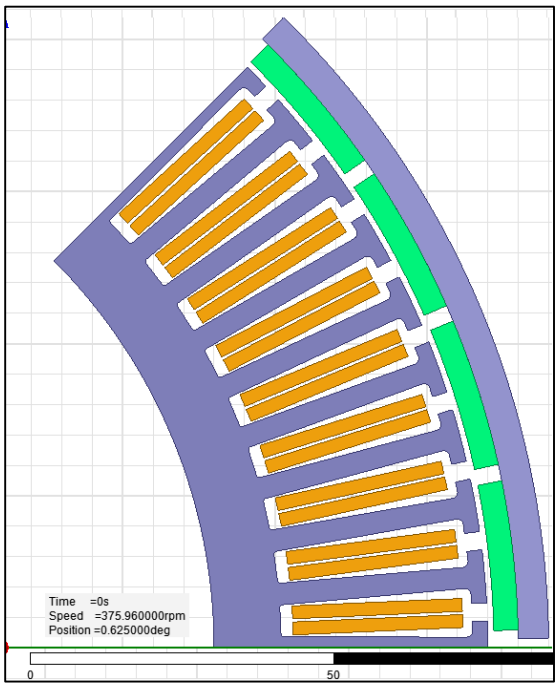

Figure 75: 2D Machine Cross – Section

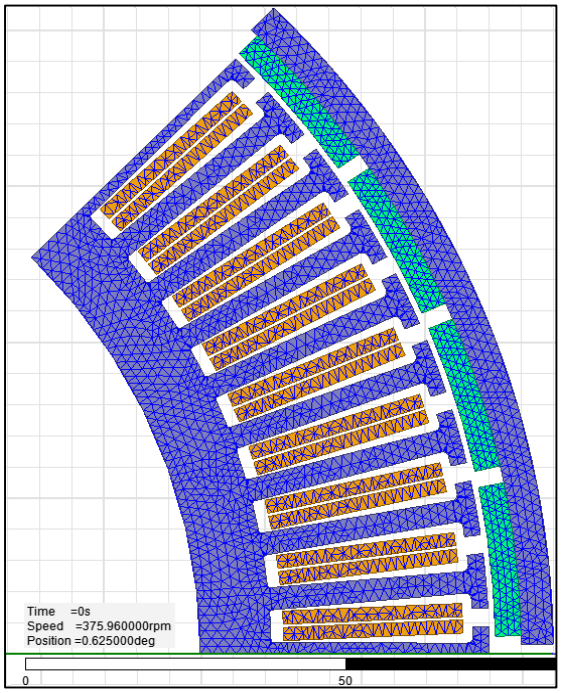

Figure 76: 2D Mesh Plot

6.4.1. Results and Field Overlays:

Shown below are the plots for Moving Torque and Winding Currents v/s time.

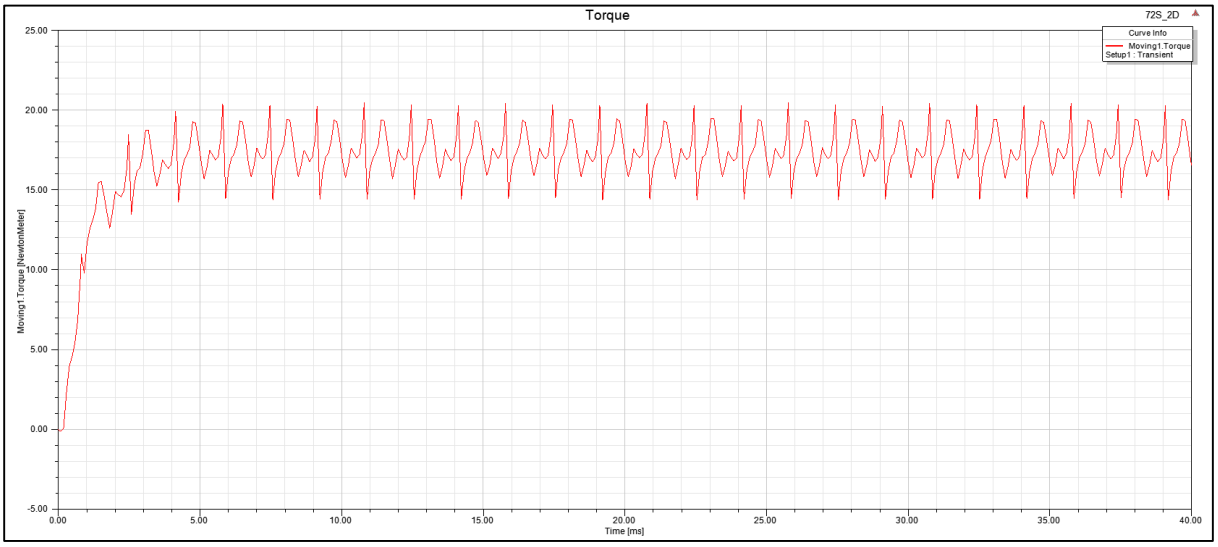

Figure 77: Moving Torque (Nm) V/s Time (ms)

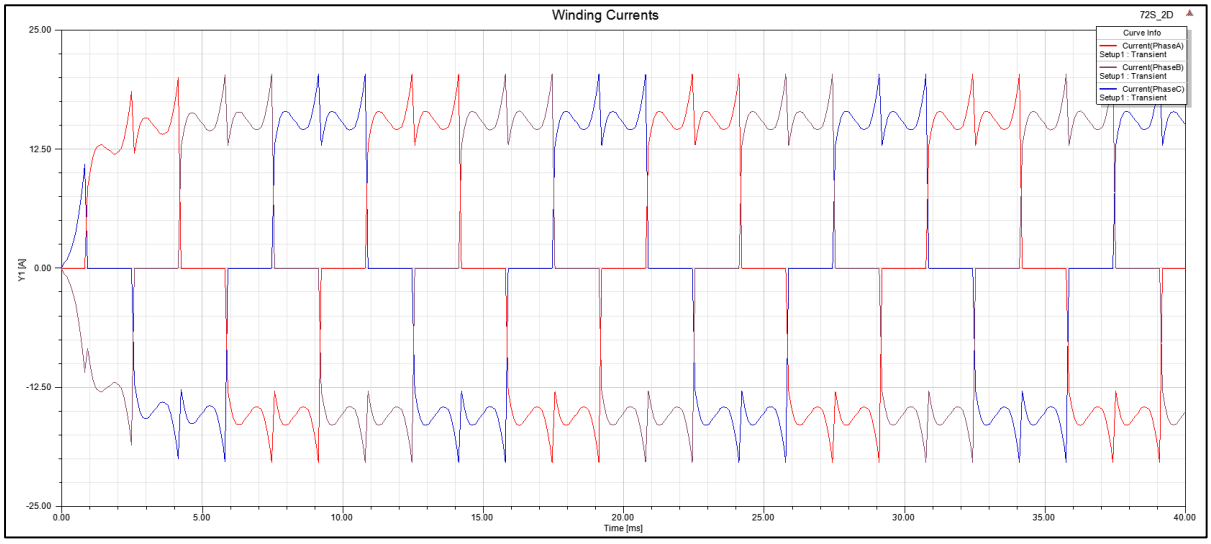

Figure 78: Winding Currents (A) V/s Time (ms)

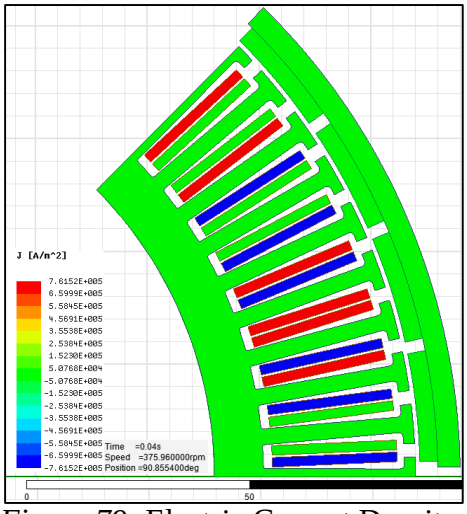

Figure 79: Electric Current Density (A/m^2)

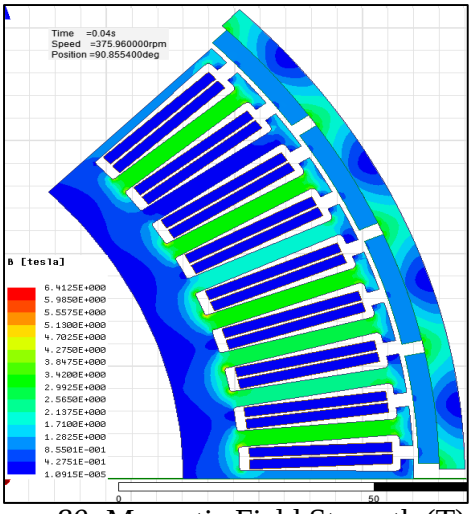

Figure 80: Magnetic Field Strength (T)

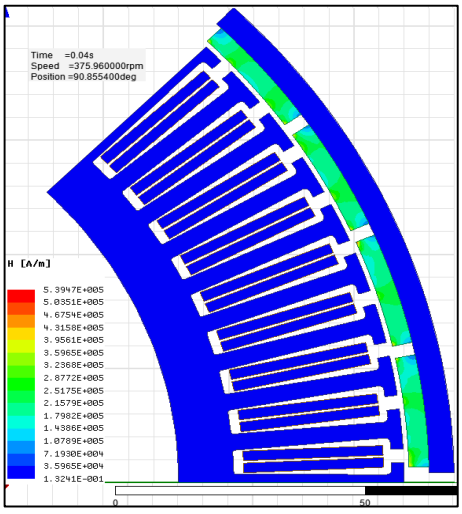

Figure 81: Magnetic Field Strength (A/m)

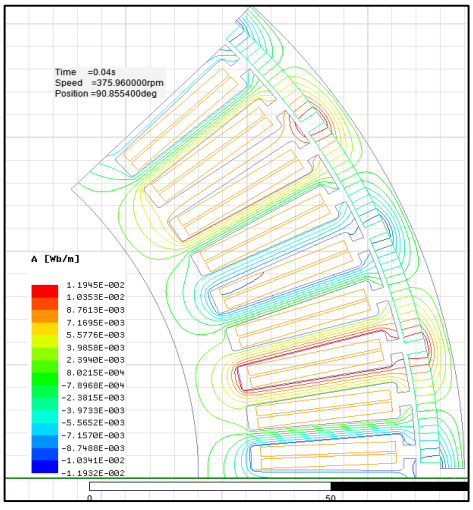

Figure 82: Flux Lines (Wb/m)

6.5. About the Maxwell Mesh

Maxwell uses the Finite Element Method (FEM) to solve Maxwell‘s electro-magnetic field equations. In order to obtain the set of algebraic equations to be solved, the geometry of the problem is discretized automatically into basic platonic solids (e.g. Triangle in 2D & Tetrahedron in 3D). The assembly of all tetrahedra/triangles is referred to as the finite element mesh of the model or simply, the mesh. [23]

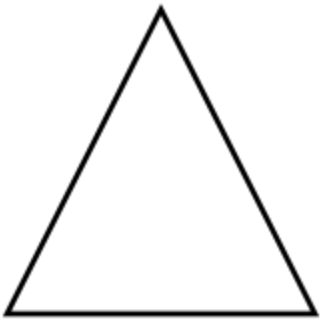

Figure 83: 2D FEM element Triangle

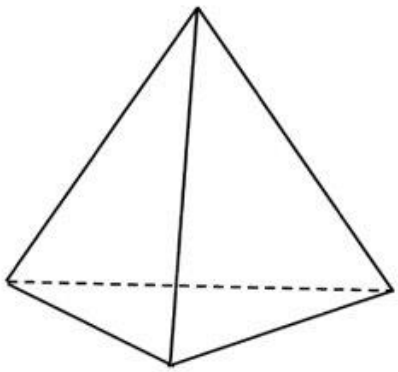

Figure 84: 3D FEM element Tetrahedron

Mesh plays important role in accuracy of the computed results and thus a higher mesh resolution is required in regions where fields intersect rapidly.

6.5.1. Meshing in Maxwell

Maxwell meshes all solids (model Objects) in the geometry automatically before solution process is started. In Maxwell’s Static Solvers, the mesh is automatically refined to achieve the required level of accuracy in field computation. This is referred as Adaptive mesh refinement Maxwell also offers wide range of mesh operations which can be utilized to achieve a mesh as required by users

6.6. 24 Slot, 16 Pole Machine 3D Model in ANSYS – Maxwell – RMxprt:

Depicted below is the 3D model of the machine along with its FE mesh plot & magnetic field density plot, the grey sections are Electrical Steel, the green sections are Permanent Magnets, while the golden ones are copper conductors.

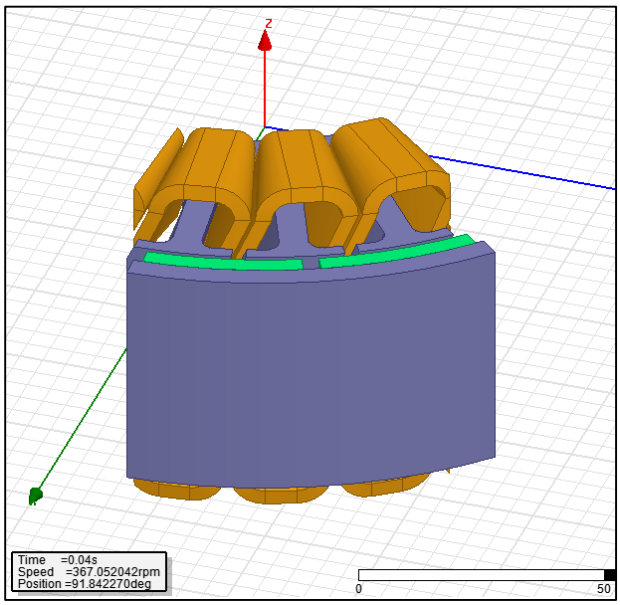

Figure 85: 3D Machine Section

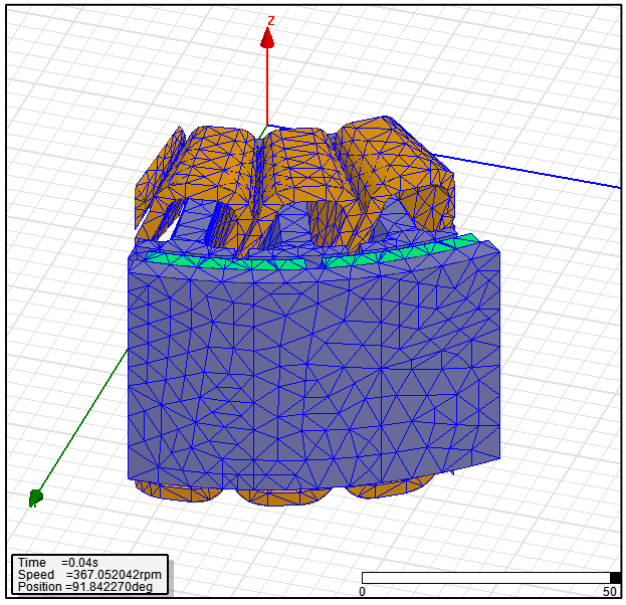

Figure 86: 3D Mesh Model

6.6.1. Results and Field Overlays:

Shown below are the plots for Moving Torque and Winding Currents v/s time along with field overlays (T).

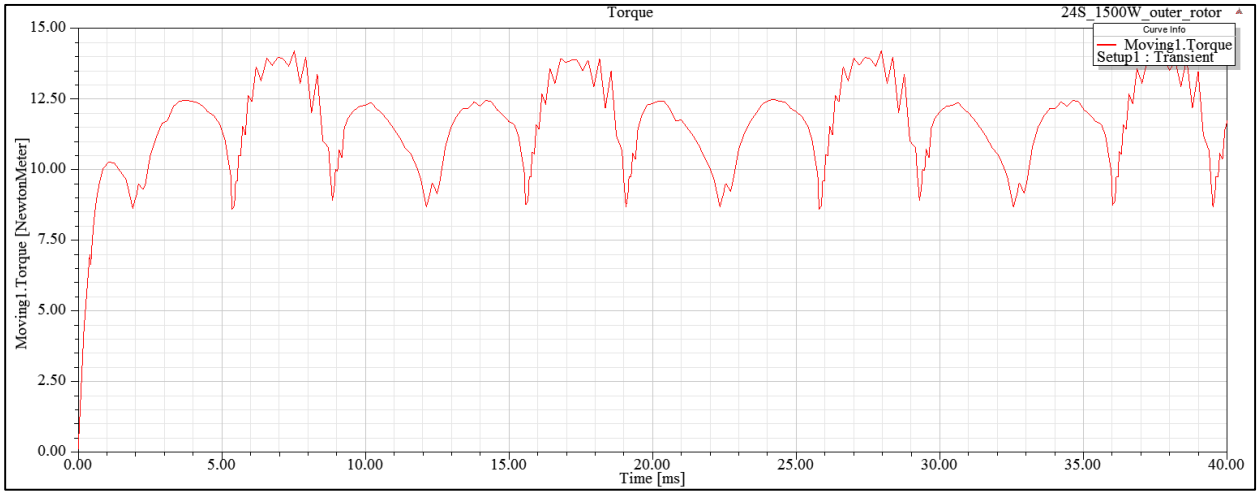

Figure 87: Moving Torque (Nm) V/s Time (ms)

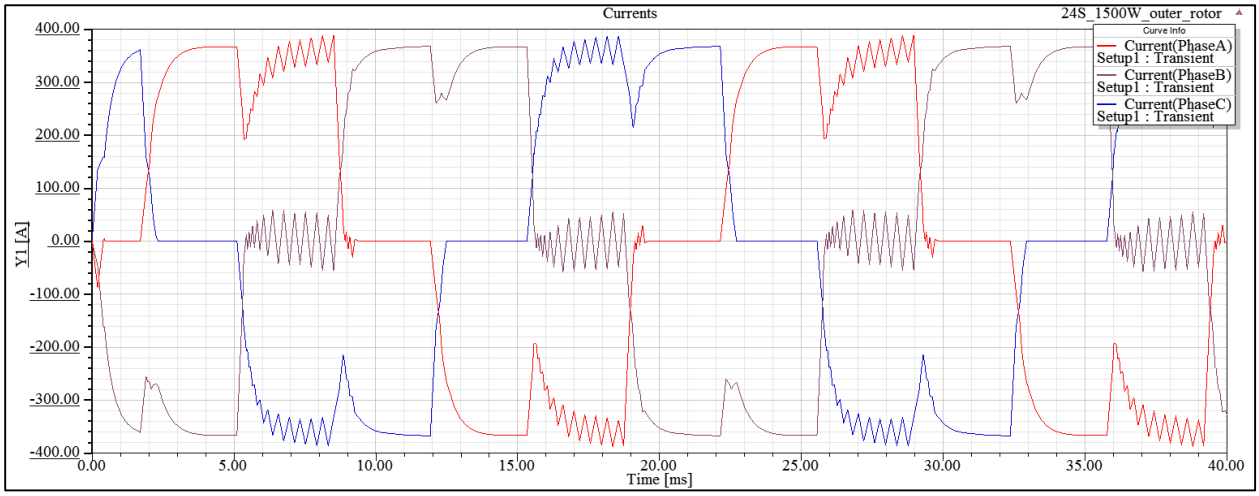

Figure 88: Winding Currents (A) V/s Time (ms)

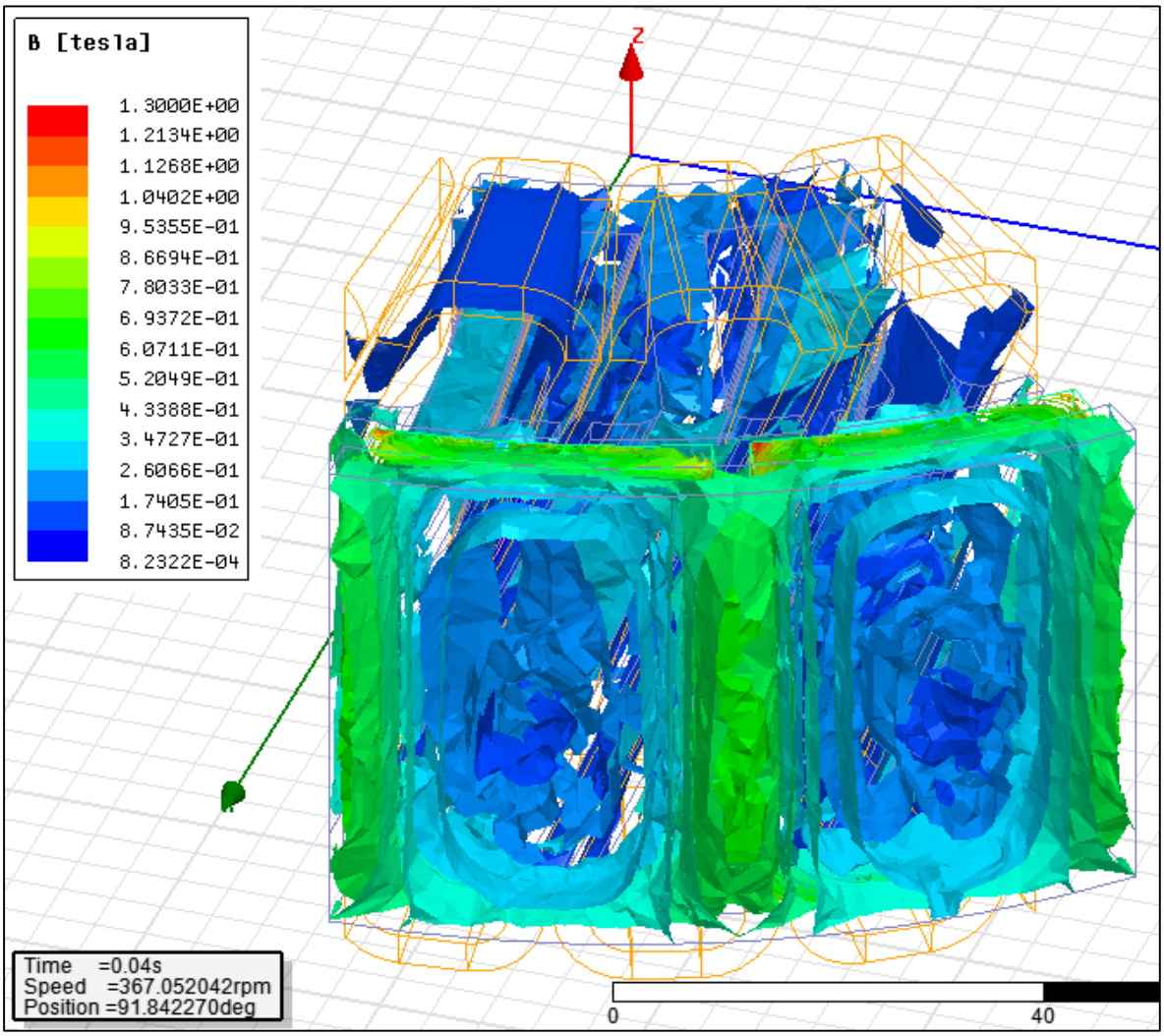

Figure 89a: Magnetic Field Strength (T)

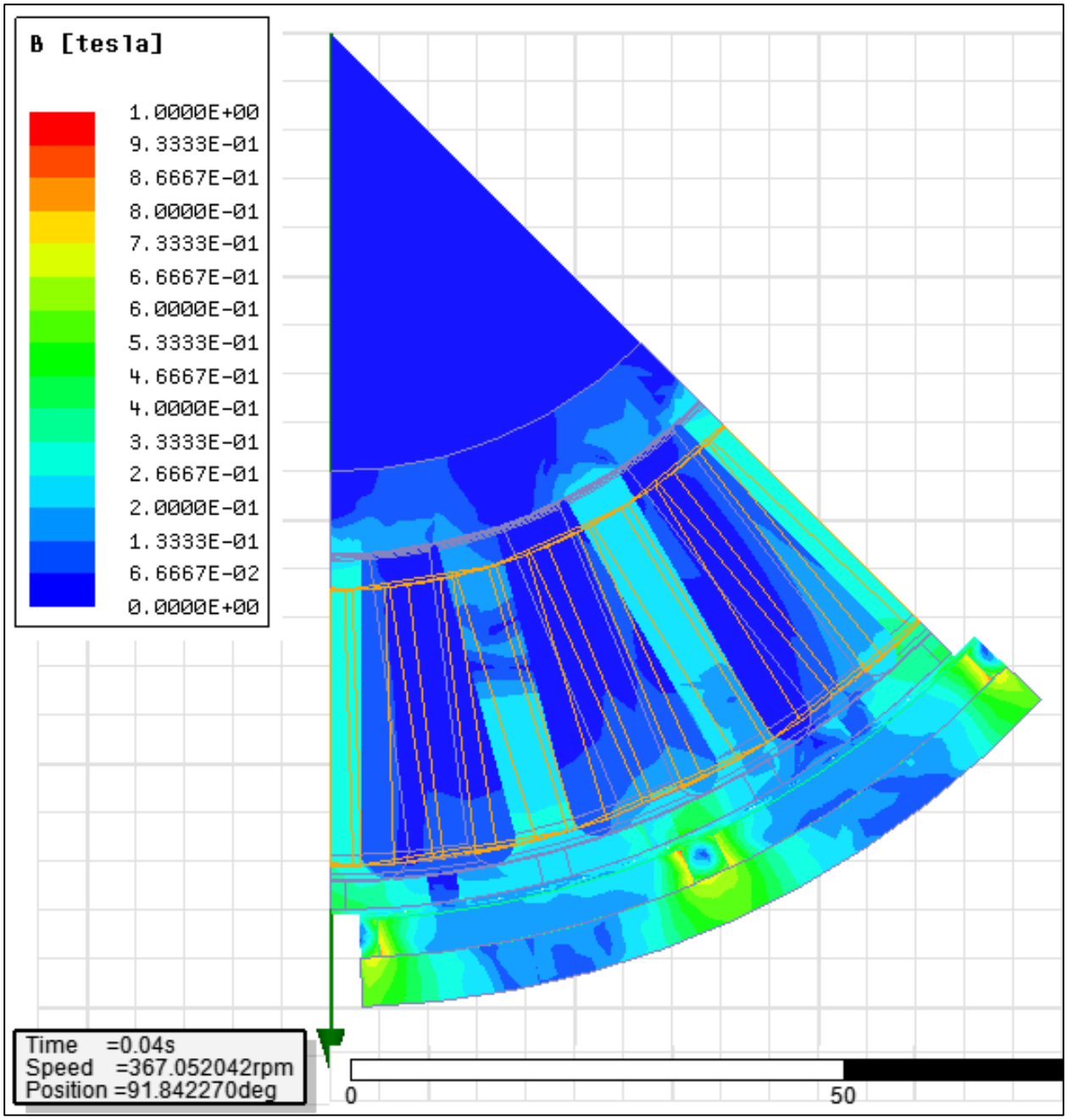

Figure 89b: Magnetic Field Strength (X-Y) (T) Plane

6.6.1.1: Observations:

Results show the torque pulsating between 10 – 15 Nm every 8 ms. Winding currents have peaks and harmonics which can be attributed to the torque pulsations, although the winding currents have abnormally high magnitude. Field Overlays of the Magnetic field show a magnitude of 1.3 T in isolated regions of the permanent magnet inner face which is the nominal expected value, while the stator tooth field density barely reaches 0.8 T, this is an abnormally low value and can be attributed to the input of inaccurate electric steel selection in the RMxprt module.

6.7. 36 Slot, 16 Pole Machine 3D Model in ANSYS – Maxwell – RMxprt:

Depicted below is the 3D model of the machine along with its FE mesh plot & magnetic field density plot, the grey sections are Electrical Steel, the green sections are Permanent Magnets, while the golden ones are copper conductors.

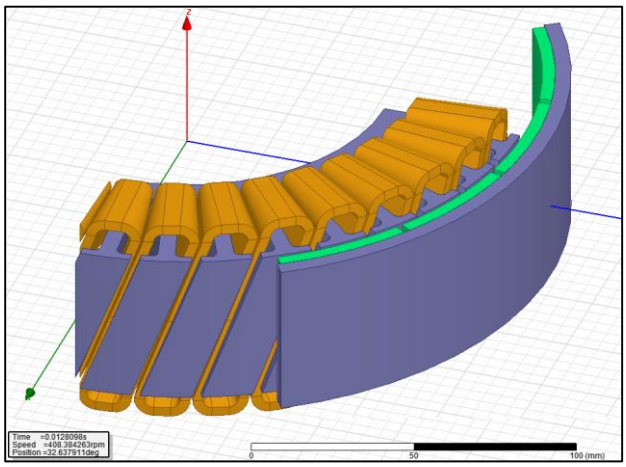

Figure 90: 3D Machine Section

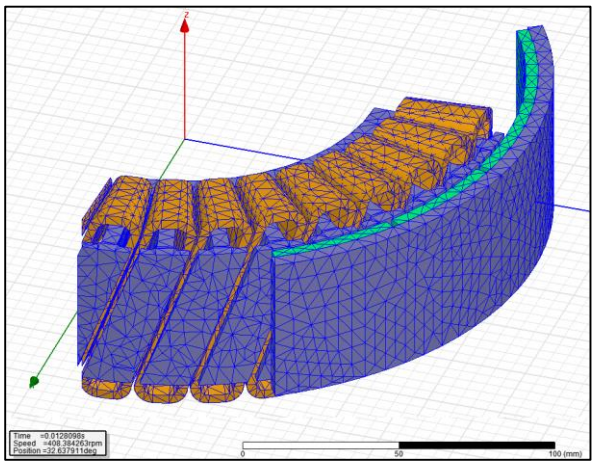

Figure 91: 3D Mesh Model

6.7.1. Results and Field Overlays:

Shown below are the plots for Moving Torque and Winding Currents v/s time along with field overlays (T).

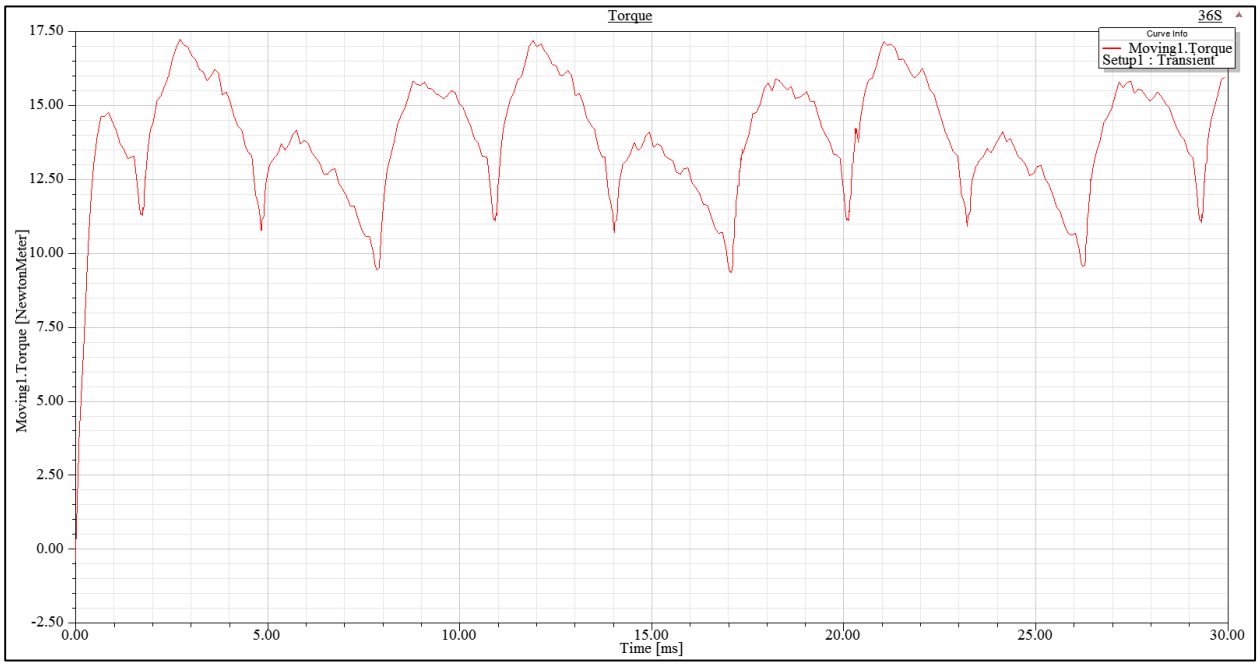

Figure 92: Moving Torque (Nm) V/s Time (ms)

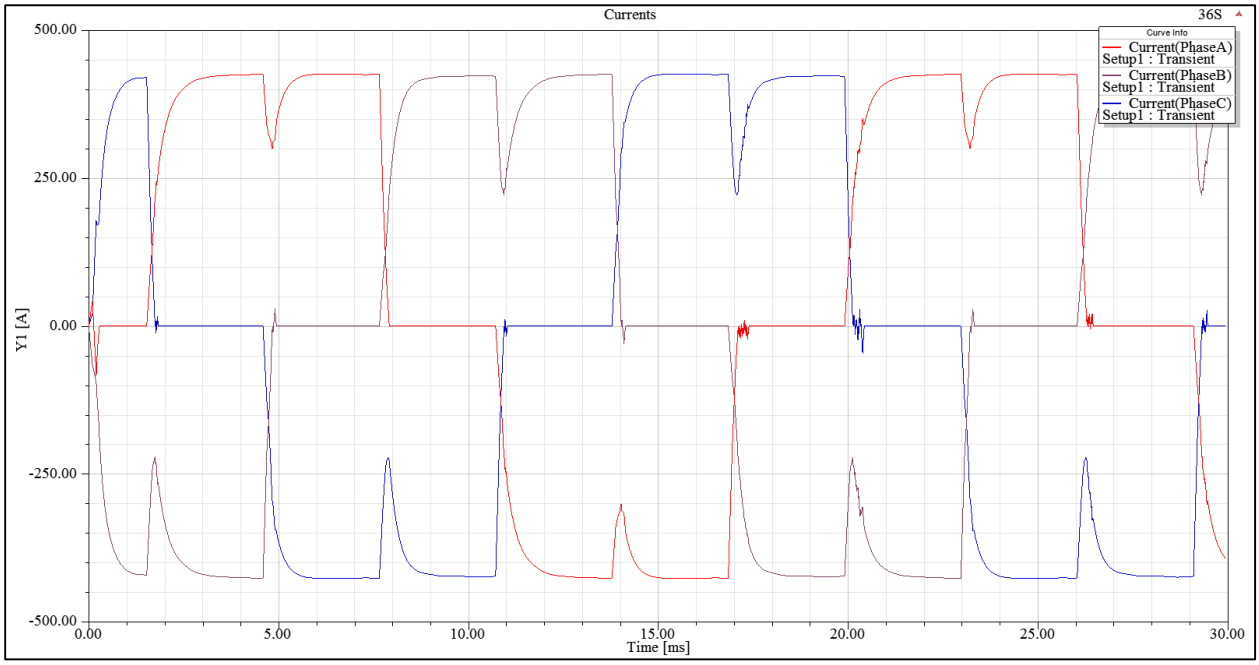

Figure 93: Winding Currents (A) V/s Time (ms)

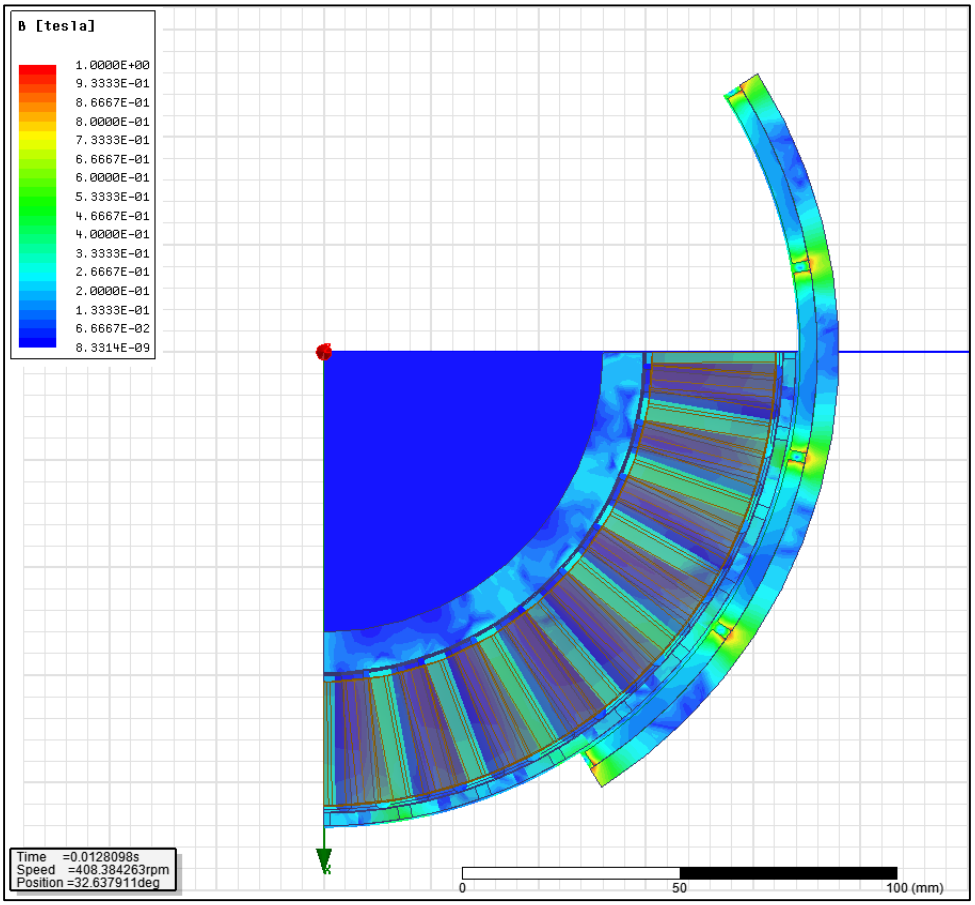

Figure 94: Magnetic Field Strength (X-Y Plane) (T)

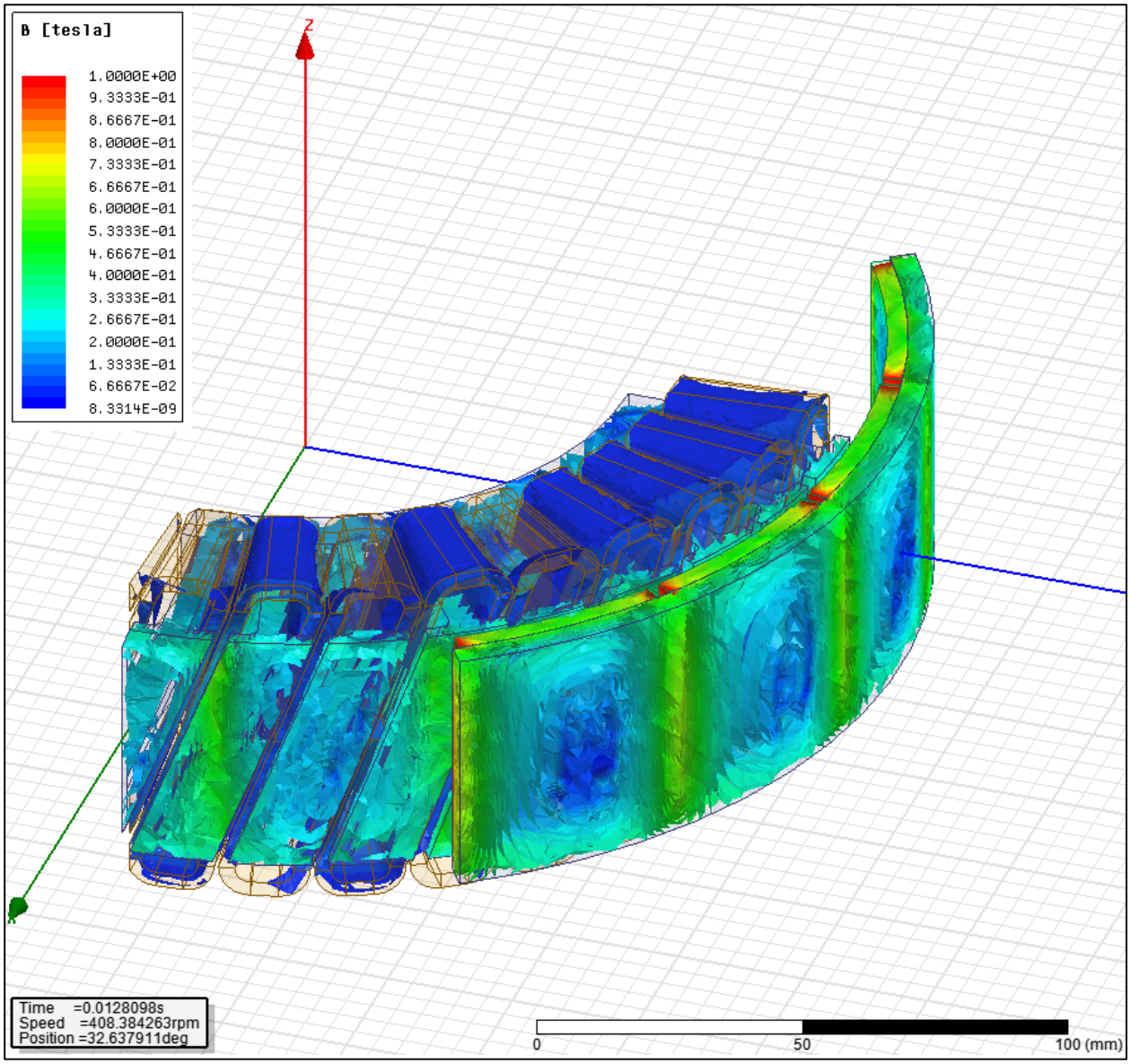

Figure 95a: Magnetic Field Strength (T)

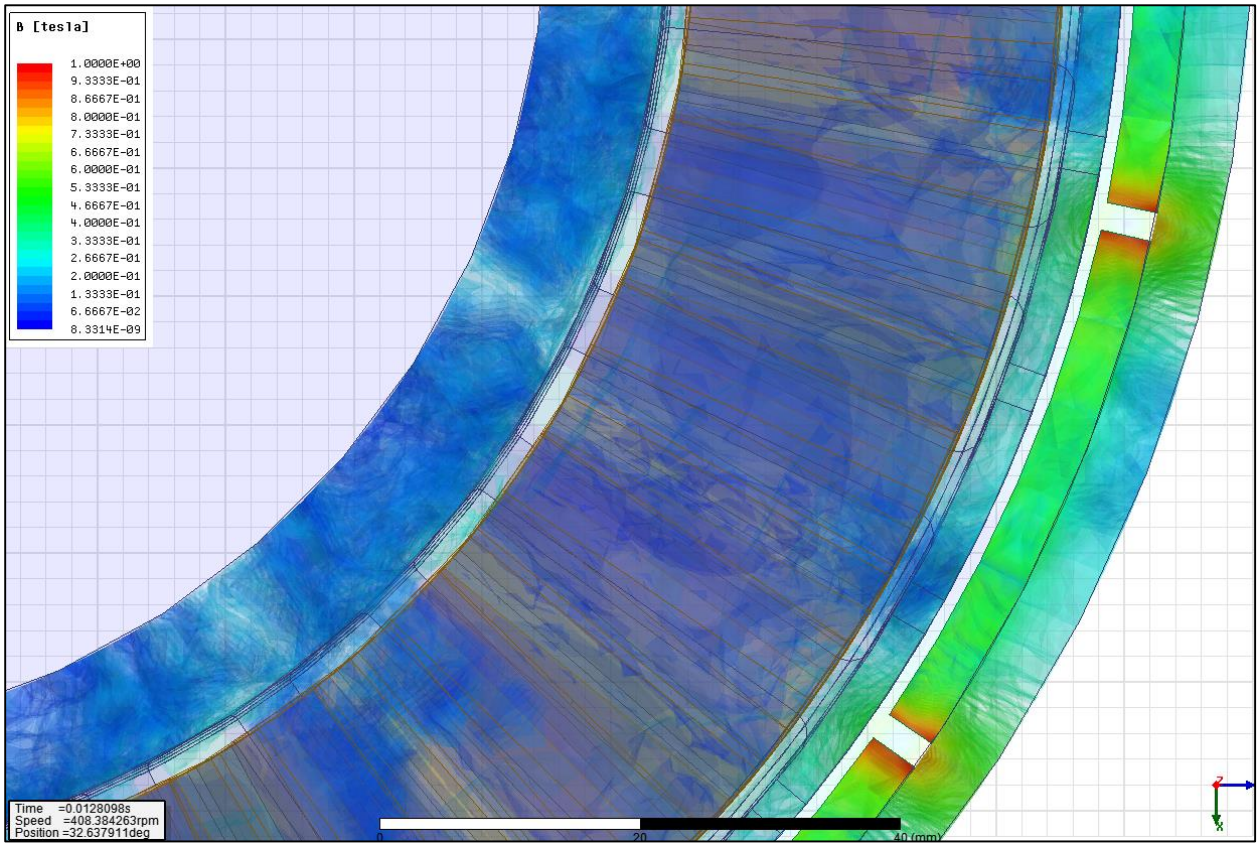

Figure 96b: Magnetic Field Strength (Streamlined Vector) (T) Plane

6.7.1.1: Observations:

Results show the torque pulsating between 10 – 17.5 Nm every 3 ms. Winding currents have plateaus and minor dips which can be attributed to the torque pulsations, although the winding currents have abnormally high magnitude. Field Overlays of the Magnetic field shows the nominal expected value, while the stator tooth field density barely reaches 0.8 T, this is an abnormally low value and can be due to the input of inaccurate electric steel selection in the RMxprt module.

6.8. 48 Slot, 22 Pole Machine 3D Model in ANSYS – Maxwell – RMxprt:

Depicted below is the 3D model of the machine along with its FE mesh plot & magnetic field density plot, the grey sections are Electrical Steel, the green sections are Permanent Magnets, while the golden ones are copper conductors.

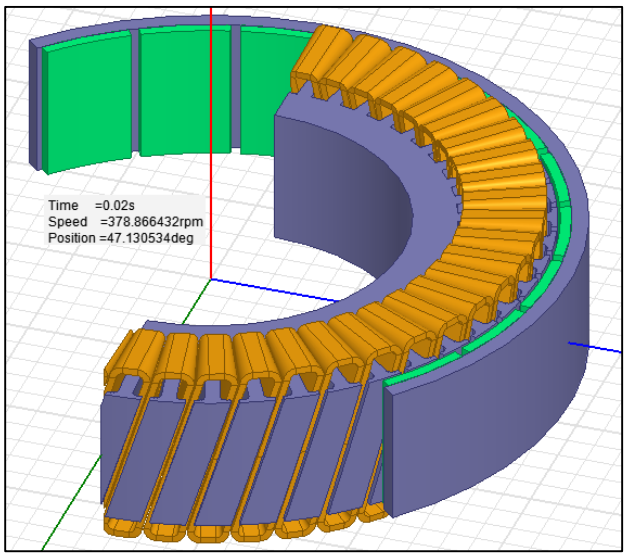

Figure 97: 3D Machine Section

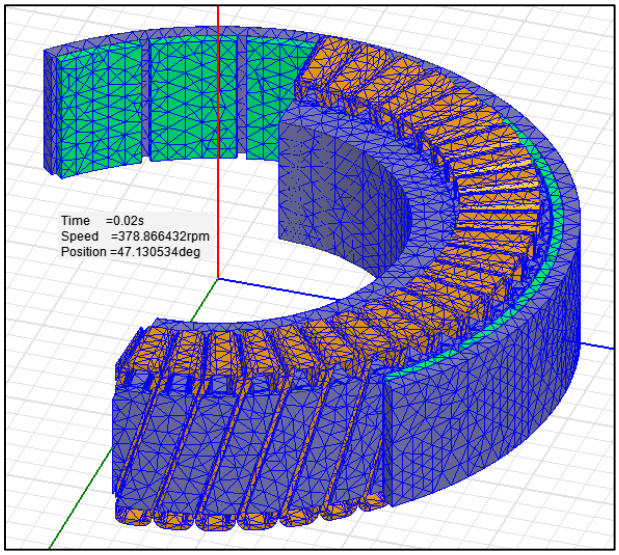

Figure 98: 3D Mesh Model

6.8.1. Results and Field Overlays:

Shown below are the plots for Moving Torque and Winding Currents v/s time along with Field Overlays (T).

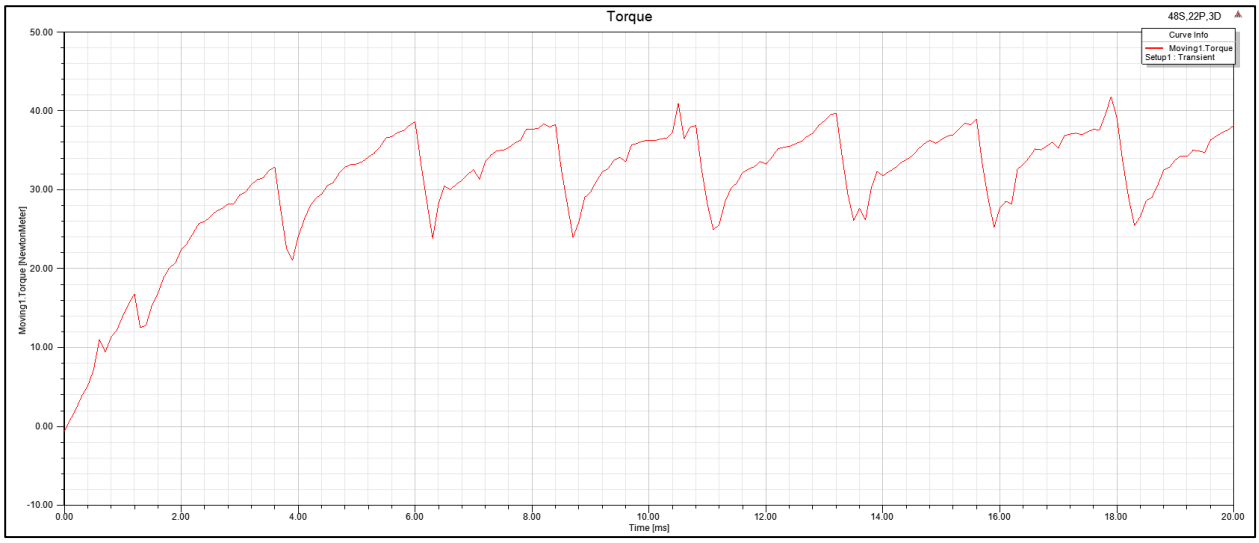

Figure 99: Moving Torque (Nm) V/s Time (ms)

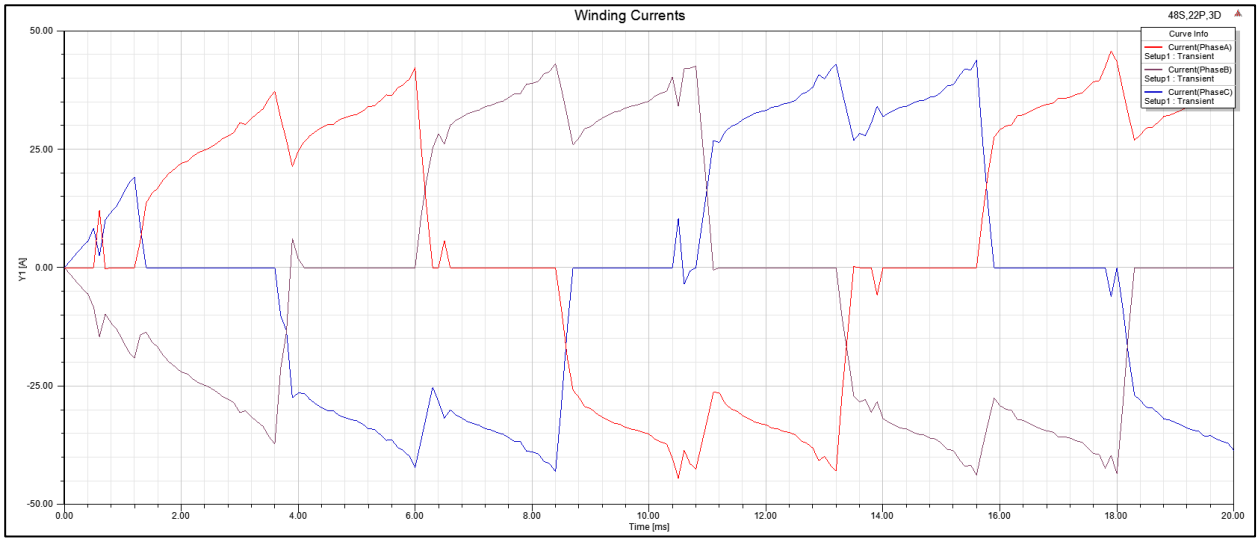

Figure 100: Winding Currents (A) V/s Time (ms)

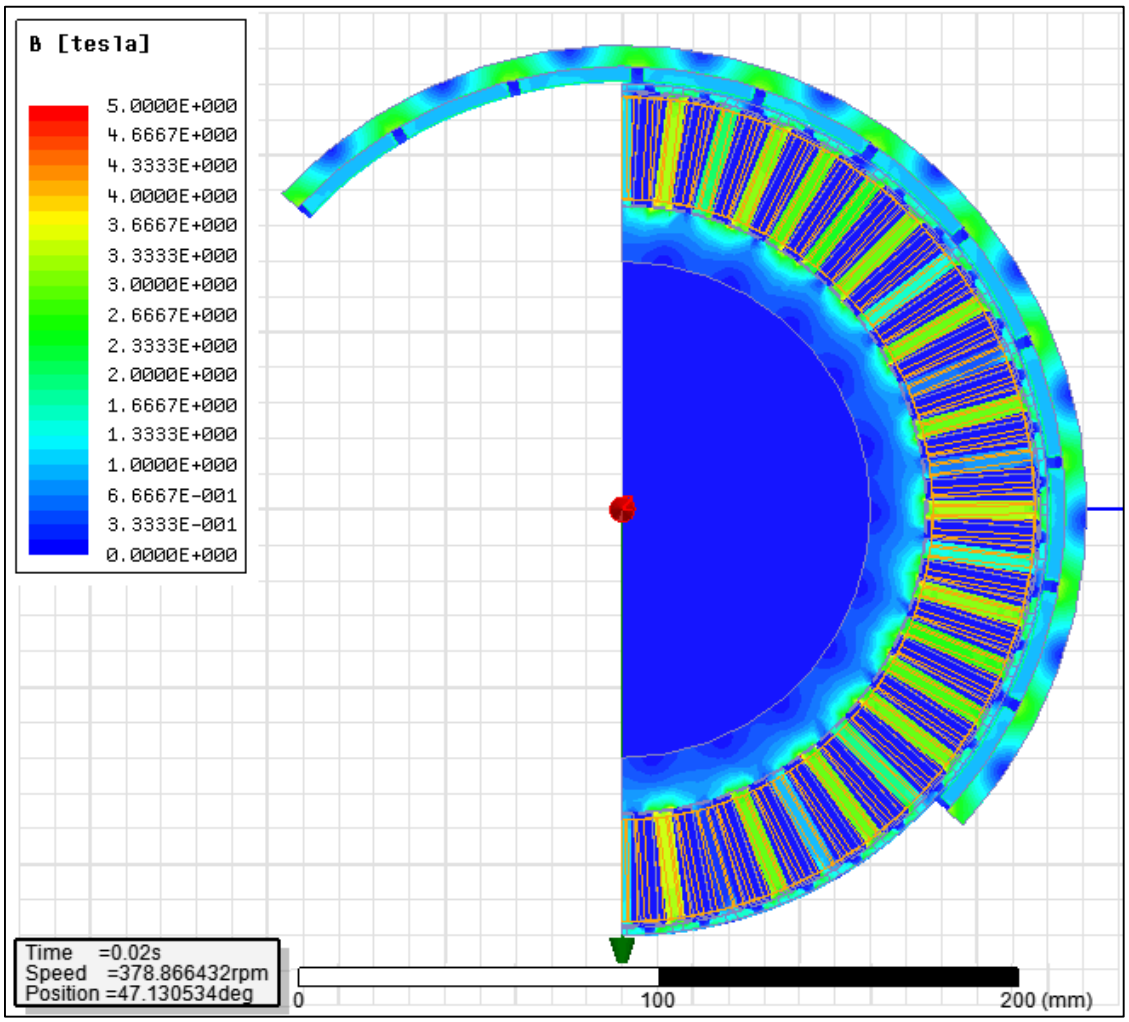

Figure 101a: Magnetic Field Strength (X-Y Plane) (T)

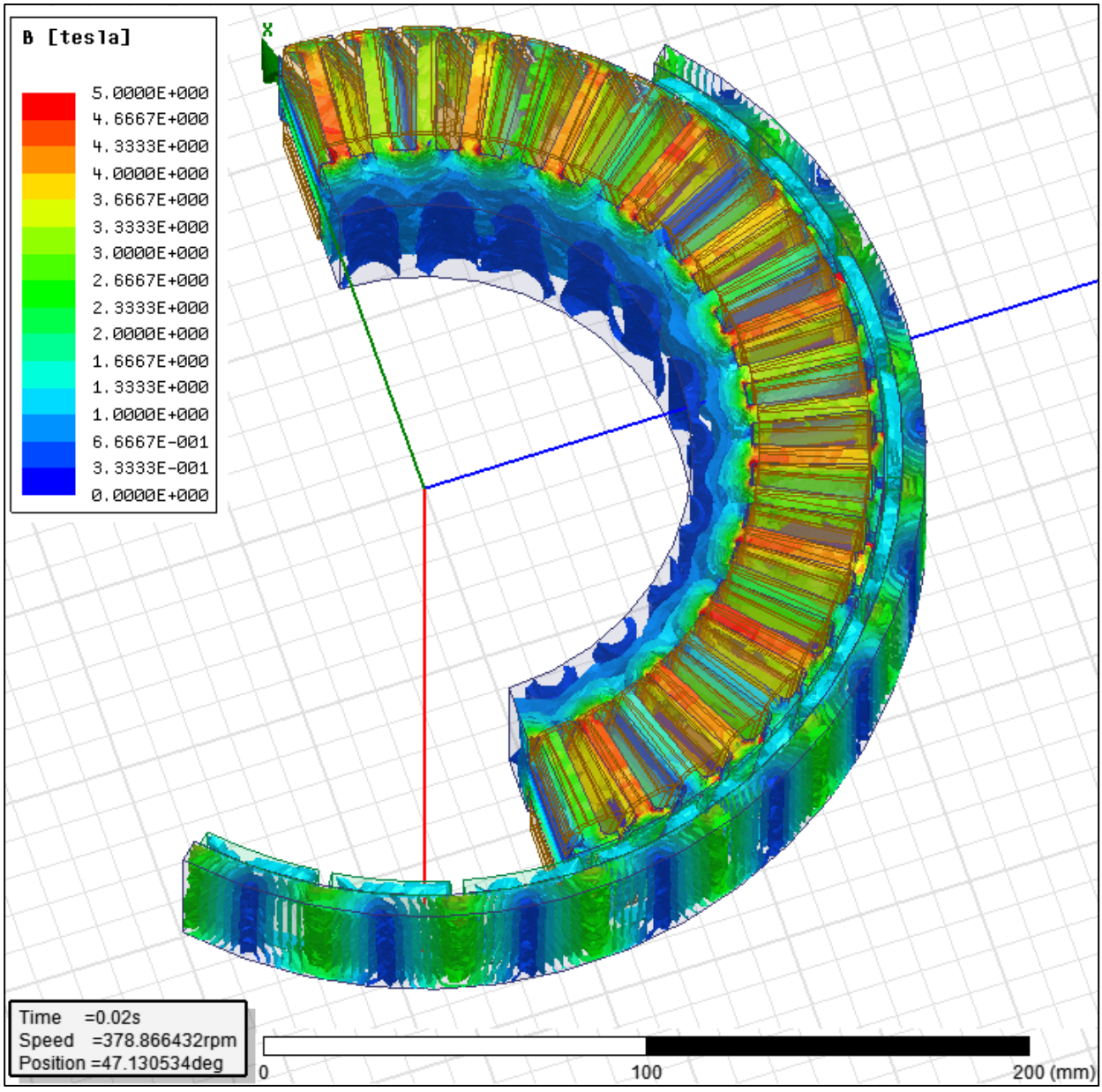

Figure 101b: Magnetic Field Strength (T)

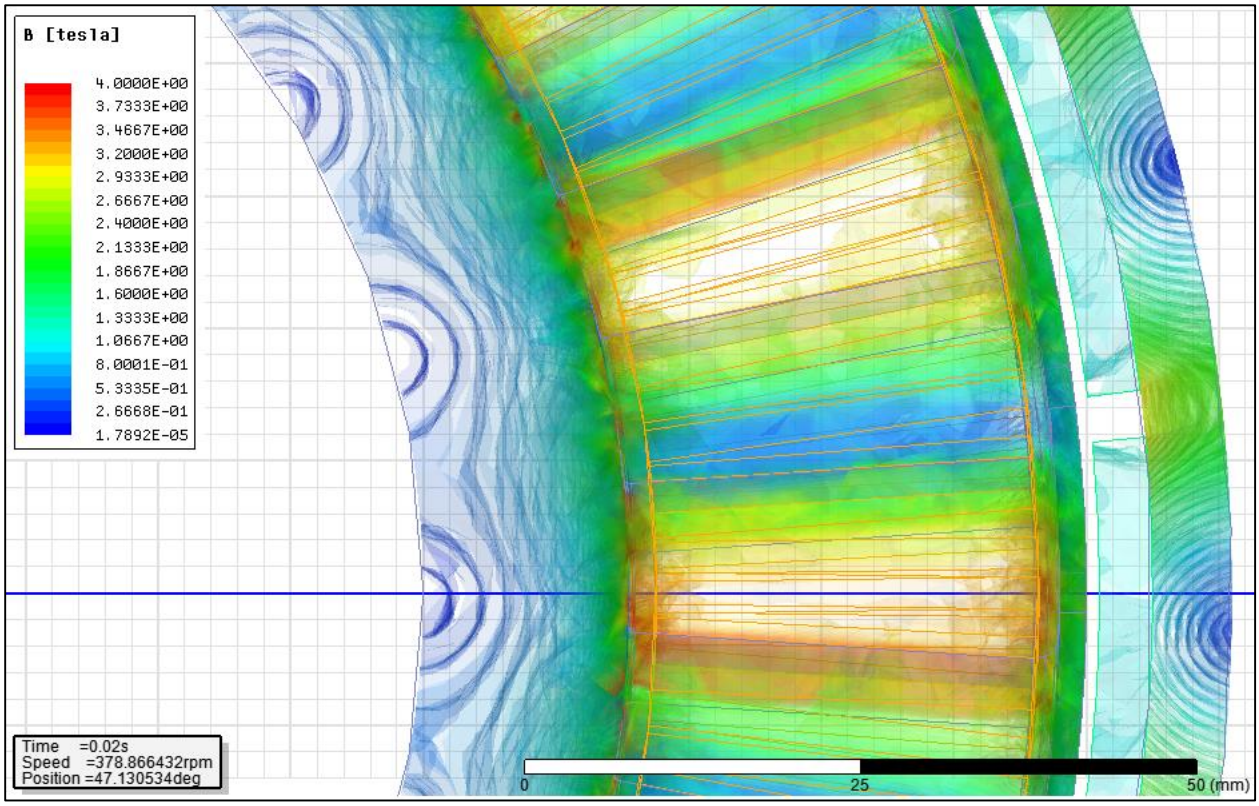

Figure 101c: Magnetic Field Strength (Streamlined Vector) (T)

6.8.1.1: Observations:

The moving torque is oscillation between 40Nm to 25Nm every 2 ms, with the magnitude of the torque same as the rated torque. The magnitude of winding currents is at an average value of 36A, which is its nominal rated value. There is approximately, an oscillation in current with a magnitude of 10A at high frequency, it is deduced that it may be due to torque pulsations. Magnetic Field plots show a density magnitude of 3T and excess in the stator teeth, which is relatively high for typical electrical steels and a machine of this size and rating. The strength of the magnet is at its nominal value of 1.3T. Streamlines show localized spots on the stator with a peak field density of 4 T. These abnormally high value can be attributed to the inaccurate core model of the machine.

6.9. 72 Slot, 32 Pole Machine 3D Model in ANSYS – Maxwell – RMxprt:

Depicted below is the 3D model of the machine along with its FE mesh plot & magnetic field density plot, the grey sections are Electrical Steel, the green sections are Permanent Magnets, while the golden ones are copper conductors.

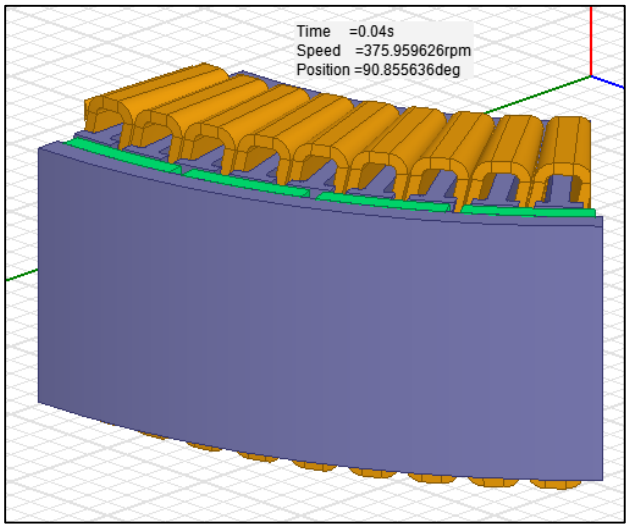

Figure 102: 3D Machine Section

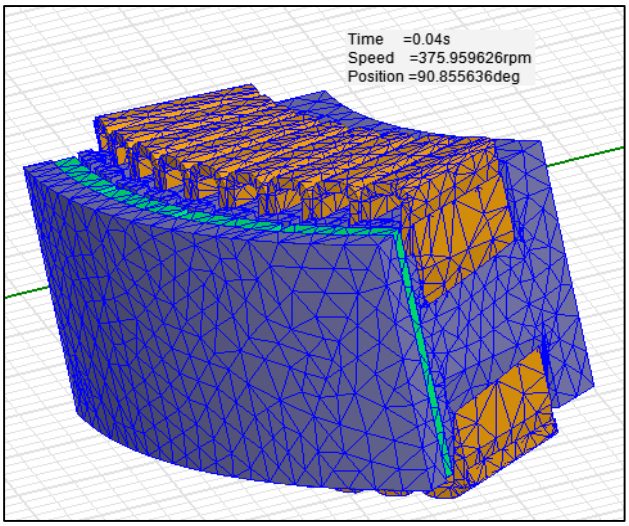

Figure 103: 3D Mesh Model

6.9.1: Results and Field Overlays

Shown below are the plots for Moving Torque and Winding Currents v/s time along with magnetic field density overlays.

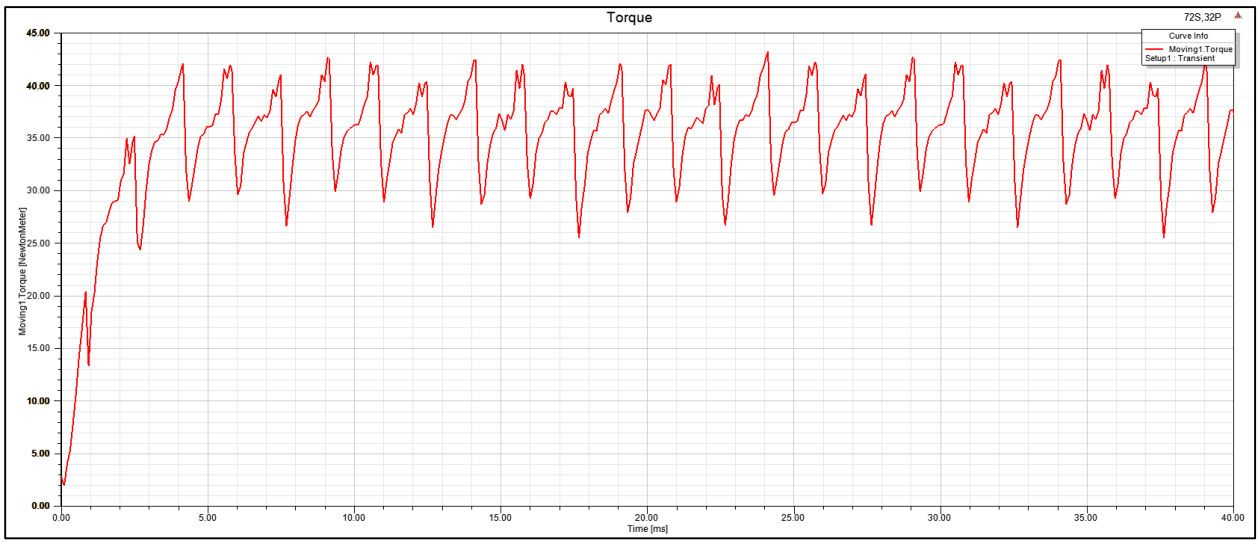

Figure 104: Moving Torque (Nm) V/s Time (ms)

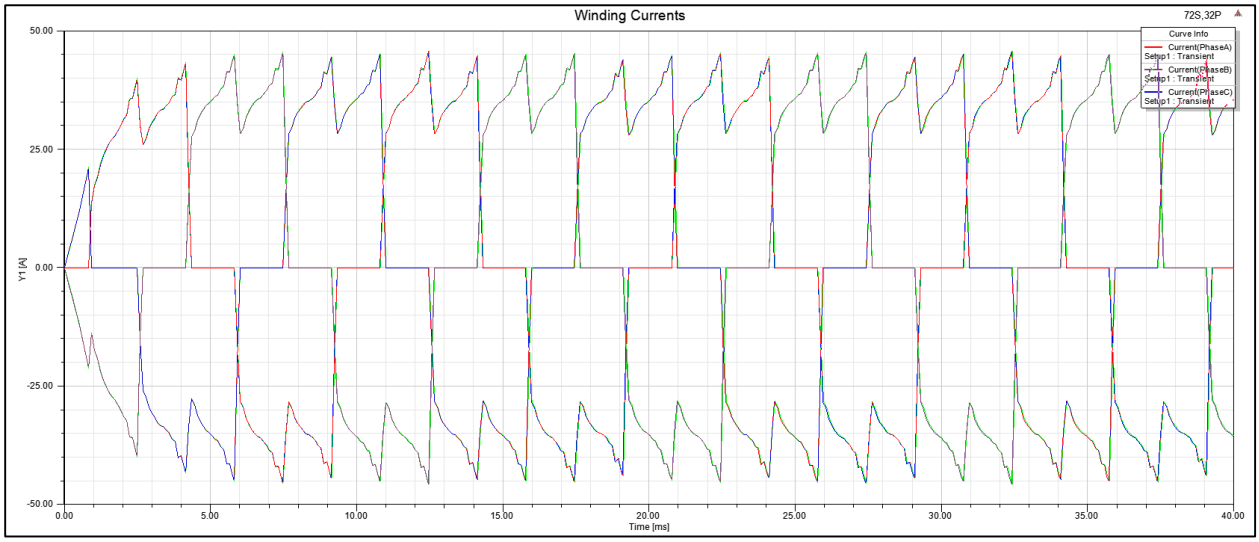

Figure 105: Winding Currents (A) V/s Time (ms)

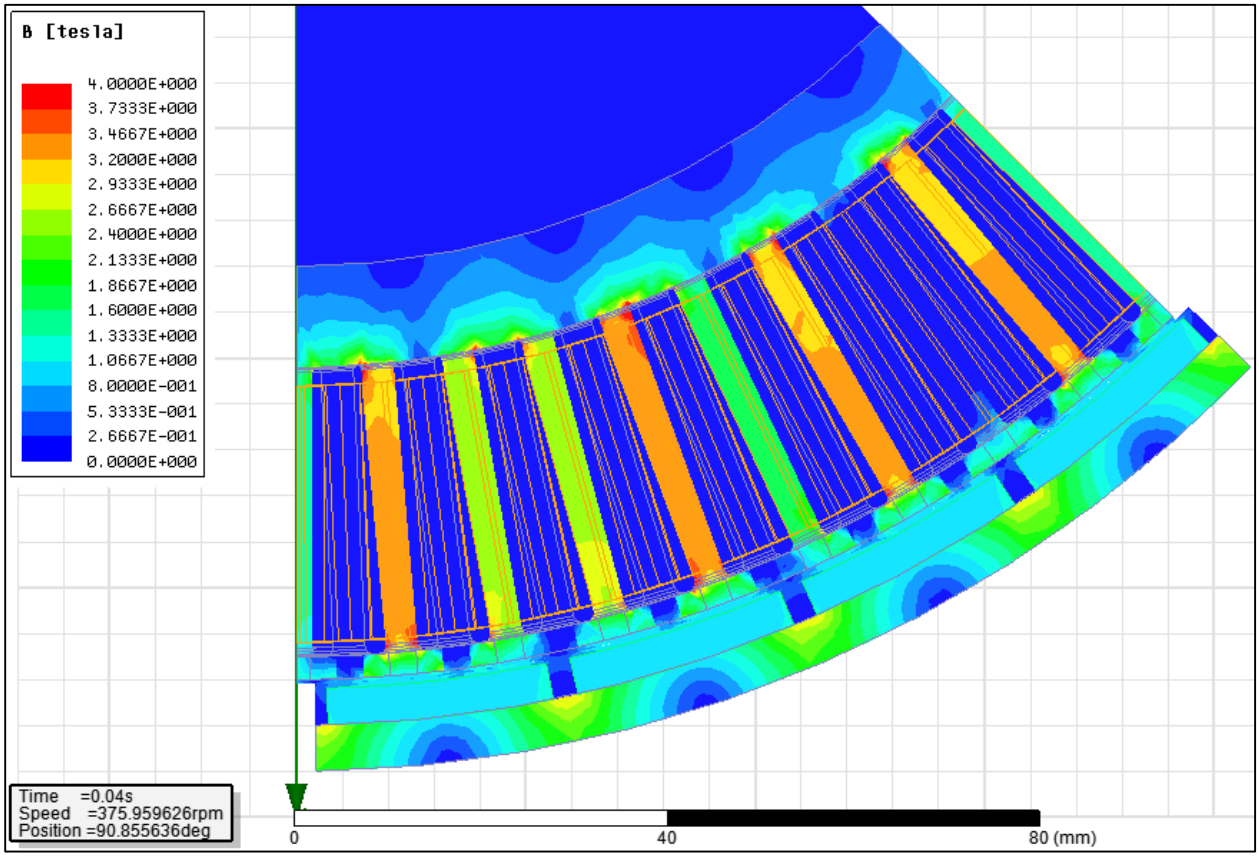

Figure 106a: Magnetic Field Strength (X-Y Plane) (T)

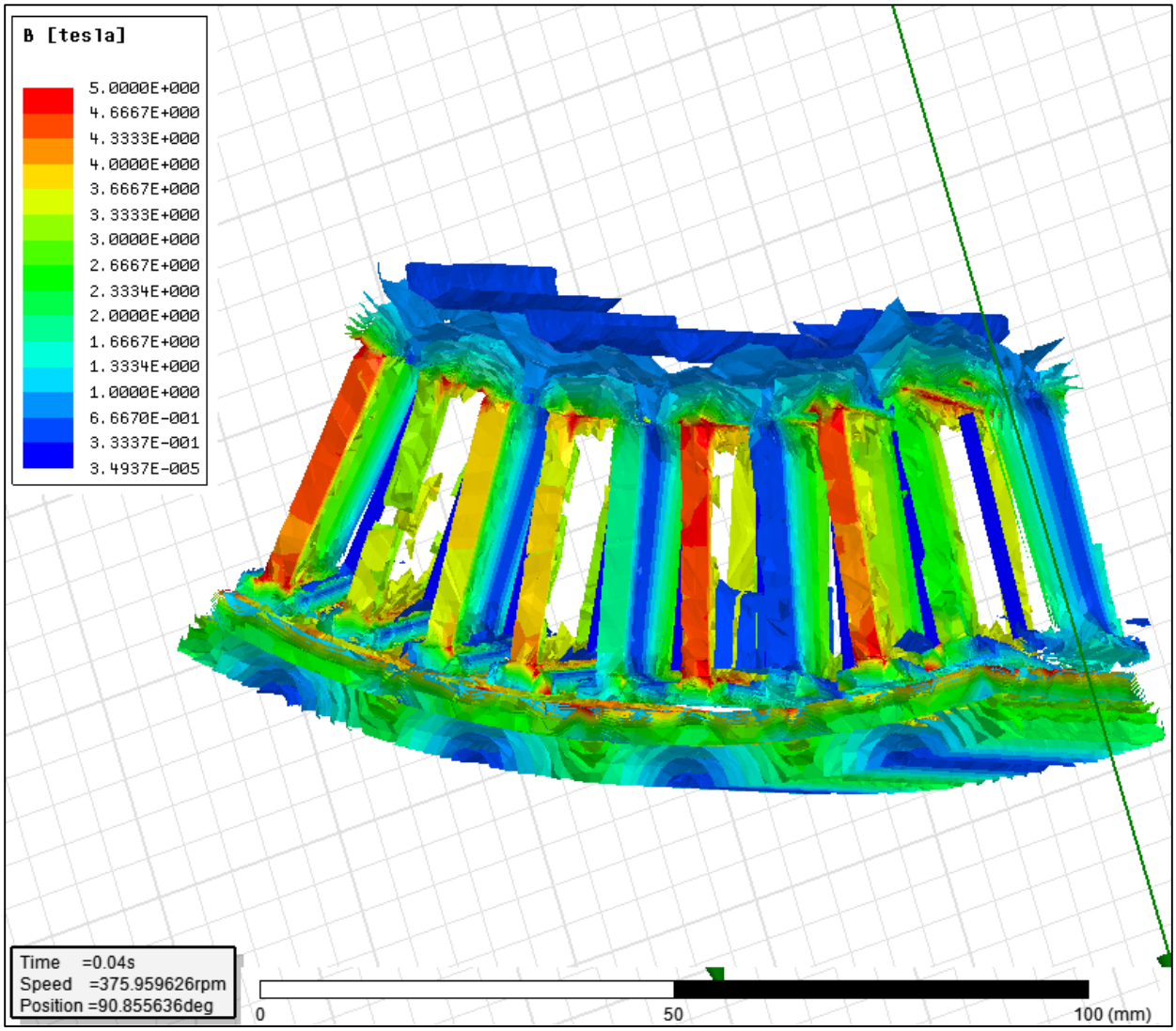

Figure 106b: Magnetic Field Strength (T)

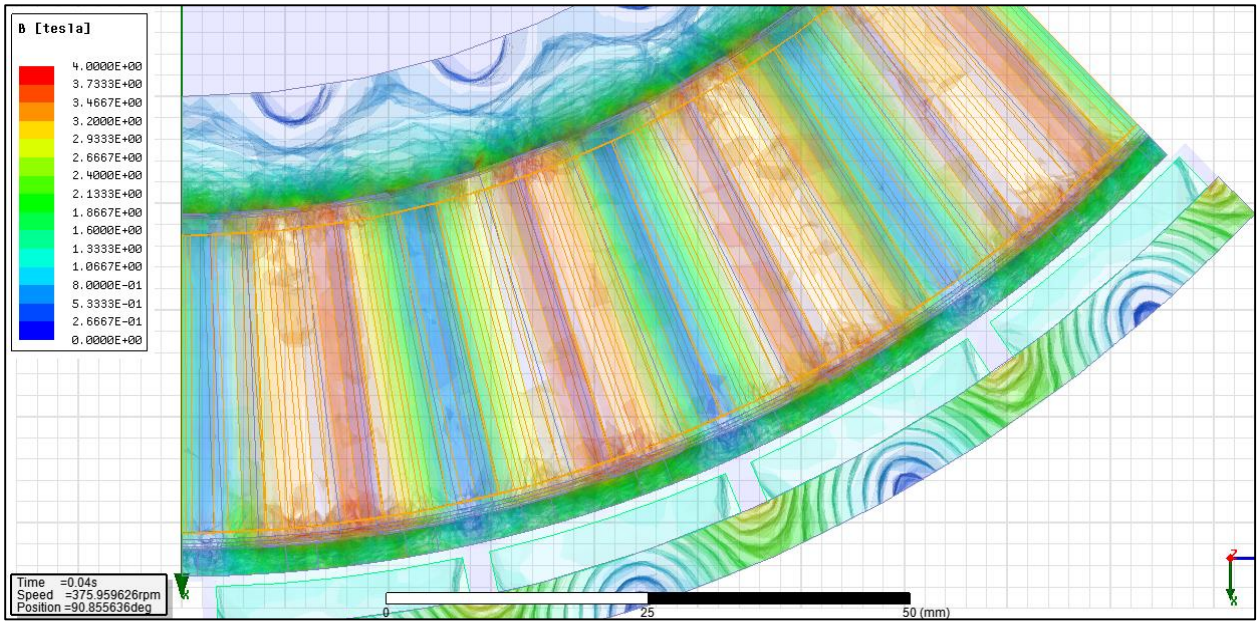

Figur1e 106c: Magnetic Field Strength (Streamlined Vector) (T)

6.9.1.1: Observations:

The moving torque is pulsating between 43 Nm to 30 Nm every 2 ms, the characteristic has sharp peaks and dips which reflect itself in the winding currents waveform, the winding current has sharp pulsation in each half cycle with an approximate magnitude of 18 A over a period of 1.2 ms with a period of 10 ms. Magnetic field density plots show a magnitude of 3 T and excess in some of the stator teeth, this value is at the operating limit of the magnetic field density in the electrical steel. It is interesting to note that the field density exactly in the central section of the rotor core behind the permanent magnet is very low compared to the side sections, this is the case with all the models.

7. 2D/3D Observations and Result Analysis:

Tabulated below are the observations from the 2D and 3D plots and field overlays.

Machine	2D Model	3D Model
24 Slot, 16 Pole	9959 Triangular Units	47655 Tetrahedra
	Moving Torque: 1. Rise Time: 11.21 ms 2. Value: 10.30 Nm 3. Pulsation: 8.4 Nm, 3.40 ms 4. Crest Factor: 1.66 5. Ripple: 43.97	Moving Torque: 1. Rise Time: 7.13 ms 2. Value: 13.89 Nm 3. Pulsation: 5.21 Nm, 1.79 ms 4. Crest Factor: 1.21 5. Ripple: 14.30
	Winding Currents: 1. RMS: 4.2 A 2. Crest Factor: 1.72 3. Rise Time: 5.81 ms 4. di/dt: 2.05 A/s	Winding Currents: 1. RMS = 272 A 2. Crest Factor: 1.37 3. Rise Time: 3.71 ms 4. di/dt: 54.83 A/s
	Induced Voltages: 1. RMS: 19.1 V 2. Distortion: 23 3. Frequency: 48.7 Hz 4. Crest Factor: 1.63	Induced Voltages: 1. RMS: 7.5 V 2. Distortion: 9000 3. Frequency: 76.27 Hz 4. Crest Factor: 4
	Stranded Losses: 1. Average: 2.85 W 2. Maximum: 4.91 W	Stranded Losses: 1. Average: 20.64 kW 2. Maximum: 34.53 kW
	Flux Linkages: 1. RMS: 0.0296 Wb 2. Crest Factor: 1.28	Flux Linkages: 1. RMS: 0.0273 Wb 2. Crest Factor: 1.38
36 Slot, 16 Pole	28795 Triangular Units	116700 Tetrahedra
	Moving Torque: 1. Rise Time: 7.40 ms 2. Value: 20.67 Nm 3. Pulsation: 11.28 Nm, 2.6 ms 4. Crest Factor: 1.28 5. Ripple: 24.29	Moving Torque: 1. Rise Time: 2.72 ms 2. Value: 17.21 Nm 3. Pulsation: 6.5 Nm, 2 ms 4. Crest Factor: 1.22 5. Ripple: 14.53
	Winding Currents: 1. RMS: 13.55 A 2. Crest Factor: 1.61 3. Rise Time: 7.66 ms 4. di/dt: 2.86 A/s	Winding Currents: 1. RMS: 319.75 A 2. Crest Factor: 1.30 3. Rise Time: 2.72 ms 4. di/dt: 165.83 A/s
	Induced Voltages: 1. RMS: 20 V 2. Distortion: 90 3. Frequency: 63.57 Hz 4. Crest Factor: 1.80	Induced Voltages: 5. RMS: 6.5 V 6. Distortion: 1500 7. Frequency: 94.6 Hz 8. Crest Factor: 8

	Stranded Losses: 1. Average: 4.42 W 2. Maximum: 7.80 W	Stranded Losses: 1. Average: 3.49 kW 2. Maximum: 4.52 kW
	Flux Linkages: 1. RMS: 0.053 Wb 2. Crest Factor: 1.32	Flux Linkages: 1. RMS: 0.068 Wb 2. Crest Factor: 1.40
48 Slot, 22 Pole	60697 Triangular Units	243530 Tetrahedra
	Moving Torque: 6. Rise Time: 9 ms 7. Value: 36.68 Nm 8. Pulsation: 14 Nm, 3.37 ms 9. Crest Factor: 1.2198 10. Ripple: 21.36	Moving Torque: 6. Rise Time: 6 ms 7. Value: 38.6Nm 8. Pulsation: 14.8 Nm, 2.4ms 9. Crest Factor: 1.312 10. Ripple: 25.15
	Winding Currents: 5. RMS: 29.5 A 6. Crest Factor: 1.57 7. Rise Time: 3.61 ms 8. di/dt: 39.75 A/s	Winding Currents: 5. RMS = 26 A 6. Crest Factor: 1.77 7. Rise Time: 2.4 ms 8. di/dt: 53.03 A/s
	Induced Voltages: 9. RMS: 20 V 10. Distortion: 86 11. Frequency: 53.24 Hz 12. Crest Factor: 1.86	Induced Voltages: 5. RMS: 19 V 6. Distortion: 50 7. Frequency: 80.25 Hz 8. Crest Factor: 1.78
	Stranded Losses: 3. Average: 28.3 W 4. Maximum: 46.21 W	Stranded Losses: 3. Average: 25.9 W 4. Maximum: 47.44 W
	Flux Linkages: 3. RMS: 0.0390 Wb 4. Crest Factor: 1.40	Flux Linkages: 3. RMS: 0.060 Wb 4. Crest Factor: 1.32
72 Slot, 32 Pole	22631 Triangular Units	89509 Tetrahedra
	Moving Torque: 1. Rise Time: 4.15 ms 2. Value: 19.77 Nm 3. Pulsation: 5.44 Nm, 0.97 ms 4. Crest Factor: 1.19 5. Ripple: 14.81	Moving Torque: 1. Rise Time: 4.15 ms 2. Value: 42 Nm 3. Pulsation: 13.14 Nm, 0.20 ms 4. Crest Factor: 1.21 5. Ripple: 16.44
	Winding Currents: 1. RMS: 12.6 A 2. Crest Factor: 1.60 3. Rise Time: 4.15 ms 4. di/dt: 4.85 A/s	Winding Currents: 1. RMS = 28.8 A 2. Crest Factor: 1.58 3. Rise Time: 4.15 ms 4. di/dt: 11.91 A/s

	Induced Voltages: 13. RMS: 19.5 V 14. Distortion: 67 15. Frequency: 107.41 Hz 16. Crest Factor: 1.80	Induced Voltages: 9. RMS: 18.4 V 10. Distortion: 64 11. Frequency: 106.65 Hz 12. Crest Factor: 1.64
	Stranded Losses: 5. Average: 2.85 W 6. Maximum: 4.91 W	Stranded Losses: 5. Average: 20.64 W 6. Maximum: 34.53 W
	Flux Linkages: 5. RMS: 0.0296 Wb 6. Crest Factor: 1.28	Flux Linkages: 5. RMS: 0.0273 Wb 6. Crest Factor: 1.38

Table 39: 2D and 3D Plot and Filed Observations

7.1. 2D & 3D Result Analysis:

Considering the resulting waveforms of torque, winding currents, induced voltages, stranded losses and flux linkages. It was observed that 24 Slot and 36 Slot Machines the moving torque for both 2D and 3D models were in agreement, the winding currents for the 3D model has abnormally high value of 300 – 600 A as compared to the 2D model which consequently resulted in high stranded losses in orders of kW, which is not true or practical, also the induced voltage waveforms for the 3D model were highly distorted. The flux linkages for both the models were in agreement with each other. For the 36 Slot and 72 Slot Machines all waveform characteristics were in complete agreement with each other except some minor fluctuations. The magnitude of waveform parameters were also in practical limits for 48 and 72 Slot Machines. This flaw in simulation result could be due to errors in converting a 2D RMxprt design to a Maxwell 3D design.

8. Conclusion:

The BLDC Machine was chosen as a motor for a high-performance e-bike. Scientific literature review and analytical model of the machine led to estimation of rated operating parameters. Four Models of a 1500 W, 48 V, 380 Rpm, 40 Nm motor were designed and simulated in Maxwell 2D and 3D. Initial machine analysis in RMxprt module of Maxwell revealed that the Transistor/Diode Drop along with the type of steel used influenced the efficiency of the machines greatly. It is advisable to have stator slot fill factors in practical limits and skewed slots to minimize cogging. 2D Analysis results reveal excessive magnetic flux densities in the stator teeth of the 24 Slot and 36 Slot Machines. The torque pulsations and wave form distortion were prominent in 24 and 36 Slot machines as compared to 48 and 72 Slot Machines. Winding currents for all machines had nominal magnitude and minor harmonics. 3D Plots show densities of 4T and excess in isolated place at the back of the lamination stack in 48 Slot and 72 Slot motor. Overall we can say that, for the decided application a higher slot and pole number BLDC machine is preferred. The increase in weight and dimensions due to high slot number is compensated well by increase in efficiency, motor constants and decrease in thermal & electrical loading. The 72 Slot, 32 Pole Machine matches best our desired performance due to its nominal magnetic field densities, lower current density, lower losses and proximity to rated operating parameters along with accordance with current similar power machines in the market make it a viable choice.

Parameters	**24 S, 16 P**	**36 S, 16 P**	**48 S, 22 P**	**72 S, 22 P**
Number of Conductors per Slot:	15	12	9	6
Length of Stator Core (mm):	50	50	50	47
Wire Diameter (mm)	1.369	1.369	1.369	1.369
Outer Diameter of Stator (mm):	180	220	240	270
Outer Diameter of Rotor (mm):	200	240	262	290
Armature Phase Resistance (Ω):	0.030	0.0253	0.025	0.021
Back-EMF Constant K_E (V/rad):	0.908	0.89	0.97	1
Torque Constant K_T (Nm/A):	1.06	0.57	1.04	1.06
Stator Slot Fill Factor (%):	60.32	61.44	68.72	53.92
Type of Steel:	M100-23P	M100-23P	M100-23P	M100-23P
Total Net Weight (kg):	7.36759	9.30647	11.57	10.4
Air-Gap Flux Density (T):	0.927284	0.92	0.92	0.91
Stator-Teeth Flux Density (T):	3.95	3.68	3.1	3.43
RMS Armature Current (A):	36.23	32.72	32.22	31.57
Stator Current Density (A/mm^2):	4.92	3.70	3.64	3.57
Iron-Core Loss (W):	0.0045419	0.0059985	0.0065836	0.0117751
Armature Copper Loss (W):	69.8671	81.2904	77.0654	64.2301
Transistor Loss (W):	159.186	154.496	152.614	150.263
Diode Loss (W):	11.5828	6.37652	5.51832	4.56598
Total Loss (W)	272.741	277.608	264.996	248.334
Output Power (W)	1500.21	1500.25	1500.14	1500.1
Input Power	1772.95	1777.86	1765.14	1748.43
Efficiency (%):	82.20	84.3853	84.9872	85.7968
Rated Speed (rpm):	359	407.744	378.866	375.96
Rated Torque (N.m):	39.92	35.13	37.8109	38.1022
No Load Speed (rpm)	465.25	473.53	434.62	422.83

Table 40: Solution Summary

9. Bibliography

[1] O. Bolton, "Electrical bicycle". Canton, Ohio Patent US 552271 A, 19 September 1895.

[2] Faulhaber Group, "www.micromo.com," [Online]. Available: http://static.micromo.com/media/wysiwyg/Technical-library/Brushless/Brushless_Application_Advantage_WP.pdf.

[3] P. T. T.G. Wilson, "D.C. Machine. With Solid State Commutation," *AIEE,* 1962.

[4] Pushek Madaan, Cypress Semiconductor, "www.edn.com," 11 February 2013. [Online]. Available: http://www.edn.com/design/sensors/4406682/Brushless-DC-Motors---Part-I--Construction-and-Operating-Principles.

[5] H. T. W. I. Muhammad Nizam, "Design of Optimal Outer Rotor Brushless DC for Minimum Cogging Torque," in *Joint International Conference on Rural Information & Communication Technology and Electric-Vehicle Technology (rICT & ICeV-T),* Bandung-Bali, Indonesia, 2013.

[6] Beikimco, "www.beikimco.com," [Online]. Available: http://www.beikimco.com/resources-downloads/about-bldc-motors/what-is-a-brushless-DC-motor.

[7] Honeywell, "www.digikey.com," June 2012. [Online]. Available: http://www.digikey.com/Web%20Export/Supplier%20Content/HoneywellSC_480/PDF/honeywell-an-ss-hall-effects.pdf.

[8] Microchip Technology Inc., "www.microchip.com," 2007. [Online]. Available: http://ww1.microchip.com/downloads/en/AppNotes/01083a.pdf.

[9] Atmel Corporation, "www.atmel.com," 2005. [Online]. Available: http://www.atmel.com/images/doc8012.pdf.

[10] A. Reinap, "Design of Powder Core Motors," Department of Industrial Electrical Engineering and Automation, Lund University , Lund, Sweden, 2004.

[11] M.-F. H. M. P. L. E. D. A. S. a. V. G. David G. Dorrell, "A Review of the Design Issues and Techniques for Radial-Flux Brushless Surface and Internal Rare-Earth Permanent-Magnet Motor," *IEEE TRANSACTIONS ON INDUSTRIAL ELECTRONICS,* vol. 58, no. 9, pp. 3741 - 3757, 2011.

[12] A. B. Nishtha Shrivastava, "Design of 3-Phase BLDC Motor for Electric Vehicle Application by Using Finite Element Simulation.," *International Journal of Emerging Technology and Advanced Engineering,* vol. IV, no. 1, pp. 140-145, 2014.

[13] P. S. A. v. d. B. Isabelle Hofman, "Influence of Soft-Magnetic Material in a Permanenet Magnet Synchronous Machine With a Commerical Induction Machine Stator," IEEE Transcations on Magnetics, Belgium, 2012.

[14] N. Abdolamir, "Design a single-phase BLDC Motor and Finite- Element Analysis of Stator Slots Structure Effects on the Efficiency," *International Journal of Electrical, Computer, Energetic, Electronic and Communication Engineering,* pp. 685 - 692, 2011.

[15] Magna Physics Corporation, James R. Hendershot, "Brushless DC Motor Phase, Pole & Slot Configurations," Hillsboro, Ohio.

[16] ANSYS, "ANSYS MAXWELL," January 2016. [Online]. Available: http://www.ansys.com/Products/Electronics/ANSYS-Maxwell.

[17] R. Nave, "www.hyperphysics.com," [Online]. Available: http://hyperphysics.phy-astr.gsu.edu/hbase/electric/maxeq.html#c1.

[18] Ansoft - ANSYS, "www.ansys.com," Ansoft, 2016. [Online]. Available: http://www.ansys.com/Products/Electronics/ANSYS-RMxprt.

[19] ANSYS, Inc, "www.scribid.com," June 2015. [Online]. Available: https://www.scribd.com/doc/129666336/RMxprt-Manual-pdf.

[20] V. P. Buhr Karel, "ANALYSIS OF THE ELECTRIC VEHICLE WITH THE BLDC PM MOTOR IN THE WHEEL BODY," Prague.

[21] S. T. L. J. H. R. K. T. C. Bo Long, "Energy-Regenerative Braking Control of Electric Vehicles Using Three-Phase Brushless Direct-Current Motors," *energies,* vol. 7, pp. 99-114, 2014.

[22] UNEP, "www.unep.org," UNEP, 2000. [Online]. Available: http://www.unep.org/transport/gfei/autotool/approaches/information/test_cycles.asp#European.

[23] Ansys , "Lecture 6: Meshing and Mesh Operations ANSYS Maxwell V16 Training Manual," 21 May 2013. [Online]. Available: http://ansoft-maxwell.narod.ru/en/Maxwell_v16_L06_Mesh_Operations.pdf.

[24] D. Koeppel, "Flight of the Pigeon," *Bicycling (Rodale, Inc.),* January 2007.

[25] V. V. H. Adrian Christen, "Analysis of a Six- and Three-Phase Interior Permanentmagnet Synchronous Machine with Flux Concentration for an Electrical Bike," in *International Symposium on Power Electronics, Electrical Drives, Automation and Motion,* Horw-Lucerne, Switzerland, 2014.

Appendix 1: 24 Slot, 16 Pole Machine Solution Set:

GENERAL DATA	
Rated Output Power (kW):	1.5
Rated Voltage (V):	48
Number of Poles:	16
Given Rated Speed (rpm):	380
Frictional Loss (W):	10
Windage Loss (W):	20
Rotor Position:	Outer
Type of Load:	Constant Power
Type of Circuit:	Y3
Lead Angle of Trigger in Elec. Degrees:	0
Trigger Pulse Width in Elec. Degrees:	120
One-Transistor Voltage Drop (V):	2
One-Diode Voltage Drop (V):	2
Operating Temperature (C):	75
Maximum Current for CCC (A):	0
Minimum Current for CCC (A):	0
STATOR DATA	
Number of Stator Slots:	24
Outer Diameter of Stator (mm):	180
Inner Diameter of Stator (mm):	90
Type of Stator Slot:	4
Stator Slot	
hs0 (mm):	4
hs1 (mm):	4
hs2 (mm):	30
bs0 (mm):	3
bs1 (mm):	15
bs2 (mm):	7
rs (mm):	0.6
Top Tooth Width (mm):	6.53136
Bottom Tooth Width (mm):	6.63135
Skew Width (Number of Slots)	0.5
Length of Stator Core (mm):	50
Stacking Factor of Stator Core:	0.95
Type of Steel:	M100-23P
Designed Wedge Thickness (mm):	1
Slot Insulation Thickness (mm):	0.5
Layer Insulation Thickness (mm):	0.5
End Length Adjustment (mm):	2
Number of Parallel Branches:	1

Number of Conductors per Slot:	15
Type of Coils:	21
Average Coil Pitch:	1
Number of Wires per Conductor:	6
Wire Diameter (mm):	1.369
Wire Wrap Thickness (mm):	0.2
Slot Area (mm^2):	399.178
Net Slot Area (mm^2):	321.76
Limited Slot Fill Factor (%):	75
Stator Slot Fill Factor (%):	68.8583
Coil Half-Turn Length (mm):	66.786
ROTOR DATA	
Minimum Air Gap (mm):	1
Outer Diameter (mm):	200
Length of Rotor (mm):	50
Stacking Factor of Iron Core:	0.95
Type of Steel:	M100-23P
Polar Arc Radius (mm):	91
Mechanical Pole Embrace:	0.9
Electrical Pole Embrace:	0.884254
Max. Thickness of Magnet (mm):	4
Width of Magnet (mm):	31.9949
Type of Magnet:	NdFe35
Type of Rotor:	1
Magnetic Shaft:	No
PERMANENT MAGNET DATA	
Residual Flux Density (Tesla):	1.23
Coercive Force (kA/m):	890
Maximum Energy Density (kJ/m^3):	273.675
Relative Recoil Permeability:	1.09981
Demagnetized Flux Density (Tesla):	7.51E-05
Recoil Residual Flux Density (Tesla):	1.23
Recoil Coercive Force (kA/m):	890
MATERIAL CONSUMPTION	
Armature Copper Density (kg/m^3):	8900
Permanent Magnet Density (kg/m^3):	7400
Armature Core Steel Density (kg/m^3):	7872
Rotor Core Steel Density (kg/m^3):	7872
Armature Copper Weight (kg):	1.88984
Permanent Magnet Weight (kg):	0.778336
Armature Core Steel Weight (kg):	3.55407
Rotor Core Steel Weight (kg):	1.14534

Total Net Weight (kg):	7.36759
Armature Core Steel Consumption (kg):	9.83492
Rotor Core Steel Consumption (kg):	5.57395
STEADY STATE PARAMETERS	
Stator Winding Factor:	0.866025
D-Axis Reactive Inductance Lad (H):	1.06E-04
Q-Axis Reactive Inductance Laq (H):	1.06E-04
D-Axis Inductance L1+Lad(H):	0.0003675
Q-Axis Inductance L1+Laq(H):	0.0003675
Armature Leakage Inductance L1 (H):	0.0002613
Zero-Sequence Inductance L0 (H):	5.29E-05
Armature Phase Resistance R1 (ohm):	0.0196915
Armature Phase Resistance at 20C (ohm):	0.0161978
D-Axis Time Constant (s):	0.0053958
Q-Axis Time Constant (s):	0.0053958
Ideal Back-EMF Constant KE (Vs/rad):	0.88399
Start Torque Constant KT (Nm/A):	0.884069
Rated Torque Constant KT (Nm/A):	1.01286
NO-LOAD MAGNETIC DATA	
Stator-Teeth Flux Density (Tesla):	3.68565
Stator-Yoke Flux Density (Tesla):	2.40341
Rotor-Yoke Flux Density (Tesla):	3.1725
Air-Gap Flux Density (Tesla):	0.927284
Magnet Flux Density (Tesla):	0.95876
Stator-Teeth By-Pass Factor:	2.83E-05
Stator-Yoke By-Pass Factor:	9.09E-07
Rotor-Yoke By-Pass Factor:	8.50E-07
Stator-Teeth Ampere Turns (A.T):	1.56826
Stator-Yoke Ampere Turns (A.T):	0.246102
Rotor-Yoke Ampere Turns (A.T):	0.600627
Air-Gap Ampere Turns (A.T):	782.694
Magnet Ampere Turns (A.T):	-785.051
Armature Reactive Ampere Turns at Start Operation (A.T):	4257.22
Leakage-Flux Factor:	1
Correction Factor for Magnetic Circuit Length of Stator Yoke:	0.785552
Correction Factor for Magnetic Circuit Length of Rotor Yoke:	0.770387
No-Load Speed (rpm):	478.439
Cogging Torque (N.m):	2.16E-11
FULL-LOAD DATA	
Average Input Current (A):	36.9364
Root-Mean-Square Armature Current (A):	34.3903
Armature Thermal Load (A^2/mm^3):	85.2521

Specific Electric Loading (A/mm):	21.8936
Armature Current Density (A/mm^2):	3.89393
Frictional and Windage Loss (W):	32.1006
Iron-Core Loss (W):	0.0045419
Armature Copper Loss (W):	69.8671
Transistor Loss (W):	159.186
Diode Loss (W):	11.5828
Total Loss (W):	272.741
Output Power (W):	1500.21
Input Power (W):	1772.95
Efficiency (%):	84.6165
Rated Speed (rpm):	391.121
Rated Torque (N.m):	36.6278
Locked-Rotor Torque (N.m):	986.927
Locked-Rotor Current (A):	1116.63
WINDING ARRANGEMENT	
The 3-phase, 2-layer winding can be arranged in 6 slots as below:	ABCABC
Angle per slot (elec. degrees):	120
Phase-A axis (elec. degrees):	60
First slot center (elec. degrees):	0
TRANSIENT FEA INPUT DATA	
For Armature Winding:	
Number of Turns:	60
Parallel Branches:	1
Terminal Resistance (ohm):	0.0196915
End Leakage Inductance (H):	1.53E-06
2D Equivalent Value:	
Equivalent Model Depth (mm):	50
Equivalent Stator Stacking Factor:	0.95
Equivalent Rotor Stacking Factor:	0.95
Equivalent Br (Tesla):	1.23
Equivalent Hc (kA/m):	890
Estimated Rotor Moment of Inertia (kg m^2):	0.0585181

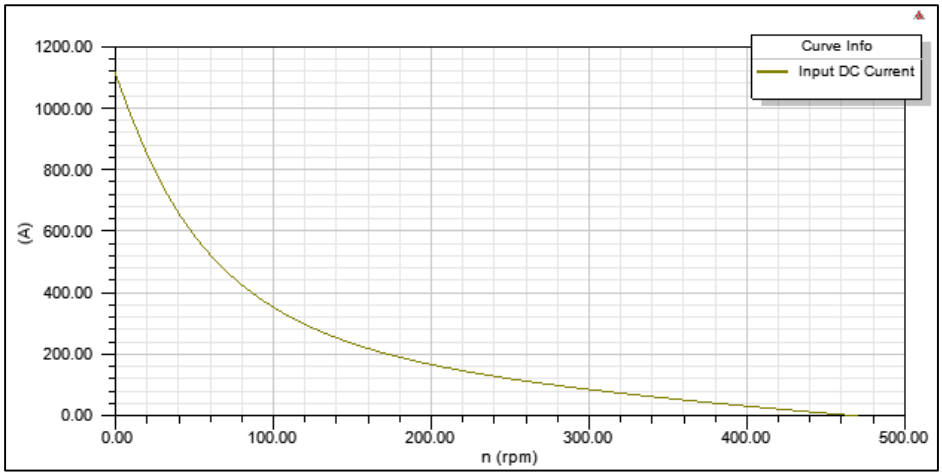

Input DC Current V/s Speed

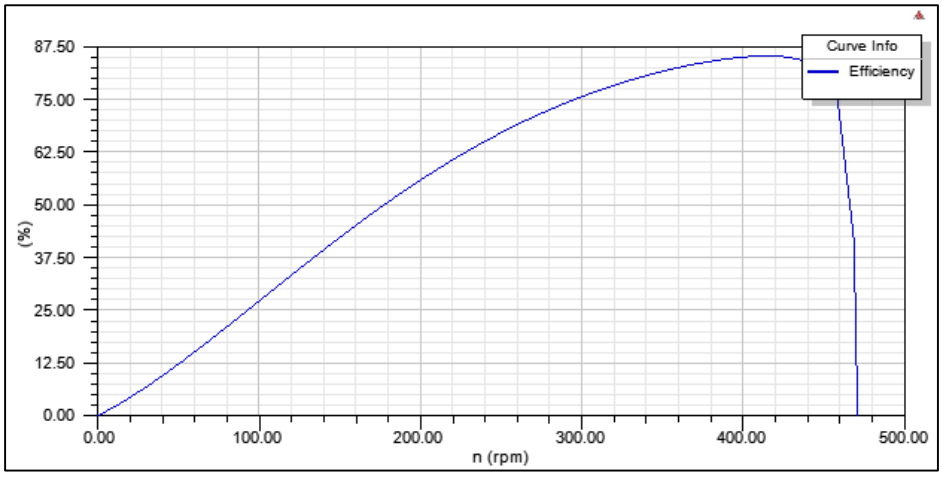

Efficiency V/s Speed

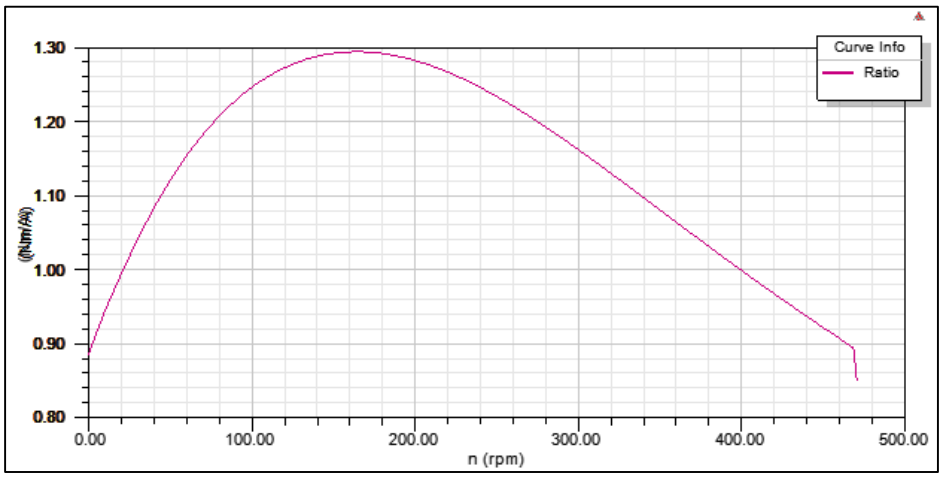

Ratio of Air-Gap Torque to DC Current V/s Speed

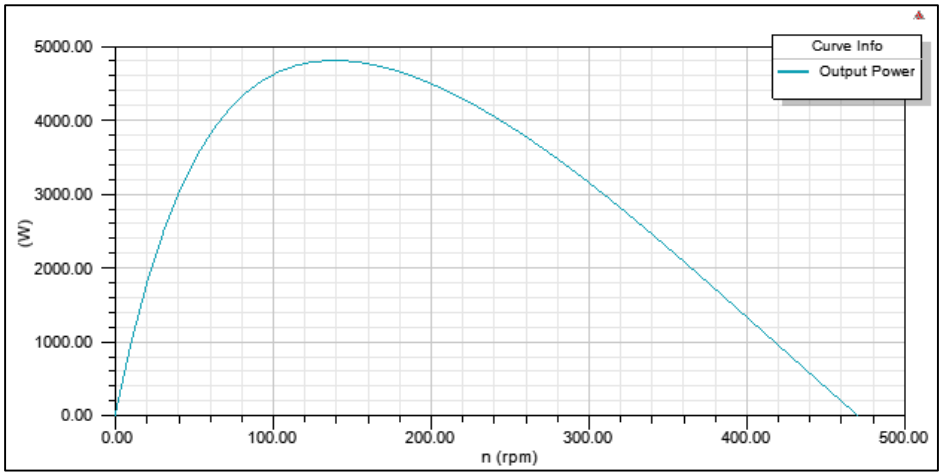

Output Power V/s Speed

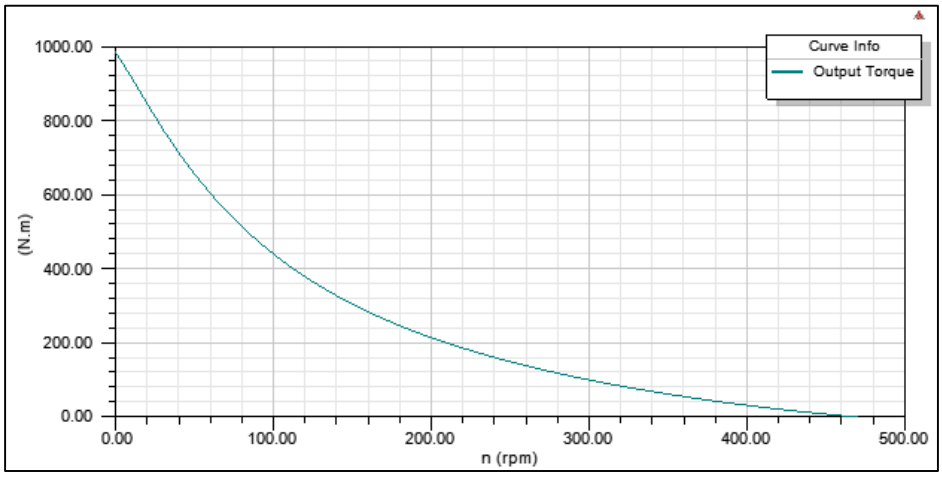

Output Torque V/s Speed

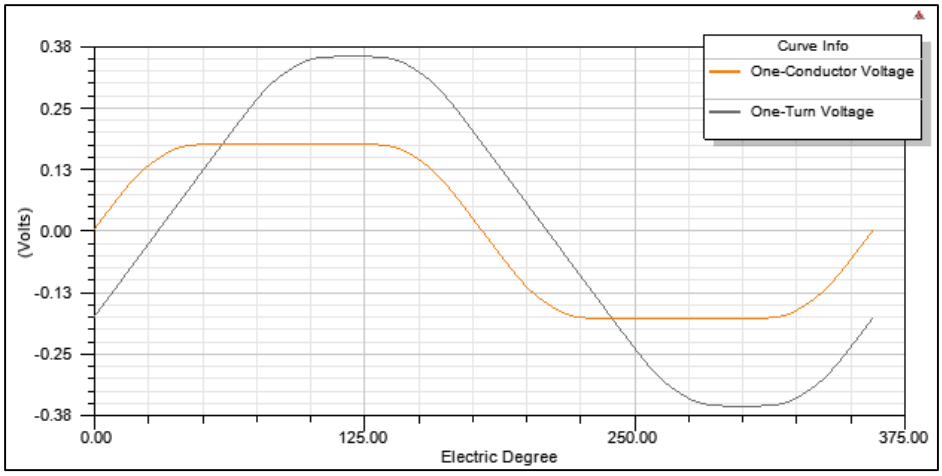

Induced Coil Voltages at rated Speed

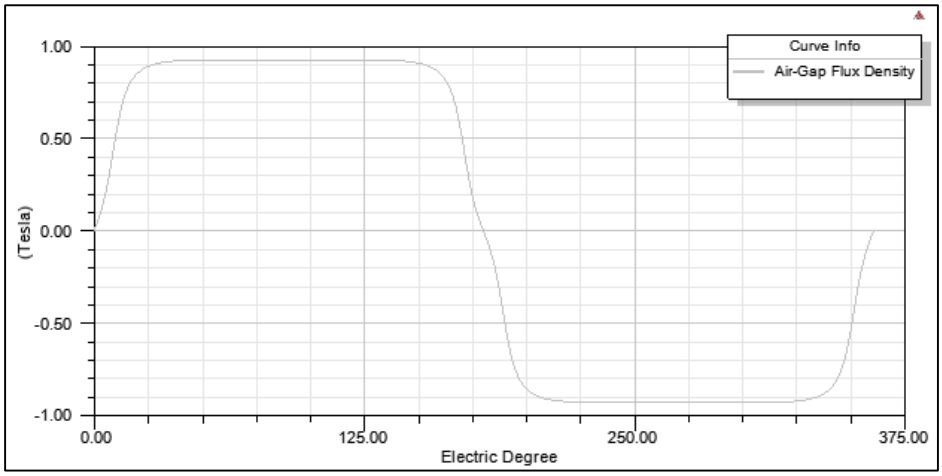

Air-Gap Flux Density

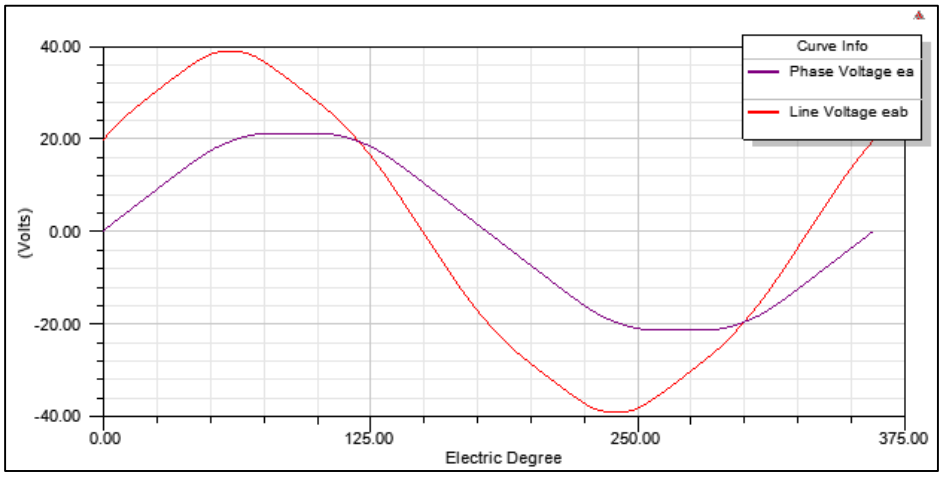

Induced Winding Voltages at Rated Speed

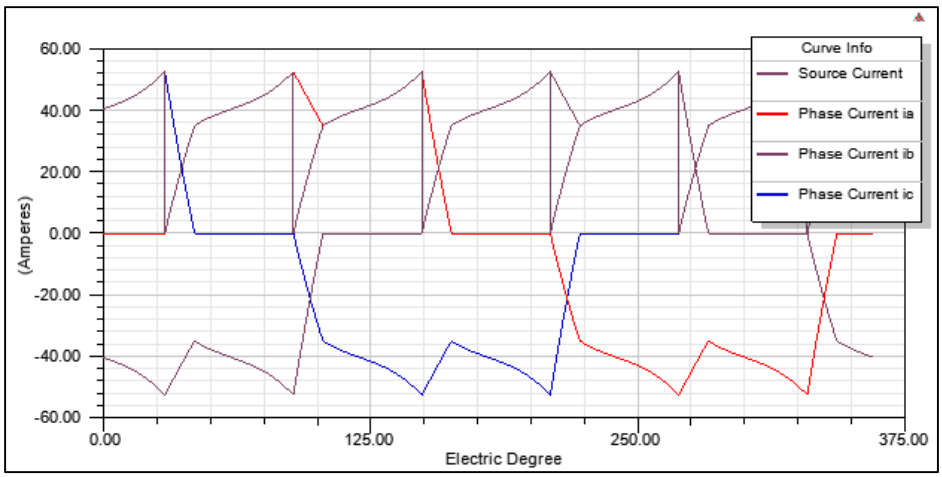

Winding Currents under Load

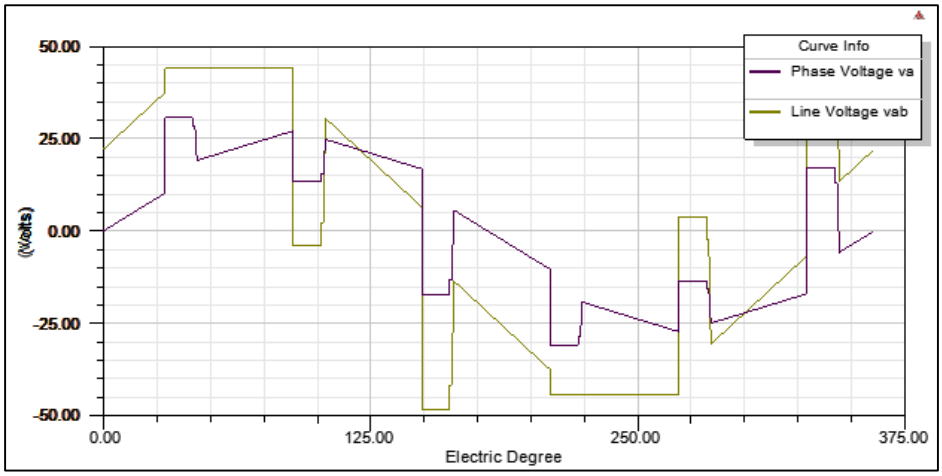

Winding Voltages under Load

Appendix 2: 36 Slot, 16 Pole Machine Solution Set:

GENERAL DATA	
Rated Output Power (kW):	1.5
Rated Voltage (V):	48
Number of Poles:	16
Given Rated Speed (rpm):	500
Frictional Loss (W):	13.1579
Windage Loss (W):	45.5606
Rotor Position:	Outer
Type of Load:	Constant Power
Type of Circuit:	Y3
Lead Angle of Trigger in Elec. Degrees:	0
Trigger Pulse Width in Elec. Degrees:	120
One-Transistor Voltage Drop (V):	2
One-Diode Voltage Drop (V):	2
Operating Temperature (C):	75
Maximum Current for CCC (A):	0
Minimum Current for CCC (A):	0
STATOR DATA	
Number of Stator Slots:	36
Outer Diameter of Stator (mm):	220
Inner Diameter of Stator (mm):	130
Type of Stator Slot:	4
Stator Slot	
hs0 (mm):	3
hs1 (mm):	2
hs2 (mm):	30
bs0 (mm):	3
bs1 (mm):	13
bs2 (mm):	8
rs (mm):	0.6
Top Tooth Width (mm):	5.35039
Bottom Tooth Width (mm):	5.10202
Skew Width (Number of Slots)	1
Length of Stator Core (mm):	50
Stacking Factor of Stator Core:	0.95
Type of Steel:	M100-23P
Designed Wedge Thickness (mm):	0.3
Slot Insulation Thickness (mm):	0.5
Layer Insulation Thickness (mm):	0.5
End Length Adjustment (mm):	5
Number of Parallel Branches:	1

Number of Conductors per Slot:	12
Type of Coils:	21
Average Coil Pitch:	1
Number of Wires per Conductor:	6
Wire Diameter (mm):	1.369
Wire Wrap Thickness (mm):	0.2
Slot Area (mm^2):	352.929
Net Slot Area (mm^2):	288.465
Limited Slot Fill Factor (%):	75
Stator Slot Fill Factor (%):	61.4448
Coil Half-Turn Length (mm):	71.502
ROTOR DATA	
Minimum Air Gap (mm):	1
Outer Diameter (mm):	240
Length of Rotor (mm):	50
Stacking Factor of Iron Core:	0.95
Type of Steel:	M100-23P
Polar Arc Radius (mm):	111
Mechanical Pole Embrace:	0.95
Electrical Pole Embrace:	0.928161
Max. Thickness of Magnet (mm):	4
Width of Magnet (mm):	41.1704
Type of Magnet:	NdFe35
Type of Rotor:	1
Magnetic Shaft:	No
PERMANENT MAGNET DATA	
Residual Flux Density (Tesla):	1.23
Coercive Force (kA/m):	890
Maximum Energy Density (kJ/m^3):	273.675
Relative Recoil Permeability:	1.09981
Demagnetized Flux Density (Tesla):	0.201572
Recoil Residual Flux Density (Tesla):	1.23
Recoil Coercive Force (kA/m):	890
MATERIAL CONSUMPTION	
Armature Copper Density (kg/m^3):	8900
Permanent Magnet Density (kg/m^3):	7400
Armature Core Steel Density (kg/m^3):	7872
Rotor Core Steel Density (kg/m^3):	7872
Armature Copper Weight (kg):	2.42795
Permanent Magnet Weight (kg):	0.99826
Armature Core Steel Weight (kg):	4.49998
Rotor Core Steel Weight (kg):	1.38028

Total Net Weight (kg):	9.30647
Armature Core Steel Consumption (kg):	14.6042
Rotor Core Steel Consumption (kg):	7.47538
STEADY STATE PARAMETERS	
Stator Winding Factor:	0.616944
D-Axis Reactive Inductance Lad (H):	9.37E-05
Q-Axis Reactive Inductance Laq (H):	9.37E-05
D-Axis Inductance L1+Lad(H):	0.0002248
Q-Axis Inductance L1+Laq(H):	0.0002248
Armature Leakage Inductance L1 (H):	0.000131
Zero-Sequence Inductance L0 (H):	0.0001843
Armature Phase Resistance R1 (ohm):	0.0252984
Armature Phase Resistance at 20C (ohm):	0.0208099
D-Axis Time Constant (s):	0.0037055
Q-Axis Time Constant (s):	0.0037055
Ideal Back-EMF Constant KE (Vs/rad):	0.892994
Start Torque Constant KT (Nm/A):	0.893053
Rated Torque Constant KT (Nm/A):	0.971026
NO-LOAD MAGNETIC DATA	
Stator-Teeth Flux Density (Tesla):	3.80224
Stator-Yoke Flux Density (Tesla):	2.10836
Rotor-Yoke Flux Density (Tesla):	4.04805
Air-Gap Flux Density (Tesla):	0.922273
Magnet Flux Density (Tesla):	0.956058
Stator-Teeth By-Pass Factor:	3.37E-05
Stator-Yoke By-Pass Factor:	9.44E-07
Rotor-Yoke By-Pass Factor:	8.09E-07
Stator-Teeth Ampere Turns (A.T):	1.51408
Stator-Yoke Ampere Turns (A.T):	0.322902
Rotor-Yoke Ampere Turns (A.T):	0.852621
Air-Gap Ampere Turns (A.T):	790.189
Magnet Ampere Turns (A.T):	-792.874
Armature Reactive Ampere Turns at Start Operation (A.T):	2808.85
Leakage-Flux Factor:	1
Correction Factor for Magnetic Circuit Length of Stator Yoke:	0.783171
Correction Factor for Magnetic Circuit Length of Rotor Yoke:	0.746887
No-Load Speed (rpm):	473.536
Cogging Torque (N.m):	4.18E-12
FULL-LOAD DATA	
Average Input Current (A):	37.0386
Root-Mean-Square Armature Current (A):	32.7275
Armature Thermal Load (A^2/mm^3):	75.8034

Specific Electric Loading (A/mm):	20.4562
Armature Current Density (A/mm^2):	3.70565
Frictional and Windage Loss (W):	35.4384
Iron-Core Loss (W):	0.0059985
Armature Copper Loss (W):	81.2904
Transistor Loss (W):	154.496
Diode Loss (W):	6.37652
Total Loss (W):	277.608
Output Power (W):	1500.25
Input Power (W):	1777.86
Efficiency (%):	84.3853
Rated Speed (rpm):	407.744
Rated Torque (N.m):	35.1355
Locked-Rotor Torque (N.m):	775.947
Locked-Rotor Current (A):	869.152
WINDING ARRANGEMENT	
The 3-phase, 2-layer winding can be arranged in 9 slots as below:	AZBCYABXC
Angle per slot (elec. degrees):	80
Phase-A axis (elec. degrees):	60
First slot center (elec. degrees):	0
TRANSIENT FEA INPUT DATA	
For Armature Winding:	
Number of Turns:	72
Parallel Branches:	1
Terminal Resistance (ohm):	0.0252984
End Leakage Inductance (H):	2.23E-06
2D Equivalent Value:	
Equivalent Model Depth (mm):	50
Equivalent Stator Stacking Factor:	0.95
Equivalent Rotor Stacking Factor:	0.95
Equivalent Br (Tesla):	1.23
Equivalent Hc (kA/m):	890
Estimated Rotor Moment of Inertia (kg m^2):	0.115407

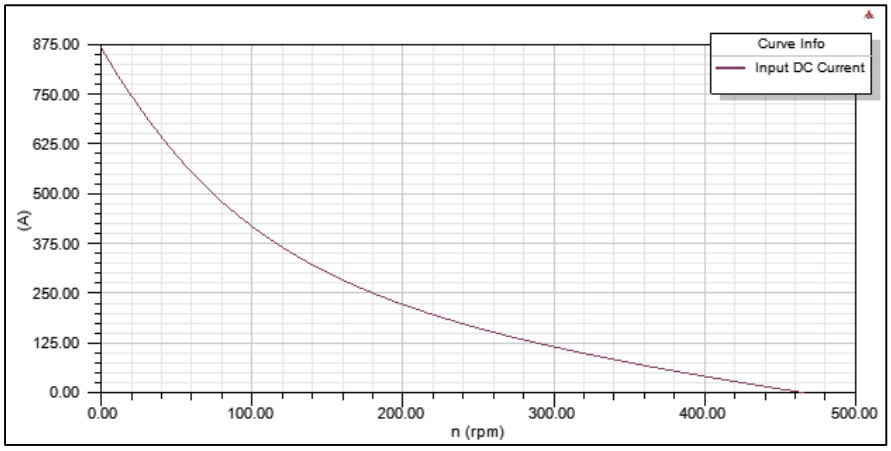

Input DC Current V/s Speed

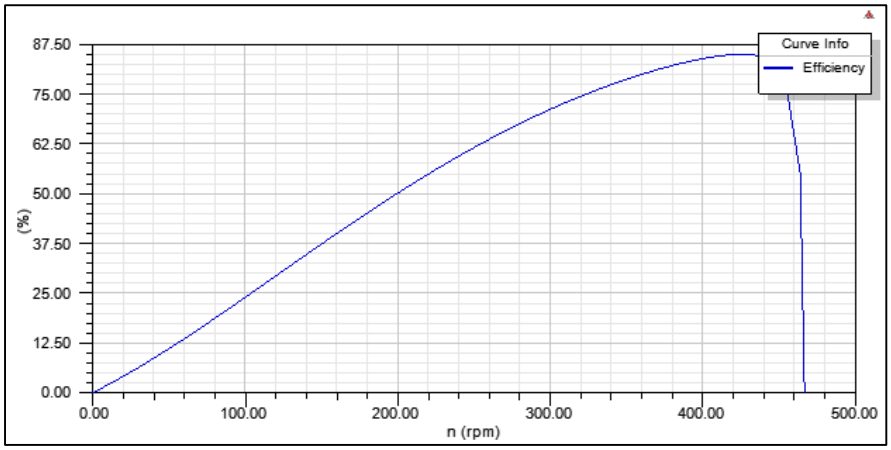

Efficiency V/s Speed

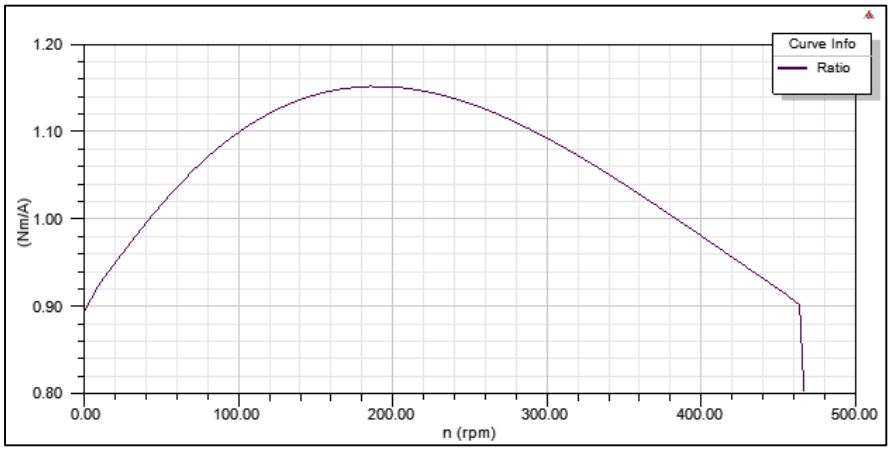

Ratio of Air-Gap torque to DC Current V/s Speed

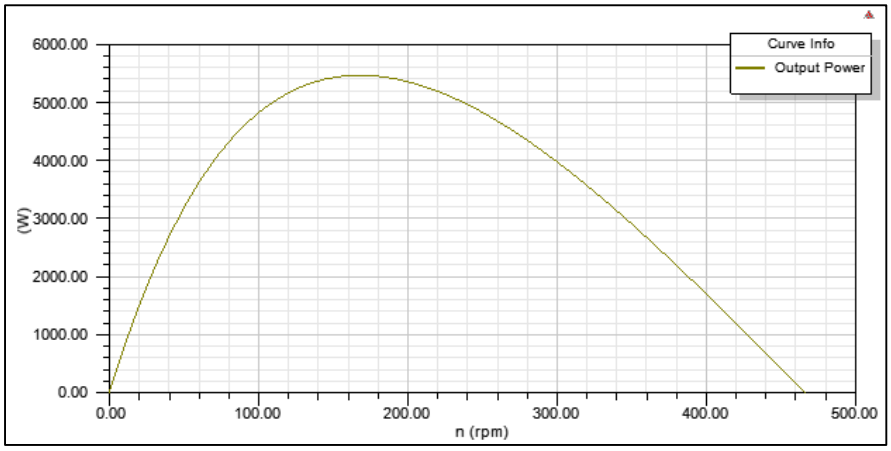

Output Power V/s Speed

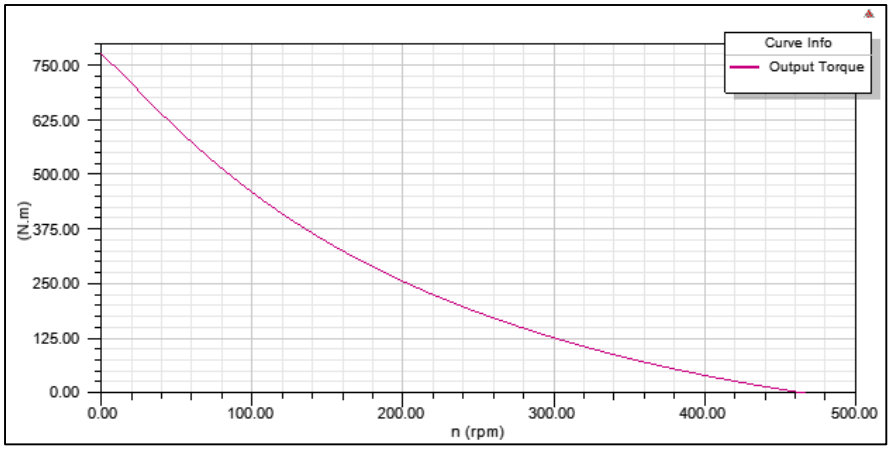

Output Torque V/s Speed

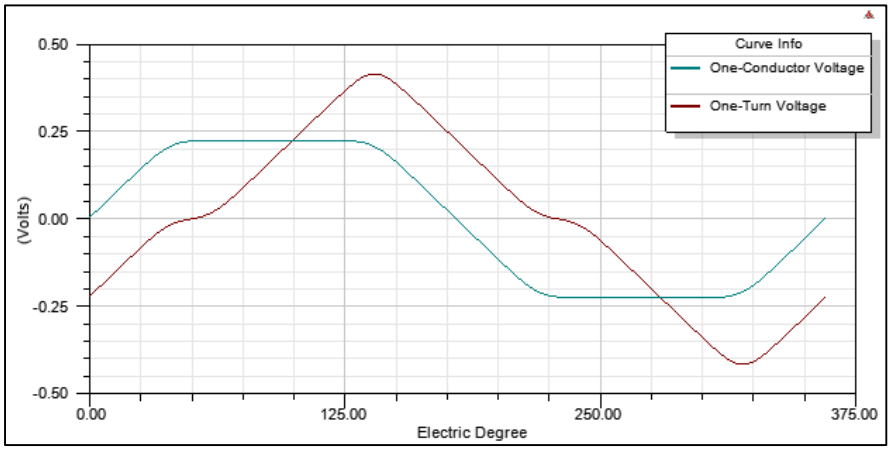

Induced Coil Voltages at Rated Speed

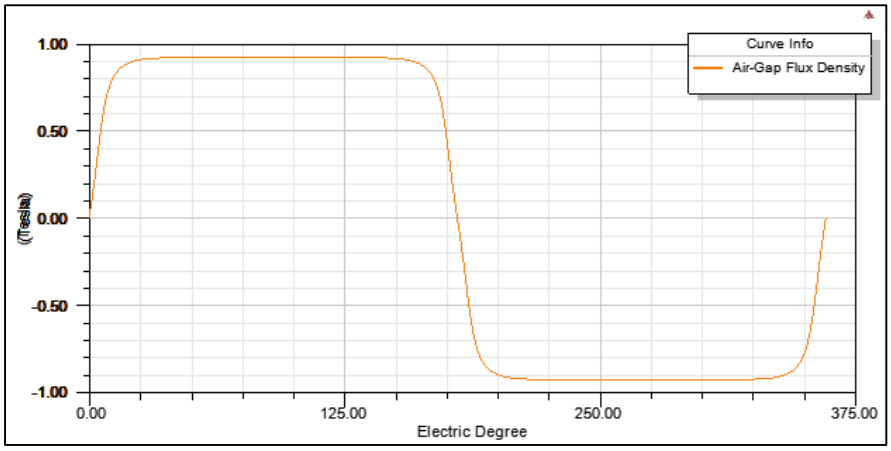

Air-Gap Flux Density

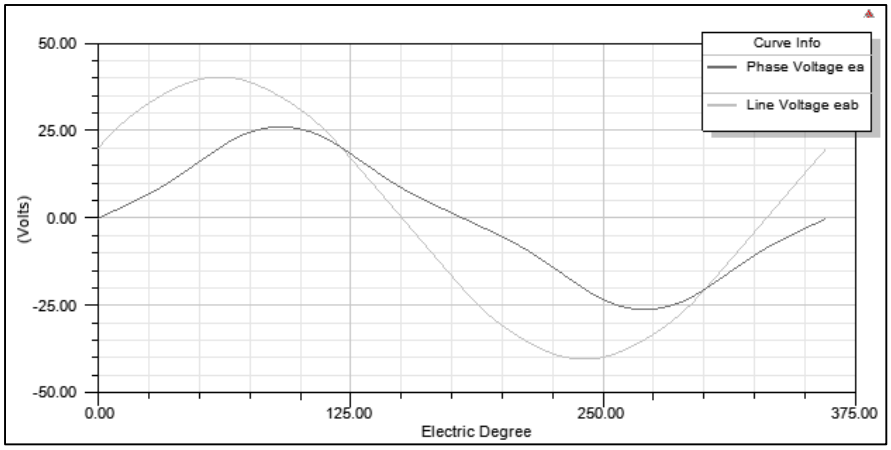

Induced Winding Voltages at Rated Speed

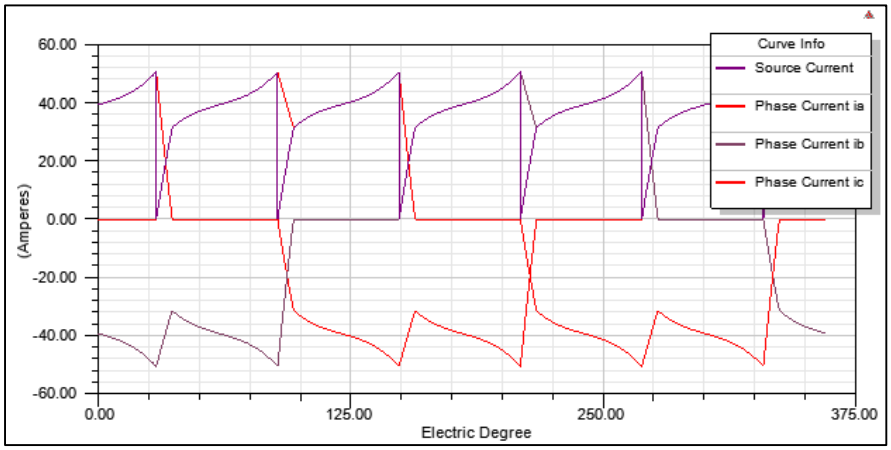

Winding Currents under Load

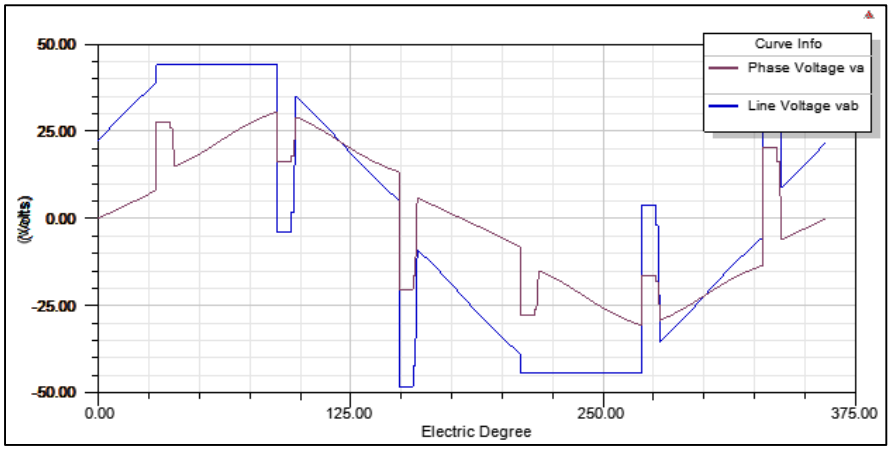

Winding Voltages under Load

Appendix 3: 48 Slot, 22 Pole Machine Solution Set:

GENERAL DATA	
Rated Output Power (kW):	1.5
Rated Voltage (V):	48
Number of Poles:	22
Given Rated Speed (rpm):	380
Frictional Loss (W):	10
Windage Loss (W):	20
Rotor Position:	Outer
Type of Load:	Constant Power
Type of Circuit:	Y3
Lead Angle of Trigger in Elec. Degrees:	0
Trigger Pulse Width in Elec. Degrees:	120
One-Transistor Voltage Drop (V):	2
One-Diode Voltage Drop (V):	2
Operating Temperature (C):	75
Maximum Current for CCC (A):	0
Minimum Current for CCC (A):	0
STATOR DATA	
Number of Stator Slots:	48
Outer Diameter of Stator (mm):	240
Inner Diameter of Stator (mm):	140
Type of Stator Slot:	4
Stator Slot	
hs0 (mm):	2
hs1 (mm):	2
hs2 (mm):	30
bs0 (mm):	3
bs1 (mm):	10
bs2 (mm):	6
rs (mm):	0.5
Top Tooth Width (mm):	5.19371
Bottom Tooth Width (mm):	5.26096
Skew Width (Number of Slots)	1
Length of Stator Core (mm):	50
Stacking Factor of Stator Core:	0.95
Type of Steel:	M100-23P
Designed Wedge Thickness (mm):	0.3
Slot Insulation Thickness (mm):	0.7
Layer Insulation Thickness (mm):	0.7

End Length Adjustment (mm):	5
Number of Parallel Branches:	1
Number of Conductors per Slot:	9
Type of Coils:	21
Average Coil Pitch:	1
Number of Wires per Conductor:	6
Wire Diameter (mm):	1.369
Wire Wrap Thickness (mm):	0.2
Slot Area (mm^2):	267.176
Net Slot Area (mm^2):	193.44
Limited Slot Fill Factor (%):	75
Stator Slot Fill Factor (%):	68.7216
Coil Half-Turn Length (mm):	69.9362
ROTOR DATA	
Minimum Air Gap (mm):	1
Outer Diameter (mm):	262
Length of Rotor (mm):	50
Stacking Factor of Iron Core:	0.95
Type of Steel:	M100-23P
Polar Arc Radius (mm):	121
Mechanical Pole Embrace:	0.9
Electrical Pole Embrace:	0.88304
Max. Thickness of Magnet (mm):	4
Width of Magnet (mm):	3.10E+01
Type of Magnet:	NdFe35
Type of Rotor:	1
Magnetic Shaft:	No
PERMANENT MAGNET DATA	
Residual Flux Density (Tesla):	1.23
Coercive Force (kA/m):	890
Maximum Energy Density (kJ/m^3):	273.675
Relative Recoil Permeability:	1.09981
Demagnetized Flux Density (Tesla):	0.376492
Recoil Residual Flux Density (Tesla):	1.23
Recoil Coercive Force (kA/m):	890
MATERIAL CONSUMPTION	
Armature Copper Density (kg/m^3):	8.90E+03
Permanent Magnet Density (kg/m^3):	7400
Armature Core Steel Density (kg/m^3):	7872
Rotor Core Steel Density (kg/m^3):	7872
Armature Copper Weight (kg):	2.37478
Permanent Magnet Weight (kg):	1.02941
Armature Core Steel Weight (kg):	6.36438

Rotor Core Steel Weight (kg):	1.80435
Total Net Weight (kg):	11.5729
Armature Core Steel Consumption (kg):	17.3413
Rotor Core Steel Consumption (kg):	8.91725
STEADY STATE PARAMETERS	
Stator Winding Factor:	0.630095
D-Axis Reactive Inductance Lad (H):	5.60E-05
Q-Axis Reactive Inductance Laq (H):	5.60E-05
D-Axis Inductance L1+Lad(H):	1.59E-04
Q-Axis Inductance L1+Laq(H):	0.0001587
Armature Leakage Inductance L1 (H):	0.0001027
Zero-Sequence Inductance L0 (H):	0.0001307
Armature Phase Resistance R1 (ohm):	0.0247444
Armature Phase Resistance at 20C (ohm):	0.0203542
D-Axis Time Constant (s):	0.0022637
Q-Axis Time Constant (s):	0.0022637
Ideal Back-EMF Constant KE (Vs/rad):	0.972909
Start Torque Constant KT (Nm/A):	0.972948
Rated Torque Constant KT (Nm/A):	1.04863
NO-LOAD MAGNETIC DATA	
Stator-Teeth Flux Density (Tesla):	3.10027
Stator-Yoke Flux Density (Tesla):	0.973274
Rotor-Yoke Flux Density (Tesla):	2.54133
Air-Gap Flux Density (Tesla):	0.920478
Magnet Flux Density (Tesla):	0.952004
Stator-Teeth By-Pass Factor:	2.70E-05
Stator-Yoke By-Pass Factor:	1.27E-06
Rotor-Yoke By-Pass Factor:	8.96E-07
Stator-Teeth Ampere Turns (A.T):	1.28673
Stator-Yoke Ampere Turns (A.T):	0.166551
Rotor-Yoke Ampere Turns (A.T):	0.49229
Air-Gap Ampere Turns (A.T):	802.471
Magnet Ampere Turns (A.T):	-804.607
Armature Reactive Ampere Turns at Start Operation (A.T):	2151.7
Leakage-Flux Factor:	1
Correction Factor for Magnetic Circuit Length of Stator Yoke:	0.799931
Correction Factor for Magnetic Circuit Length of Stator Yoke:	0.782633
No-Load Speed (rpm):	434.642
Cogging Torque (N.m):	7.81E-12
FULL-LOAD DATA	
Average Input Current (A):	36.7737
Root-Mean-Square Armature Current (A):	32.2204

Armature Thermal Load (A^2/mm^3):	67.3498
Specific Electric Loading (A/mm):	18.4609
Armature Current Density (A/mm^2):	3.64824
Frictional and Windage Loss (W):	29.7917
Iron-Core Loss (W):	0.0065836
Armature Copper Loss (W):	77.0654
Transistor Loss (W):	152.614
Diode Loss (W):	5.51832
Total Loss (W):	264.996
Output Power (W):	1500.14
Input Power (W):	1765.14
Efficiency (%):	84.9872
Rated Speed (rpm):	378.866
Rated Torque (N.m):	37.8109
Locked-Rotor Torque (N.m):	864.32
Locked-Rotor Current (A):	888.611
WINDING ARRANGEMENT	
The 3-phase, 2-layer winding can be arranged in 24 slots as below:	AZBCYABXYAZXCYZ BCYABXCAZ
Angle per slot (elec. degrees):	82.5
Phase-A axis (elec. degrees):	67.0827
First slot center (elec. degrees):	0
TRANSIENT FEA INPUT DATA	
For Armature Winding:	
Number of Turns:	72
Parallel Branches:	1
Terminal Resistance (ohm):	0.0247444
End Leakage Inductance (H):	1.56E-06
2D Equivalent Value:	
Equivalent Model Depth (mm):	50
Equivalent Stator Stacking Factor:	0.95
Equivalent Rotor Stacking Factor:	0.95
Equivalent Br (Tesla):	1.23
Equivalent Hc (kA/m):	890
Estimated Rotor Moment of Inertia (kg m^2):	0.164846

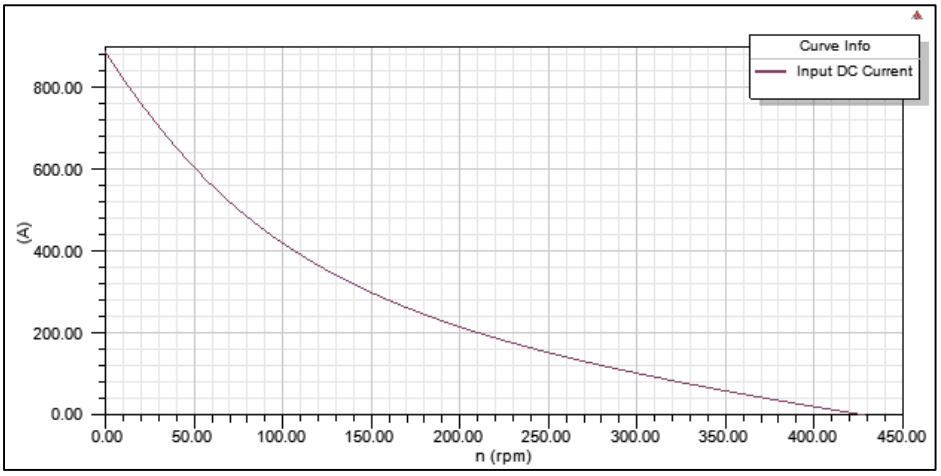

Input DC Current V/s Speed

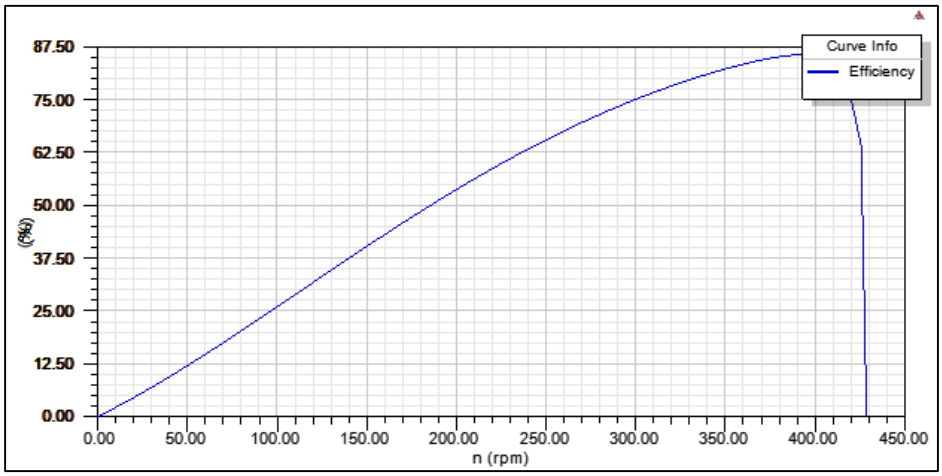

Efficiency V/s Speed

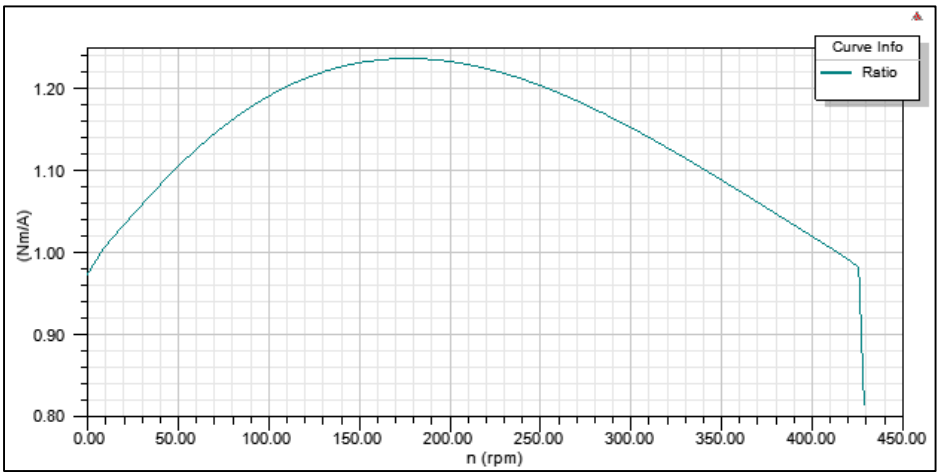

Ratio of Air-Gap Torque to DC Current V/s Speed

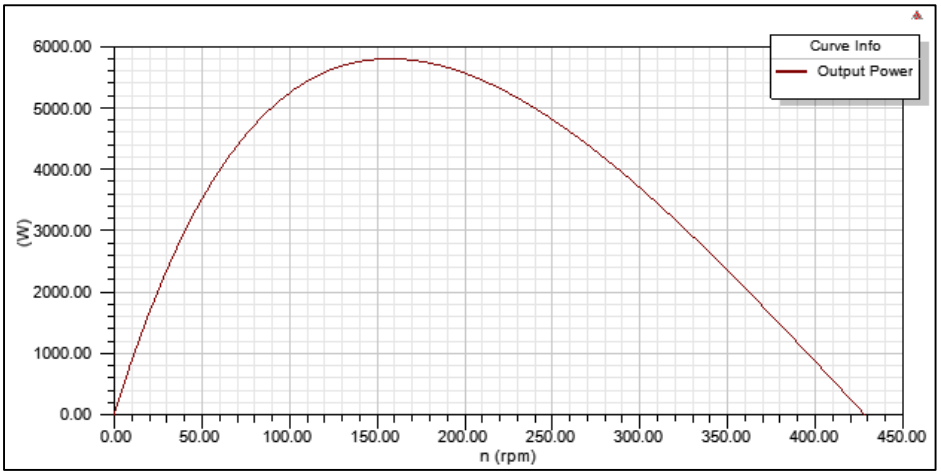

Output Power V/s Speed

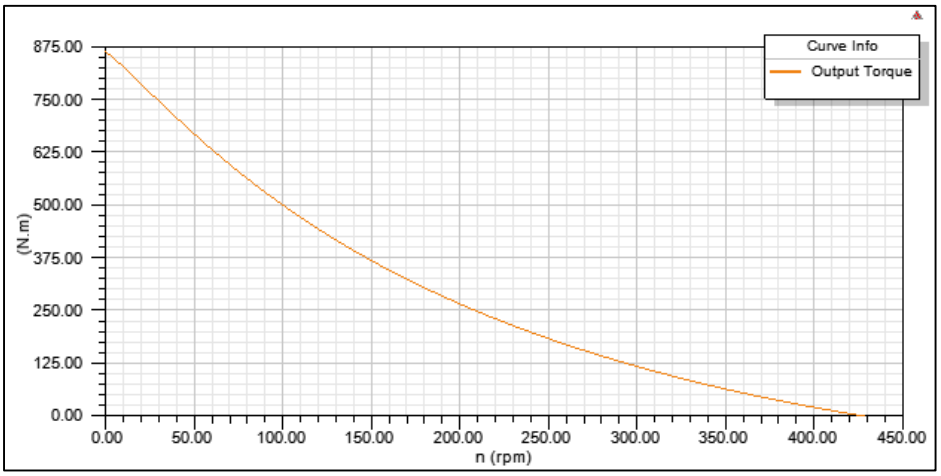

Output Torque V/s Speed

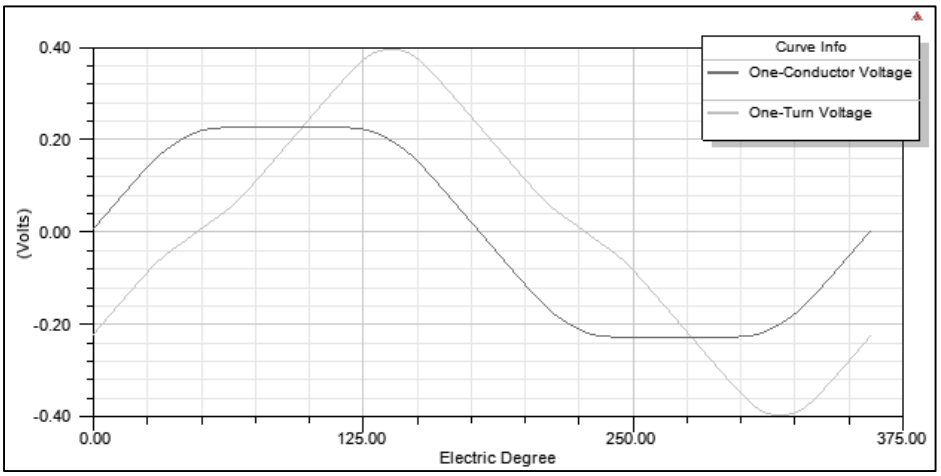

Induced Coil Voltages at Rated Speed

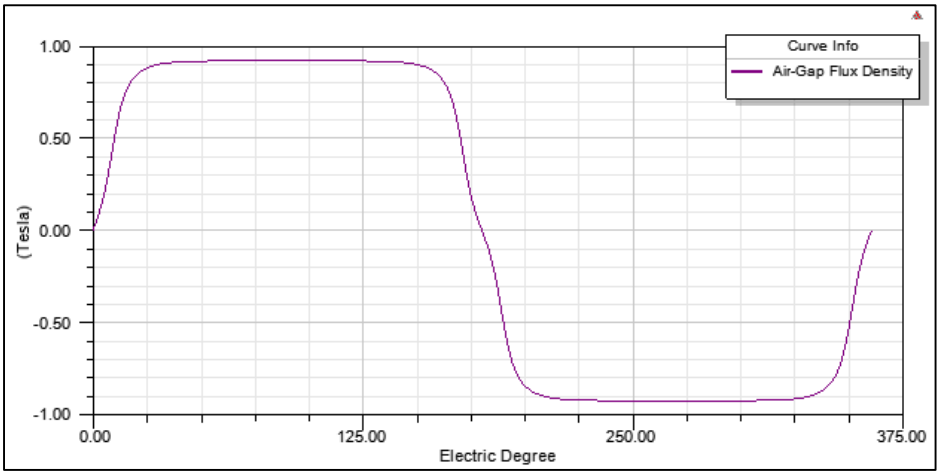

Air-Gap Flux Density

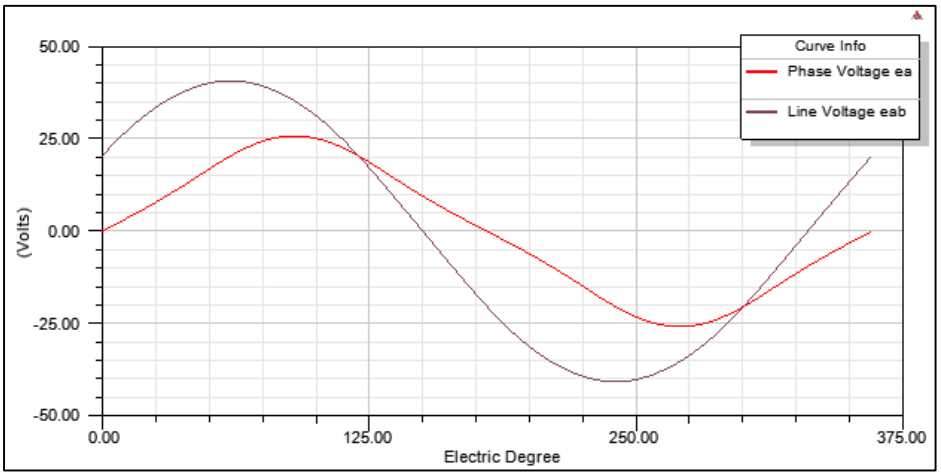

Induced Winding Voltages at Rated Speed

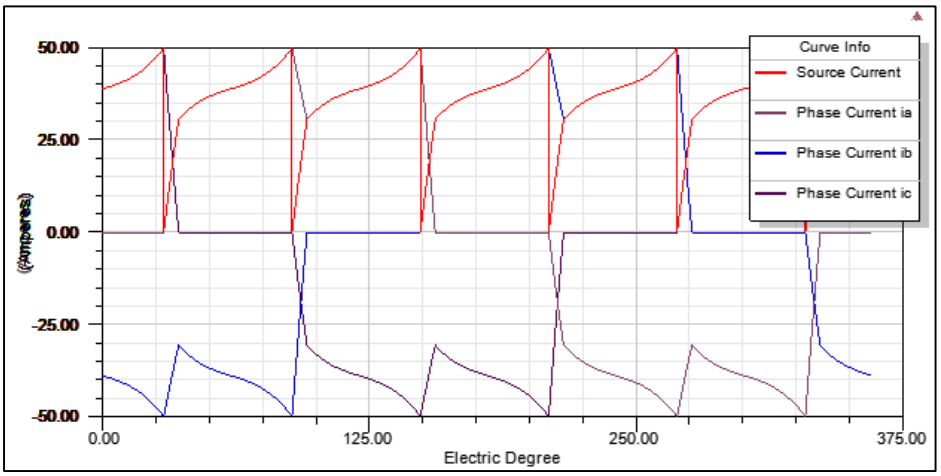

Winding Currents under Load

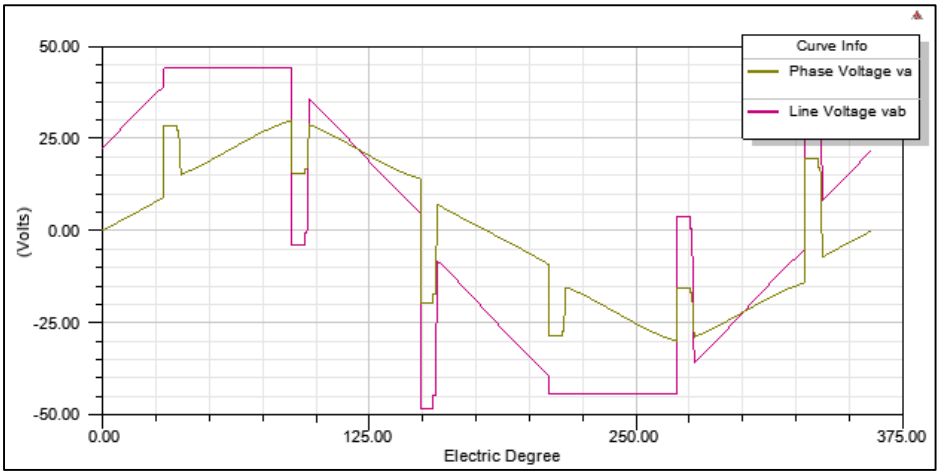

Winding Voltages under Load

Appendix 4: 72 Slot, 32 Pole Machine Solution Set:

GENERAL DATA	
Rated Output Power (kW):	1.5
Rated Voltage (V):	48
Number of Poles:	32
Given Rated Speed (rpm):	330
Frictional Loss (W):	8.68421
Windage Loss (W):	13.0985
Rotor Position:	Outer
Type of Load:	Constant Power
Type of Circuit:	Y3
Lead Angle of Trigger in Elec. Degrees:	0
Trigger Pulse Width in Elec. Degrees:	120
One-Transistor Voltage Drop (V):	2
One-Diode Voltage Drop (V):	2
Operating Temperature (C):	75
STATOR DATA	
Number of Stator Slots:	72
Outer Diameter of Stator (mm):	270
Inner Diameter of Stator (mm):	180
Type of Stator Slot:	4
Stator Slot	
hs0 (mm):	2.5
hs1 (mm):	1
hs2 (mm):	30
bs0 (mm):	3
bs1 (mm):	8
bs2 (mm):	5.3
rs (mm):	0.5
Top Tooth Width (mm):	3.47879
Bottom Tooth Width (mm):	3.55905
Skew Width (Number of Slots)	1
Length of Stator Core (mm):	47
Stacking Factor of Stator Core:	0.95
Type of Steel:	M100-23P
Designed Wedge Thickness (mm):	0.2
Slot Insulation Thickness (mm):	0.5
Layer Insulation Thickness (mm):	0.5
End Length Adjustment (mm):	3
Number of Parallel Branches:	1
Number of Conductors per Slot:	6
Type of Coils:	21

Average Coil Pitch:	1
Number of Wires per Conductor:	6
Wire Diameter (mm):	1.369
Wire Wrap Thickness (mm):	0.2
Slot Area (mm^2):	217.113
Net Slot Area (mm^2):	164.332
Limited Slot Fill Factor (%):	75
Stator Slot Fill Factor (%):	53.9295
Coil Half-Turn Length (mm):	60.6786
ROTOR DATA	
Minimum Air Gap (mm):	1
Outer Diameter (mm):	290
Length of Rotor (mm):	47
Stacking Factor of Iron Core:	0.95
Type of Steel:	M100-23P
Polar Arc Radius (mm):	136
Mechanical Pole Embrace:	0.9
Electrical Pole Embrace:	0.870756
Max. Thickness of Magnet (mm):	4
Width of Magnet (mm):	2.40E+01
Type of Magnet:	NdFe35
Type of Rotor:	1
Magnetic Shaft:	No
PERMANENT MAGNET DATA	
Residual Flux Density (Tesla):	1.23
Coercive Force (kA/m):	890
Maximum Energy Density (kJ/m^3):	273.675
Relative Recoil Permeability:	1.09981
Demagnetized Flux Density (Tesla):	0.501114
Recoil Residual Flux Density (Tesla):	1.23E+00
Recoil Coercive Force (kA/m):	8.90E+02
MATERIAL CONSUMPTION	
Armature Copper Density (kg/m^3):	8900
Permanent Magnet Density (kg/m^3):	7400
Armature Core Steel Density (kg/m^3):	7872
Rotor Core Steel Density (kg/m^3):	7872
Armature Copper Weight (kg):	2.06043
Permanent Magnet Weight (kg):	1.08565
Armature Core Steel Weight (kg):	5.68578
Rotor Core Steel Weight (kg):	1.57352
Total Net Weight (kg):	10.4054
Armature Core Steel Consumption (kg):	20.5741

Rotor Core Steel Consumption (kg):	9.60048
STEADY STATE PARAMETERS	
Stator Winding Factor:	0.616944
D-Axis Reactive Inductance Lad (H):	2.66E-05
Q-Axis Reactive Inductance Laq (H):	2.66E-05
D-Axis Inductance L1+Lad(H):	9.47E-05
Q-Axis Inductance L1+Laq(H):	9.47E-05
Armature Leakage Inductance L1 (H):	6.81E-05
Zero-Sequence Inductance L0 (H):	9.50E-05
Armature Phase Resistance R1 (ohm):	0.0214689
Armature Phase Resistance at 20C (ohm):	0.0176599
D-Axis Time Constant (s):	0.0012389
Q-Axis Time Constant (s):	0.0012389
Ideal Back-EMF Constant KE (Vs/rad):	1.00006
Start Torque Constant KT (Nm/A):	1.00008
Rated Torque Constant KT (Nm/A):	1.06643
NO-LOAD MAGNETIC DATA	
Stator-Teeth Flux Density (Tesla):	3.43167
Stator-Yoke Flux Density (Tesla):	1.03492
Rotor-Yoke Flux Density (Tesla):	2.31132
Air-Gap Flux Density (Tesla):	0.912484
Magnet Flux Density (Tesla):	0.945547
Stator-Teeth By-Pass Factor:	3.24E-05
Stator-Yoke By-Pass Factor:	1.24E-06
Rotor-Yoke By-Pass Factor:	9.19E-07
Stator-Teeth Ampere Turns (A.T):	1.35
Stator-Yoke Ampere Turns (A.T):	0.145211
Rotor-Yoke Ampere Turns (A.T):	0.355407
Air-Gap Ampere Turns (A.T):	821.691
Magnet Ampere Turns (A.T):	-823.293
Armature Reactive Ampere Turns at Start Operation (A.T):	1673.22
Leakage-Flux Factor:	1
Correction Factor for Magnetic Circuit Length of Stator Yoke:	0.799752
Correction Factor for Magnetic Circuit Length of Rotor Yoke:	7.91E-01
No-Load Speed (rpm):	422.834
Cogging Torque (N.m):	6.21E-12
FULL-LOAD DATA	
Average Input Current (A):	36.4257
Root-Mean-Square Armature Current (A):	31.5794
Armature Thermal Load (A^2/mm^3):	57.5081
Specific Electric Loading (A/mm):	16.0832
Armature Current Density (A/mm^2):	3.57566
Frictional and Windage Loss (W):	29.2626

Iron-Core Loss (W):	0.0117751
Armature Copper Loss (W):	64.2301
Transistor Loss (W):	150.263
Diode Loss (W):	4.56598
Total Loss (W):	248.334
Output Power (W):	1500.1
Input Power (W):	1748.43
Efficiency (%):	85.7968
Rated Speed (rpm):	375.96
Rated Torque (N.m):	38.1022
Locked-Rotor Torque (N.m):	1024.02
Locked-Rotor Current (A):	1024.18
WINDING ARRANGEMENT	
The 3-phase, 2-layer winding can be arranged in 9 slots as below:	AZBCYABXC
Angle per slot (elec. degrees):	80
Phase-A axis (elec. degrees):	6.00E+01
First slot center (elec. degrees):	0
TRANSIENT FEA INPUT DATA	
For Armature Winding:	
Number of Turns:	72
Parallel Branches:	1
Terminal Resistance (ohm):	0.0214689
End Leakage Inductance (H):	6.11E-07
2D Equivalent Value:	
Equivalent Model Depth (mm):	47
Equivalent Stator Stacking Factor:	0.95
Equivalent Rotor Stacking Factor:	0.95
Equivalent Br (Tesla):	1.23
Equivalent Hc (kA/m):	890
Estimated Rotor Moment of Inertia (kg m^2):	0.215067

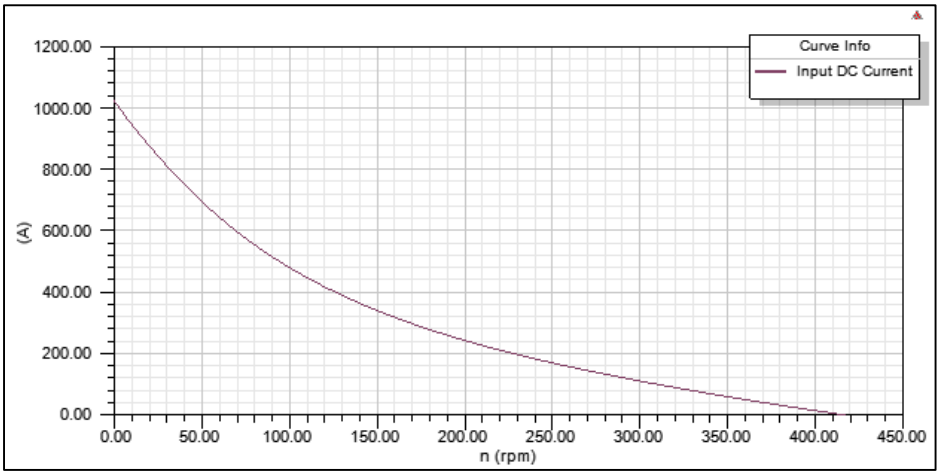

Input DC Current V/s Speed

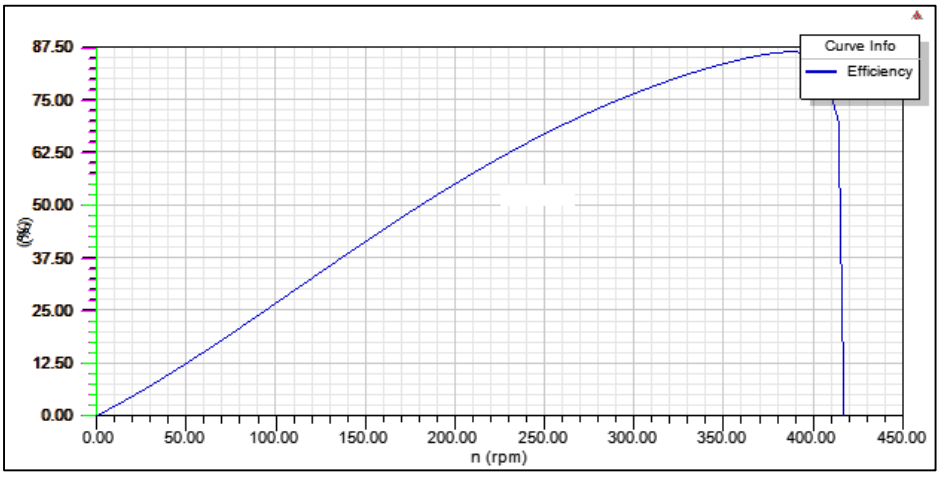

Efficiency V/s Speed

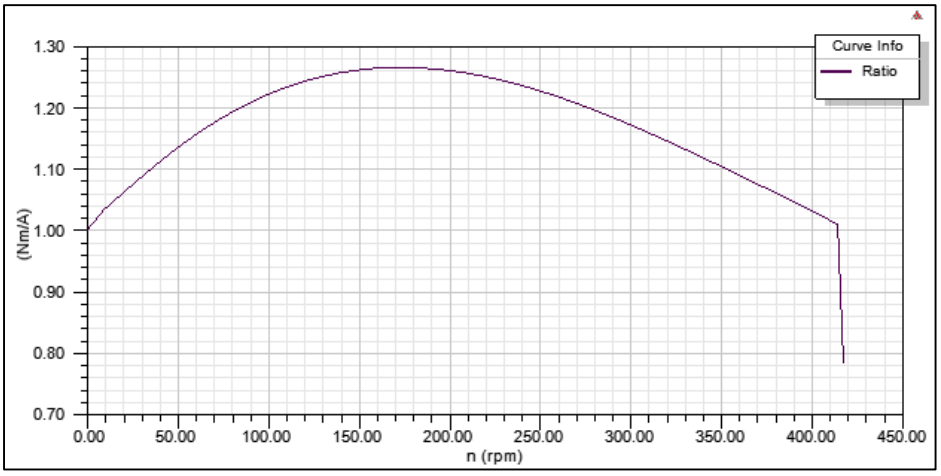

Ratio of Air-Gap Torque to DC Current V/s Speed

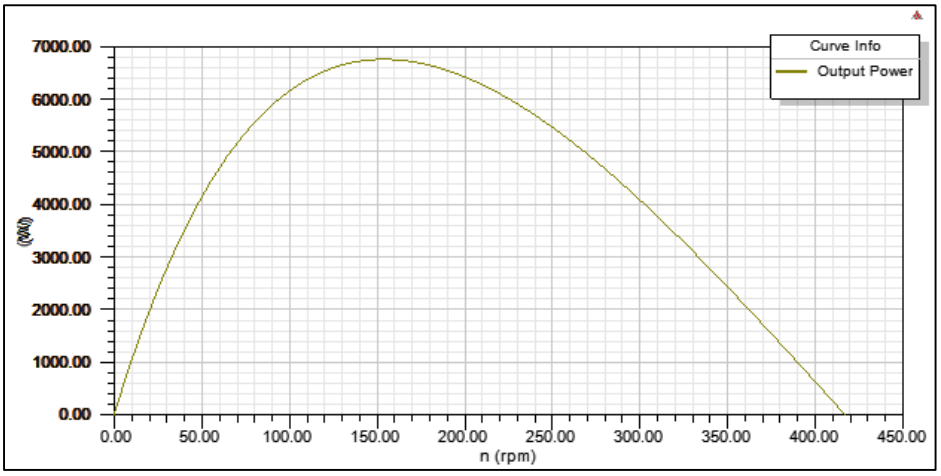

Output Power V/s Speed

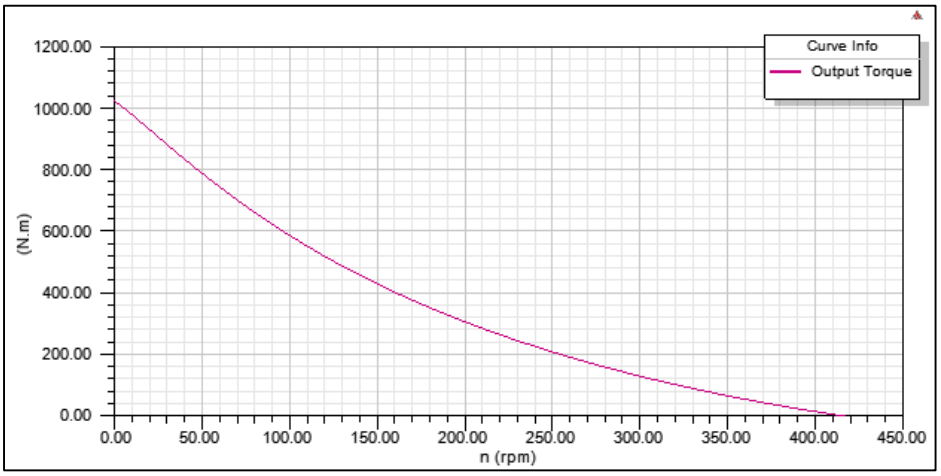

Output Torque V/s Speed

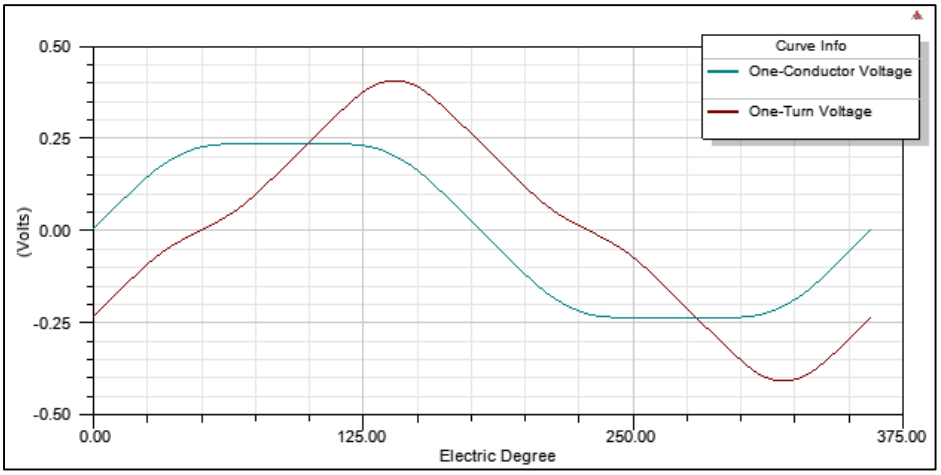

Induced Coil Voltages at Rated Speed

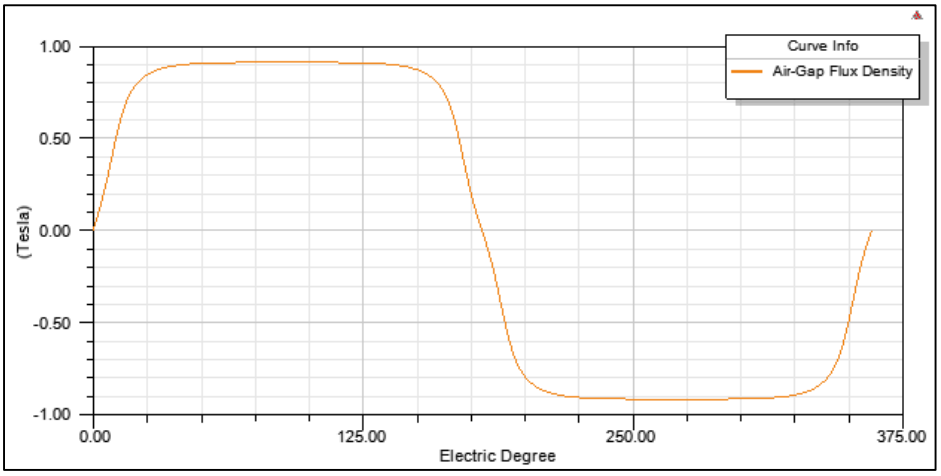

Air-Gap Flux Density

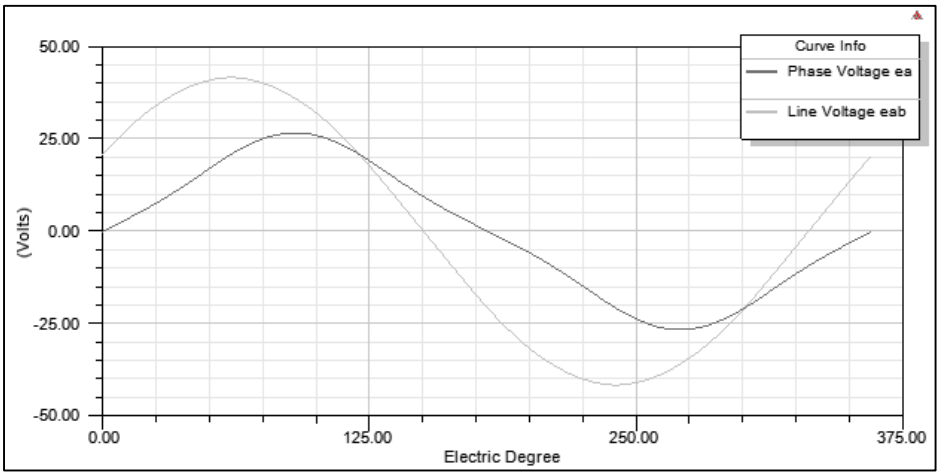

Induced Winding Voltages at Rated Speed

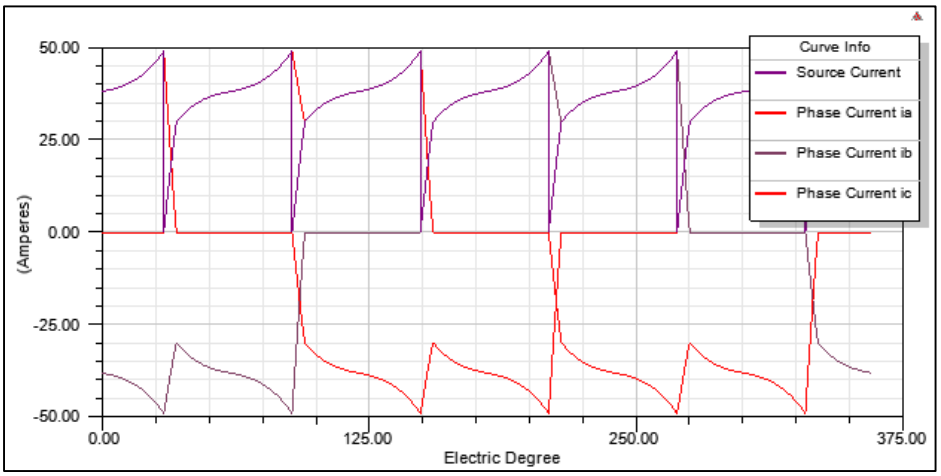

Winding Currents under Load

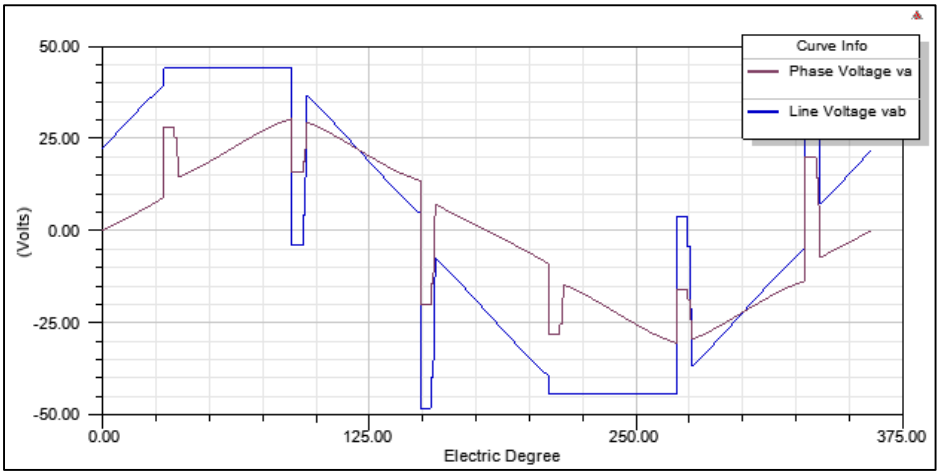

Winding Voltages under Load

Appendix 5: Steel Data:

1. Name: Unisil – H M100 – 23P
2. Manufacturer: Cogent

Name	Maximum specific loss (W/kg) at 1.7T		Typical specific loss (W/kg) at 1.7T		Polarization at H=800 A/m 1
	50Hz	60Hz	50Hz	60Hz	50 Hz Min T / Typical T
M10023P	1.00	1.32	0.92	1.19	1.88/1.91

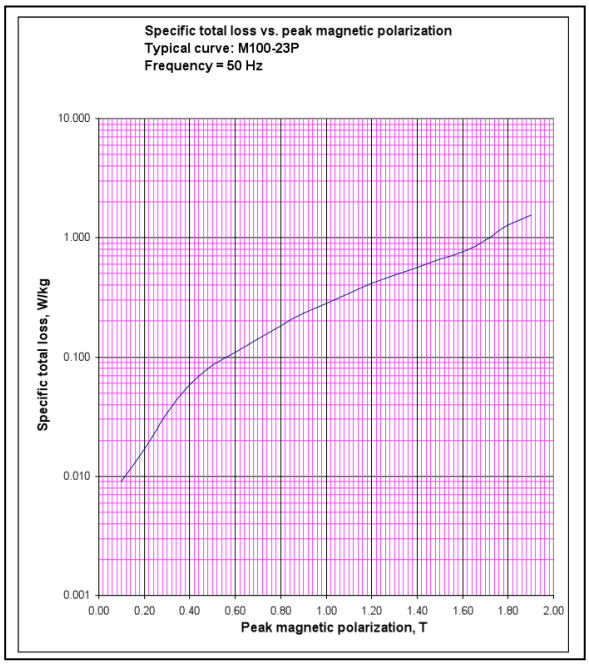

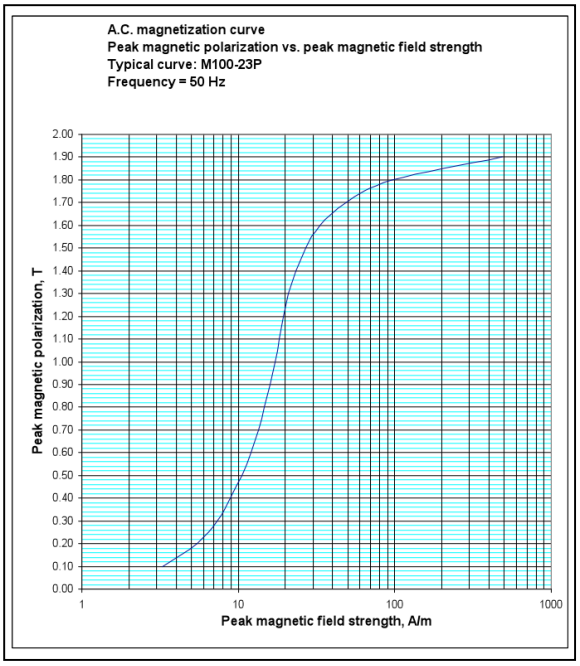

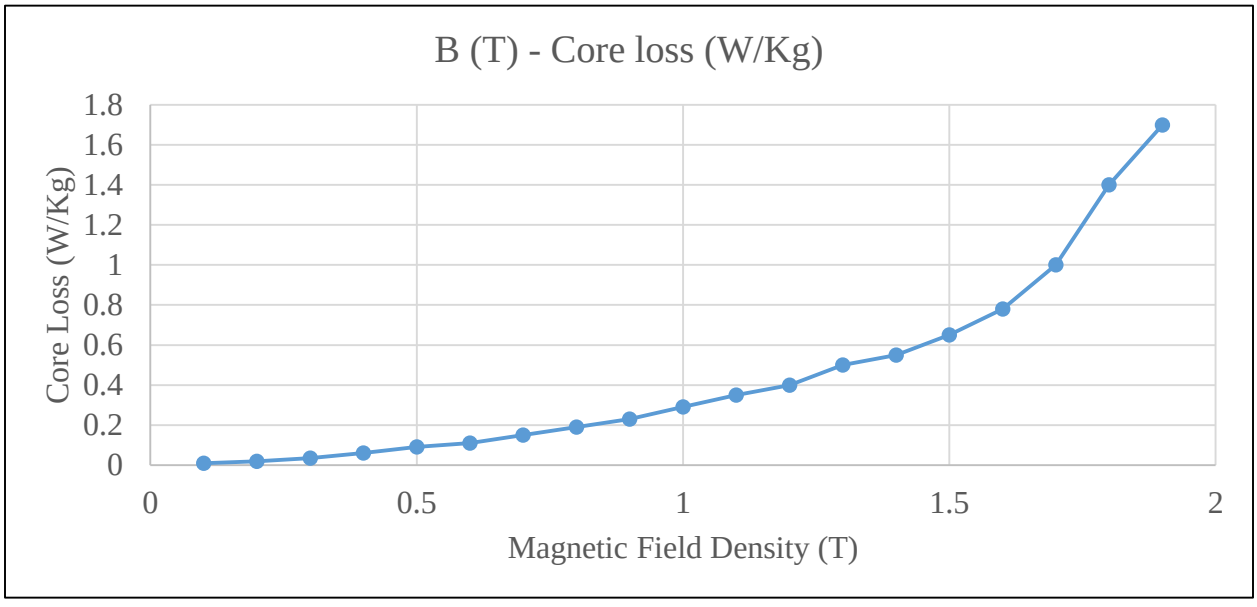

Magnetization Data		Core Loss Data	
B (T)	**B (T)**	**Core loss (W/Kg)**	**H (A/m)**
0.1	0.1	0.009	3.5
0.2	0.2	0.018	5.8
0.3	0.3	0.035	8
0.4	0.4	0.06	9.5
0.5	0.5	0.09	12
0.6	0.6	0.11	14
0.7	0.7	0.15	15
0.8	0.8	0.19	17
0.9	0.9	0.23	18
1	1	0.29	19
1.1	1.1	0.35	20
1.2	1.2	0.4	21
1.3	1.3	0.5	22
1.4	1.4	0.55	24
1.5	1.5	0.65	30
1.6	1.6	0.78	41
1.7	1.7	1	75
1.8	1.8	1.4	200
1.9	1.9	1.7	1000